PERCEPTUALLY MOTIVATED SIGNAL PROCESSING FOR DIGITAL HEARING AIDS

by

Ashutosh Pandey

A dissertation submitted to the faculty of
The University of Utah
in partial fulfillment of the requirements for the degree of

Doctor of Philosophy

Department of Electrical and Computer Engineering

The University of Utah

May 2011

The University of Utah Graduate School

STATEMENT OF DISSERTATION APPROVAL

The dissertation of **Ashutosh Pandey**

has been approved by the following supervisory committee members:

V. John Mathews	, Chair	**Feb 28, 2011** Date Approved
Behrouz Farhang-Boroujeny	, Member	**Feb 28, 2011** Date Approved
Michelle Hicks	, Member	**Jan 20, 2011** Date Approved
Michael Nilsson	, Member	**Jan 14, 2011** Date Approved
Marc Bodson	, Member	Date Approved

and by **Gianluca Lazzi**, Chair of the Department of **Electrical and Computer Engineering**

and by Charles A. Wight, Dean of The Graduate School.

ABSTRACT

Hearing aids suffer from the problem of acoustic feedback that limits the gain provided by hearing aids. Moreover, the output sound quality of hearing aids may be compromised in the presence of background acoustic noise. Digital hearing aids use advanced signal processing to reduce acoustic feedback and background noise to improve the output sound quality. However, it is known that the output sound quality of digital hearing aids deteriorates as the hearing aid gain is increased. Furthermore, popular subband or transform domain digital signal processing in modern hearing aids introduces analysis-synthesis delays in the forward path. Long forward-path delays are not desirable because the processed sound combines with the unprocessed sound that arrives at the cochlea through the vent and changes the sound quality.

In this dissertation, we employ a variable, frequency-dependent gain function that is lower at frequencies of the incoming signal where the information is perceptually insignificant. In addition, the method of this dissertation automatically identifies and suppresses residual acoustical feedback components at frequencies that have the potential to drive the system to instability. The suppressed frequency components are monitored and the suppression is removed when such frequencies no longer pose a threat to drive the hearing aid system into instability. Together, the method of this dissertation provides more stable gain over traditional methods by reducing acoustical coupling between the microphone and the loudspeaker of a hearing aid. In addition, the method of this dissertation performs necessary hearing aid signal processing with low-delay characteristics. The central idea for the low-delay hearing aid signal processing is a spectral gain shaping method (SGSM) that employs parallel parametric equalization (EQ) filters. Parameters of the parametric EQ filters and associated gain values are selected using a least-squares approach to obtain the desired spectral response. Finally, the method of this dissertation switches to a least-squares adaptation scheme with linear complexity at the onset of howling. The method adapts to the altered feedback path quickly and allows the patient to not lose perceivable information. The complexity of the least-squares estimate is reduced by reformulating the least-squares estimate into a Toeplitz system and solving it with a direct Toeplitz solver.

The increase in stable gain over traditional methods and the output sound quality were evaluated with psychoacoustic experiments on normal-hearing listeners with speech and music signals. The results indicate that the method of this dissertation provides 8 to 12 dB more hearing aid gain

than feedback cancelers with traditional fixed gain functions. Furthermore, experimental results obtained with real world hearing aid gain profiles indicate that the method of this dissertation provides less distortion in the output sound quality than classical feedback cancelers, enabling the use of more comfortable style hearing aids for patients with moderate to profound hearing loss. Extensive MATLAB simulations and subjective evaluations of the results indicate that the method of this dissertation exhibits much smaller forward-path delays with superior howling suppression capability.

To my parents.

CONTENTS

LIST OF FIGURES

LIST OF TABLES

ACKNOWLEDGEMENTS

I am thankful to my advisor, Dr. V. John Mathews, for his immense guidance and motivation on this project. I thank my committee members, Dr. Michael Nilsson, Dr. Michelle Hicks, Dr. Behrouz Farhang and Dr. Marc Bodson for supervising research in this dissertation. I am especially thankful to Dr. Michael Nilsson and Dr. Michelle Hicks, for their time providing me better insight about hearing aids from an audiological point of view. I am thankful to the faculty and staff of the Department of Communications Sciences and Disorders at the University of Utah for letting me use facilities in their department. In particular, I would like to thank Prof. Kumiko Boike, Prof. Lisa Hunter and Prof. Michelle Hicks from the above department for their help on several occasions. I would like to thank my professors at the University of Utah, especially Dr. Behrouz Farhang, Mr. Darrel Judd, Dr. Michael Nilsson, Dr. Michelle Hicks and Dr. Bomjun Kwon, from whom I had the benefit of learning in great deal to complete this research.

I am grateful to Keith Davis, Director of Engineering at Sonic Innovations, for providing me with equipment and data that were extensively used in this research. I am particularly thankful to Jeff Bullough, Jim Wellington and Jay Kirsch, engineers at Sonic Innovations, for their many hours of help in the beginning of this project to troubleshoot the hardware and experimental setup. I certainly learned a lot from them. I would like to thank Analog Devices for providing us the computing platforms that were used in this work. I would like to acknowledge some of my colleagues at work, David Lambert, Russell Ericksen, Mario Ninic, Pitchet Ong and Senad Tursic, for their valuable insight on audio signal processing that was useful for this research. I am grateful to my employers at ClearOne Communications for their support during this work that was critical in finishing it. I am especially thankful to my boss at ClearOne Communications, Derek Graham for allowing me to continue on this research while working there.

I would like to thank my former colleagues at the Signal Processing Group, University of Utah, Janez Jeraj, Ying Deng, Lanka Fernando, Harsha Rao and Lekun Lin, for helping me in my early years as a graduate student. I would like to thank my brother, Dr. Devashish Srivastava, and sister-in-law, Dr. Rachana Visaria, for their support and encouragement during my graduate years. I acknowledge the financial support received from the Department of Electrical and Computer Engineering for my initial graduate years.

This work would not have been possible without the support of all my friends and well-wishers.

I would especially like to thank my friends, Paul Warner, Laurie Warner, Mary Halbosted, Vineet Kumar, Susan and Randy Bartholomew, for their constant support over several years while I worked on this project. I am thankful to my family, Preeti Pandey, Umakant Pandey, Dipali Dutta, Aditi Dutta, Naresh Panda, Aditya Panda and Shreya Pandey, for their continual love and support. I owe a huge gratitude to my wife, Swati, for her love, support and motivation through the many hardships and uncertainties during this project. Finally, I am indebted to my parents, for their perpetual love that has ultimately made this dissertation possible.

CHAPTER 1

INTRODUCTION

Hearing aids provide frequency-dependent amplification of incoming signals to compensate for hearing loss in hearing-impaired patients. A typical hearing loss is a sensorineural hearing loss at higher frequencies with normal hearing at lower frequencies. Approximately, 10% (30 million people) of the US population suffers from some hearing loss and most of them need hearing aids. However, only a small portion of that population wear hearing aids [1]. There are several reasons why hearing aids have not penetrated a significant segment of the potential market. Among various reasons, the acoustic feedback problem is one of the biggest concerns for many hearing aid users. The acoustic feedback is present mostly because of a vent that provides patients comfort from the acoustic pressure difference at the ear drum. An adaptive filter is often used to continuously estimate the feedback path and cancel the acoustic feedback in hearing aids [2]. Figure 1.1 shows the block diagram of a typical digital hearing aid with a single microphone where thin and thick lines indicate scalar and vector quantities, respectively. It is common to implement the system in a transform or subband domain [3] where each band operates at a slower rate than the full band rate. Throughout the dissertation, we assume discrete time signal processing, with m and n denoting the time indices for the subband domain and fullband signals, respectively. The signal transformation results in spectrally distributed signals at a decimated rate.

Digital hearing aids use discrete signal samples of the microphone signal $u(n)$ and the speaker signal $x(n)$ to perform the necessary signal processing for hearing-impaired listeners. Such processes include adaptive feedback cancellation, noise suppression, hearing loss compensation and dynamic range compression (DRC) applied on the spectrally distributed signals. In general, a hearing aid performs compensation of hearing loss, noise suppression to reduce ambient noise in the incoming signal and DRC to provide a comfortable listening experience in the forward path [4, 5]. In Figure 1.1, the gain function $\mathbf{g}(m)$, where the entries of the gain vector are the gain values for the subbands, may vary with time and is designed to perform all three operations. We refer to DRC and noise suppression as dynamic signal processing in this dissertation. In Figure 1.1, due to the closed loop nature of the hearing aid system, a decorrelator is used to decorrelate the reference signal $x(n)$ from the input signal $u(n)$.

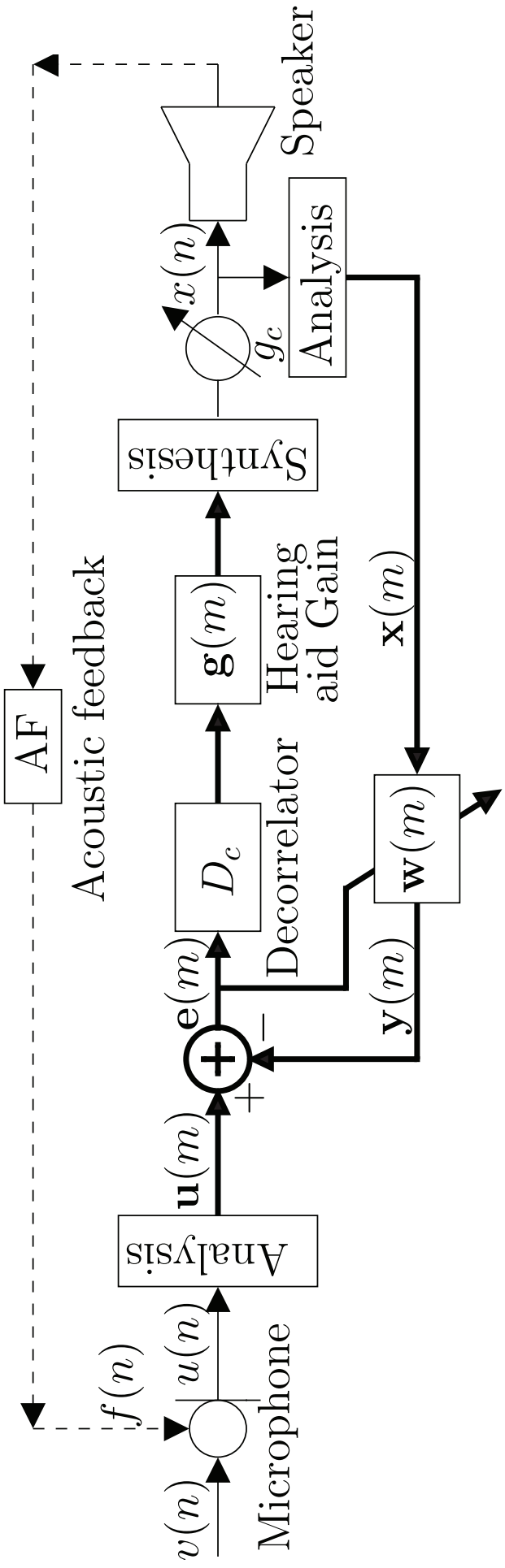

Figure 1.1: Block diagram showing the signal processing components of a typical digital hearing aid.

The use of a decorrelator can in general improve the adaptive filter estimate of the feedback path.[1] Introducing a delay in the forward path is the most popular decorrelation method employed in hearing aids due to its simplicity [6, 7]. Delays in the forward path can result in improved adaptive filter performance and additional stable gains [7–9]. There are also several shortcomings to the use of delays as decorrelators. They include slower convergence with longer delays [7–9], smaller decorrelation of tonal signals in the input signal such as voiced segments in speech [10] and coloration effects at the cochlea for longer delays (usually greater than 4 ms to 8 ms) [10]. Many researchers have proposed the use of additional decorrelators such as adding probe noise [6], frequency shifting [10] and continuous phase shifting [11] along with the delay in the forward path to alleviate some of the above difficulties. The broadband variable gain function g_c in Figure 1.1 can be used to adjust the overall output sound level in changing acoustic environments and is often available to hearing aid users as a volume control on the face plate of the hearing aid.

Processing the signals in transform or subband domain results in three advantages: easy adjustment of the gain value $g_i(m)$ in the i^{th} band, faster adaptive filter convergence and overall computational savings [12]. Adaptive feedback cancellation improves the output sound quality and provides an additional gain over the critical gain[2] for which the hearing aid is stable [3, 6, 13, 14]. The additional gain made possible by feedback cancellation is termed the added stable gain (ASG). Dynamic signal processing provides better output sound quality by reducing background noise with comfortable output sound levels [13, 15].

Together, the classical subband scheme discussed above provides added stable gain with good output sound quality. However, when the amplification in a hearing aid is more than the limits of the added stable gain, the hearing aid becomes unstable or the quality of the signal degrades to below acceptable levels [6]. A major source of this loss of performance of the system is the presence of residual feedback components in the signal. If acoustical feedback components are reduced, the stability and the output sound quality of a hearing aid can be further improved. Many researchers have proposed to change the characteristics of the signal in the forward path by changing its phase, shifting its frequency components or modifying its spectral magnitude with a notch filter to suppress the feedback and hence provide added stable gains [6, 16].

Although these methods keep the hearing aid stable, the output sound quality degrades as the signal characteristics are changed. In this dissertation, we present an approach that alters the hearing aid gain in the forward path to enhance the stability of the hearing aid system. The

[1] The feedback path is the combined response of the speaker, the microphone and the acoustic feedback.

[2] Critical gain refers to the maximum amplification for which the output signal quality is acceptable without feedback cancellation.

method of this dissertation modifies the hearing aid gain in two ways for reducing the acoustical coupling between the loudspeaker and the microphone. First, the hearing aid gain values $\mathbf{g}(m)$ are reduced intermittently at perceptually redundant components of the incoming signal. Research in psychoacoustics has shown that humans have difficulty hearing weak signals that fall in the frequency (frequency masking) or time vicinity (temporal masking) of stronger signals [17–21]. Such components do not contribute to the understanding of speech regardless of whether they are amplified or not. Such redundancies were successfully used in the past in the area of coding and noise suppression [22–24]. Second, the forward path gain is reduced at frequencies in the signal that are more likely to drive the system to unstable behavior. We refer to the frequencies so identified as the *offending frequencies* (OF). If offending frequencies are detected accurately and gain is reduced in a narrowband frequency region around these frequencies, the gain reduction is not audible for a few offending frequencies [25, 26]. This approach is similar to methods for controlling acoustical feedback in public address (PA) systems using narrowband parametric equalization (EQ) filters [27].

The offending frequencies are detected as they begin to develop instabilities in the system. The gain is reduced with narrowband parametric equalization (EQ) filters. While offending frequency suppression results in more stable hearing aids, the changes in offending frequencies are not tracked in traditional methods [26]. This can result in unwanted gain reductions at several frequencies in the signal over long periods of time. Traditionally, in public address (PA) systems, parametric EQ filters are reset (removed from the forward path) periodically and new offending frequencies are detected upon reset. However, this is not the most desired method because until the offending frequencies are reset, there may be unnecessary distortion in the system. In this dissertation, we develop a method that monitors the adaptive feedback canceller coefficients to reset the parametric EQ filters when the offending frequencies change. The offending frequency suppression and reset method provide a substantial amount of added stable gain with minimal impact on the perceptual quality of the output signal.

The classical subband-based method discussed earlier is a simple and computationally efficient way of implementing necessary signal processing for digital hearing aids. However, transform domain signal processing introduces an undesirable broadband delay in the forward path [4,28,29]. This is in addition to the processing delays such as analog-to-digital converter (ADC) and digital-to-analog converter (DAC) delays that are unavoidable in any realization of the hearing aid and the delay due to the decorrelator. Typically, the ADC/DAC adds $0.4 - 2$ ms of delay in hearing aids [30]. In practice, these time delays cause coloration effects when a hearing-aid user is talking. The talker's own voice reaches the cochlea with minimal delay via bone conduction and through

the hearing-aid vent and interacts with the delayed and amplified sound produced by the hearing aid signal processing to produce the coloration effect. Broadband delays as short as 4 to 8 ms have been reported to be detectable and to degrade the perceived output sound quality [31–33]. This dissertation presents a digital hearing aid design that retains the benefits of transform domain signal processing with a small forward path delay.

Our method accomplishes this objective by combining a low-delay spectral gain shaping method (SGSM) with a low-delay adaptive feedback cancellation system in the hearing aid. The low-delay SGSM uses a set of parallel second-order parametric equalization (EQ) IIR filters [34, 35] to obtain the desired response. The desired response depends on the prescribed hearing aid gain to compensate for the hearing loss, amount of noise suppression and dynamic range compression. The parametric EQ filters are known for their low group delays and are widely used in professional audio systems for audio equalization [36–38]. The coefficients of a parametric EQ filter are selected in this dissertation to match properties of the human auditory system that are relevant to hearing aid design [39].

The hearing aid signal processing structure presented in this dissertation employs an off-the-forward-path adaptive feedback cancellation system in the frequency domain similar to the system proposed by Morgan *et al.* [40] for acoustic echo cancellation. The feedback canceller employs a two-stage process. First, the adaptive filter estimates the feedback path using a frequency domain implementation of the filtered-XLMS algorithm [14]. Second, the estimated coefficients are used to cancel the feedback signal in the time domain. Separation of the estimation of the feedback path and cancellation of the feedback allows the system to use delays in the adaptation process without inserting delays in the cancellation process.

Finally, the method of this dissertation improves upon the howling scenario due to rapid or sudden change in the acoustic feedback path [13]. This problem is annoying and occurs often in a daily routine whenever a reflective surface such as a telephone receiver is brought near the face plate of the hearing aid, and in many other ways [13, 14, 41]. The majority of the feedback canceller systems employ gradient adaptive algorithms. They have relatively low computational complexity and therefore can be implemented within the small chip areas available in hearing aids. Unfortunately, gradient adaptive filters have slow convergence characteristics and may not be able to track the high rate of build up of the output signal during times of sudden or rapid changes in the feedback path, thus giving rise to howling behavior [13]. One approach to tackling this problem is to use a howling detector to sense the start of howling. In order to avoid prolonged howling, the gain function of the hearing aid is reduced when howling is detected. Subsequently, the gain is increased slowly while the adaptive filter estimates the altered feedback path and the hearing aid system is

stable [13]. The problem with this approach is that the gain has to be increased gradually over several seconds to keep the hearing aid system stable and produce an output with low distortion. This may cause the patient to miss some information because of inadequate sound pressure levels at the eardrum while ramping up the gain function. It is highly desirable to develop an adaptive filter with fast convergence and low computational complexity to suppress howling in hearing aids.

It is well known that least-squares adaptive filters converge faster than gradient-based algorithms in general [42–44]. However, even the most efficient least-squares algorithms [12, 42] have much higher computational complexity than most gradient adaptive filters. In our approach, we use the least-squares method to obtain an initial estimate of the altered feedback path immediately after howling is detected and switch to a gradient algorithm after a predetermined number of iterations. The computational complexity of the least-squares adaptive filter is comparable to that of the gradient algorithm because we make use of the efficiencies available during the initialization of the LS estimation process. The least-squares problem $Ax = B$, where A is an $N \times N$ known Toeplitz matrix, B is an $N \times 1$ known vector and x is an $N \times 1$ unknown vector can be solved in $O(N^2)$ operations using a direct Toeplitz solver [45–51]. These operations are spread over N iterations in our approach to maintain the linear complexity of the adaptive filter. Feedback cancellation is not performed during the LS adaptation process immediately after howling is detected. During the transition period, the hearing aid gain is reduced and increased periodically so as to prevent the hearing aid from becoming unstable. The gain is reduced for short durations so that the user will not perceive a loss of information because of the posttemporal masking effect [39].

1.1 Organization of the dissertation

The rest of this dissertation is organized as follows. Chapter 2 reviews the background literature for the research presented in this dissertation. Some of the popular decorrelators used in digital hearing aids for adaptive feedback cancellation are evaluated in Chapter 3. An experimental method for MATLAB simulations that is suitable for testing adaptive feedback cancellation algorithms employed in hearing aids is also developed in Chapter 3. The adaptive gain processing is described and compared against the classical methods with fixed gain functions in Chapter 4. The low-delay structure employed in this dissertation and relevant signal processing is described and evaluated in Chapter 5. Chapter 6 formulates the howling suppression algorithm using a least-squares approach and presents the experimental results from MATLAB simulations to demonstrate the capability of the howling suppression algorithm. The perceptually motivated signal processing method that combines the methods presented in Chapters 4, 5 and 6 is described in Chapter 7. Concluding remarks and future work for this research are discussed in Chapter 8.

CHAPTER 2

BACKGROUND

In this chapter, we present the background for the research presented in this dissertation. The work in the dissertation provides a better feedback control solution than the state-of-the-art techniques. The acoustic feedback control for hearing aids has been a topic of research for over 30 years [6, 52, 53]. In this chapter, we will briefly go through the different types of feedback control algorithms presented to date in the literature to the best of the author's knowledge. This research also improves upon the gain shaping methods in hearing aids. We will discuss various gain shaping methods presented in literature for hearing aids. Finally, this research is motivated by signal processing techniques used in the human auditory system. We present details about the human auditory signal processing relevant to this research in Section 2.3.

2.1 Acoustic feedback control for hearing aids

In this section, we illustrate various methods described in the literature for feedback control in hearing aids. Let the frequency response of the forward path of a hearing aid be $G(e^{j\omega})$. It can be said that sound arriving at the hearing aid microphone is amplified in accordance with a frequency response $G(e^{j\omega})$ in the forward path. The amplified sound at the receiver gets fed back to the microphone through transfer function $H(e^{j\omega})$ and re-amplified in a closed loop. As a result, the digital hearing aid works in a closed loop structure with the closed loop response $G(e^{j\omega})/(1 - G(e^{j\omega})H(e^{j\omega}))$. If the open loop gain

$$\Gamma_o(e^{j\omega}) = G(e^{j\omega})H(e^{j\omega}) \tag{2.1}$$

meets the Nyquist criteria (2.2, 2.3) [54,55] at some frequency ω_{osc} for many consecutive iterations, the hearing aid system is prone to instability and may oscillate at those frequencies. The Nyquist criteria are given by

$$|\Gamma(\omega_{osc})| \geq 1 \tag{2.2}$$

$$\angle\Gamma(\omega_{osc}) = n \times \pi \quad \text{for} \quad n = 0, 2, 4, \cdots\cdots \tag{2.3}$$

The oscillation may occur at one frequency or at a band of frequencies depending on the nature of the feedback path and the gain profile in the forward path. The oscillation results in a narrow bandwidth peak in the output spectrum that causes whistling in the hearing aid. Moreover, if the Nyquist criteria sustain for many iterations, it causes the output of the hearing aid to grow in an unbounded fashion creating the howling.

One way to avoid howling is to modify the forward path response so that the Nyquist conditions are not satisfied in consecutive iterations. Many researchers have proposed such techniques by modifying the magnitude and phase in the forward path of hearing aids to provide additional hearing aid gain. Such techniques are discussed in Sections 2.1.1 and 2.1.2. Some other techniques identify the feedback path and cancel the feedback signal to enhance the hearing aid system stability. These methods are known as adaptive feedback cancellation and are discussed in Section 2.1.3

2.1.1 Oscillation suppression by modifying forward path magnitude response

In this method, a notch filter is used in the forward path of a hearing aid to reduce the gain at frequencies where oscillations are likely to occur [52]. The notch filter is used in the forward path of the hearing aid in cascade with the amplifier. The authors of [56] have suggested that the oscillation frequencies may be identified at the time of hearing aid fitting. Once the frequencies are identified, narrow notches are placed in the forward path using a digital notch filter. After manually tuning the notch filters, authors in [56] demonstrated 8 to 10 dB of gain above the critical gain. Unfortunately, the oscillation frequencies are not fixed over time. If the earmold moves a little bit in the ear, or the patient moves his/her jaw, wears a hat, or brings a telephone receiver near his/her ear, the characteristics of the feedback path, and consequently, the oscillation frequencies, can change. To circumvent problems due to change in the feedback path, researchers have used adaptive notch filters to continuously monitor large spectral peaks in the output signal [57–59]. Results in [57–59] have shown up to 4 dB of additional gain above the critical gain. Evaluations of the adaptive notch filter (ANF) in [6] have suggested that the method employing ANFs is not suitable for detecting oscillation frequencies at low frequencies.

2.1.2 Oscillation suppression using phase variation

Feedback oscillation occurs if the sound gets larger every time it goes around the loop. If the characteristics of the sound coming back to the microphone is different from those of the original input so that frequency components of the input signal and the feedback signal do not remain continuously in phase with each other, they may not add up constructively. Consequently, the chances of the system going into oscillations are greatly reduced. Authors in [60–62] suggested to continuously modify the phase response with all-pass filters at oscillation frequencies so that a

negative feedback is maintained. Published results in the literature have indicated that continuous phase variation can provide 2 to 6 dB of additional gain without deteriorating the output sound quality.

2.1.3 Adaptive feedback cancellation

The methods given in Sections 2.1.1-2.1.2 do not reduce feedback. Instead, they modify the open loop gain so that instability in a hearing aid system can be avoided and more additional stable gain can be provided to the hearing aid user. On the other hand, adaptive feedback cancellation techniques estimate the feedback signal and the estimated feedback signal is subtracted from the output of the microphone. Adaptive feedback cancellation (AFC) is one of the most attractive approaches to reducing acoustic feedback in digital hearing aids [5, 6, 13, 52, 59, 63]. In adaptive feedback cancellation, digital hearing aids use adaptive filters to estimate acoustic feedback and cancel it in the digital domain [6,63]. A block diagram of a typical digital hearing aid with adaptive feedback cancellation (AFC) is shown in Figure 2.1.

The input signal $v(n)$ is corrupted by the feedback signal $f(n)$ and is picked up by the microphone. An adaptive filter $\mathbf{w}(n)$ is used to estimate the feedback signal using the reference signal $x(n)$ and the primary input signal $u(n)$ to produce the signal $y(n)$. The adaptive filter $\mathbf{w}(n)$ estimates the combined response of the speaker, the microphone and the acoustic feedback. It is desired that the signal $y(n)$ be close to the feedback signal $f(n)$ so that the output of the hearing aid is close to the input signal $v(n)$. The gain function G of the hearing aid is typically frequency dependent. The output limiter (OL) limits the amplitude of the output signal $x(n)$ which is used here in place of an output compression limiter (OCL) for simplicity [7]. The OCL reduces the gain of the system to mitigate clipping [13, 64]. Due to the closed loop nature of the hearing aid system, a delay is used to decorrelate the reference signal $x(n)$ from the input signal $u(n)$. Introducing

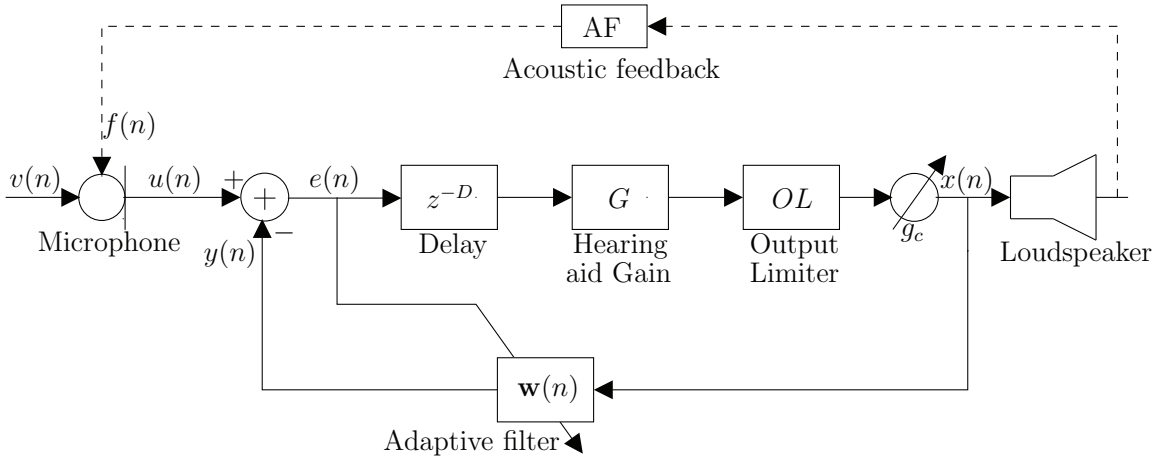

Figure 2.1: Simplified block diagram of a digital hearing aid with AFC.

a delay in the forward path or in the cancellation path is the most popular decorrelation method employed in hearing aids due to its simplicity [6, 7]. Bustamante *et al.* [56] were the first to suggest the use of a delay to estimate the feedback path. Use of delays can result in improved adaptive filter performance in steady state, as shown analytically by Siqueria *et al.* [7]. Siqueria *et al.* in [7] have also shown that the delay in the forward path provides more bias reduction than the delay in the cancellation path.

Adaptive filters model the feedback path with a finite impulse response filter with N coefficients. In what follows, we denote the coefficient vector as $\mathbf{w}(n)$. Among the many gradient adaptive filters available, the normalized least-mean-squares (NLMS) algorithm is the most popular scheme in hearing aids due to its simplicity. The update equations for the NLMS adaptation for estimating the feedback path are given in Table 2.1. In the update equations, α is a small positive constant that controls the adaptation speed of the system and ϵ is another small positive constant designed to prevent singularities [36]. The adaptive feedback cancellation described above improves the output sound quality and provides amplification levels larger than the critical gain [6]. However, there are also shortcomings to the use of delays as decorrelators. They include slower convergence with longer delays [7], smaller decorrelation of tonal signals in the input signal such as voiced segments in speech [10, 65] and coloration effects at the cochlea for longer delays (usually greater than 4 ms to 8 ms) [10]. A number of researchers have proposed and evaluated variations of adaptive feedback cancellation techniques to reduce the requirement of delay and distortions at low frequencies [6, 8, 10, 13, 14, 59, 66].

Various types of decorrelators have been suggested in literature to reduce the requirements of the forward path delay [6]. These decorrelators include intermittent probe noise [67–70], phase modulation [11] and frequency compression [10]. While the use of probe noise reduces the requirements of the delay, often, the power of the probe noise required to get sufficient decorrelation is large and so noise can be heard at the output of the hearing aid. This is annoying to the user and hence not a preferred method except for profoundly hearing impaired patients who are not affected by the additional noise. The use of phase modulation or frequency compression also reduces the

Table 2.1: Update equations for the classical adaptive feedback canceller.

$$\mathbf{x}(n) = \begin{bmatrix} x(n) & x(n-1) & \cdots & x(n-N+1) \end{bmatrix}^T$$
$$e(n) = u(n) - y(n) = u(n) - \mathbf{w}^T(n)\mathbf{x}(n)$$
$$\mathbf{w}(n+1) = \mathbf{w}(n) + \frac{\alpha}{\|\mathbf{x}(n)\|^2 + \epsilon} e(n)\mathbf{x}(n)$$

delay requirements and can improve output sound quality for tonal components in the input signals. Frequency-dependent phase modulation can be achieved with all-pass filters [16, 71]. Frequency shifting is done with Hilbert transform [36] or compression of the spectrum with the sampling approach [10, 72]. It must be mentioned that the increased use of decorrelators may harm the output sound quality of hearing aids [11, 16, 72]. It is reported that frequency shifting up to 5 Hz or slow phase modulation is not perceivable by human ears [11, 39].

In another improvement for AFC in hearing aids, Kates [73] suggested constraining the magnitude of the adaptive filter coefficients [73] to stop the divergence of the adaptive filter coefficients when tonal signals are input to the hearing aid. In a different implementation of adaptive feedback cancellation, a noncontinuous adaptive feedback cancellation (AFC) was proposed to improve the hearing aid stability and to provide more feedback cancellation [6, 59, 74, 75]. It was argued that the noncontinuous AFC would be less susceptible to the instability problems because it is implemented in the open loop. The block diagram of the noncontinuous AFC is shown in Figure 2.2. In this method, the forward signal path is broken and the adaptive filter is adapted with some predetermined condition. Such adaptation was first proposed by Graupe *et al.* [74]. The adaptation is performed at turn on, periodically and/or when a threshold change in the gain is sensed. Kates [59] proposed adaptation using probe noise when strong oscillations are detected. The oscillation is detected using an adaptive notch filter (ANF). Maxwell and Zurek [6] proposed the adaptation in quiet intervals or at the onset of oscillations. The quiet intervals are detected using an energy-based voice activity detector (VAD).

There are several problems associated with the noncontinuous AFC. First, since the adaptation is not carried out all the time, it compromises the output sound quality of the hearing aid. Second, if the hearing aid system is in suboscillatory situations, the adaptation will not be evoked and hence

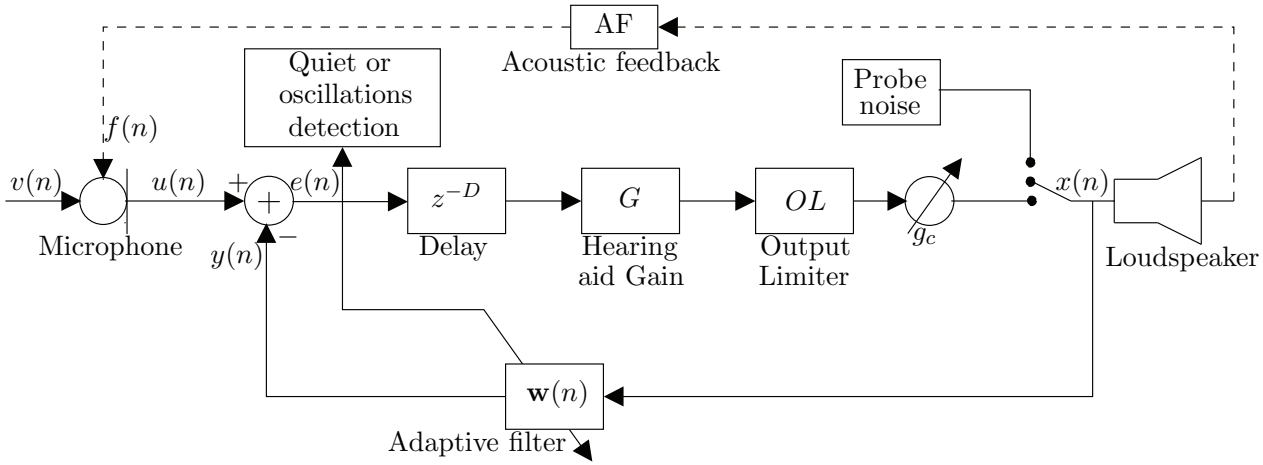

Figure 2.2: A block diagram of noncontinuous acoustic feedback cancellation in hearing aids.

the output sound quality will be poor. Moreover, the intermittent probe signal introduced into the signal to help the adaptive filter to adapt reduces the signal-to-noise ratio and may not be acceptable to the hearing aid user. Greenberg *et al.* [2] evaluated continuous and noncontinuous AFC with different signals, vent conditions and feedback paths. The results in [2] indicate that the continuous adaptive feedback cancellation is the better choice for the feedback reduction in hearing aids than its noncontinuous counterpart.

A few researchers have suggested feedback cancellation with an adaptive filter for limited frequencies - band-limited adaptive feedback cancellation, to provide smaller distortions at low-frequencies in the output sound [8, 76]. In this approach, adaptive feedback cancellation is done for frequencies in which oscillations are likely to occur. Such frequencies are determined at the time of hearing aid fitting based on the Nyquist criteria. The idea of the band-limited adaptation is attractive for speech signals, because most of the correlated part of speech is at low frequencies, while oscillation normally occurs at high frequencies. In addition, band-limited signals will have lower spectral dynamics compared to original signals. Consequently, the band-limited algorithm should have faster convergence than wide-band algorithms. The band-limited algorithm may improve the output sound quality if the feedback path contains oscillation frequencies in higher frequency regions. However, it is not suitable for all types of hearing aids and may not work well if the feedback path is changing frequently during the operation of hearing aids.

In a significant contribution towards improving adaptive feedback cancellation in hearing aids, Hellgren *et al.* [77] proposed an idea for adaptive feedback cancellation to reduce the bias of the adaptive filter in hearing aids using a filtered-XLMS type adaptive filter [63]. Hellgren *et al.* showed that the bias in the adaptive filter estimate with the NLMS adaptive filter can be reduced if the mean of the square filtered error $E[(e_w(n))^2]$ is minimized. The error $e(n)$ is filtered through a filter $\mathbf{L}_w(n)$ to obtain the filtered error $e_w(n)$, where $L_w(e^{j\omega})$ is a whitening filter and is the inverse of the filter that generates the input signal $v(n)$ from a white noise signal or an impulse train signal [78]. The block diagram of adaptive feedback cancellation with the filtered-XLMS algorithm is shown in Figure 2.3.

Spriet *et al.* [79] proposed a two-channel identification approach to identify $L_w^{-1}(e^{j\omega})$ with the assumption that the input signal $v(n)$ is an autoregressive signal of fixed order, *i.e.* the filter $L_w^{-1}(e^{j\omega})$ is a fixed order all pole filter [12]. Spriet *et al.* used two FIR adaptive filters $A(e^{j\omega})$ and $B(e^{j\omega})$ to simultaneously identify $L_w(e^{j\omega})$ and $-L_w(e^{j\omega})H(e^{j\omega})$. The adaptation is performed to minimize the error $e_t(n)$

$$e_t(n) = \mathbf{B}^T(n)\mathbf{x_t}(n) + \mathbf{A}^T(n)\mathbf{u_t}(n) \tag{2.4}$$

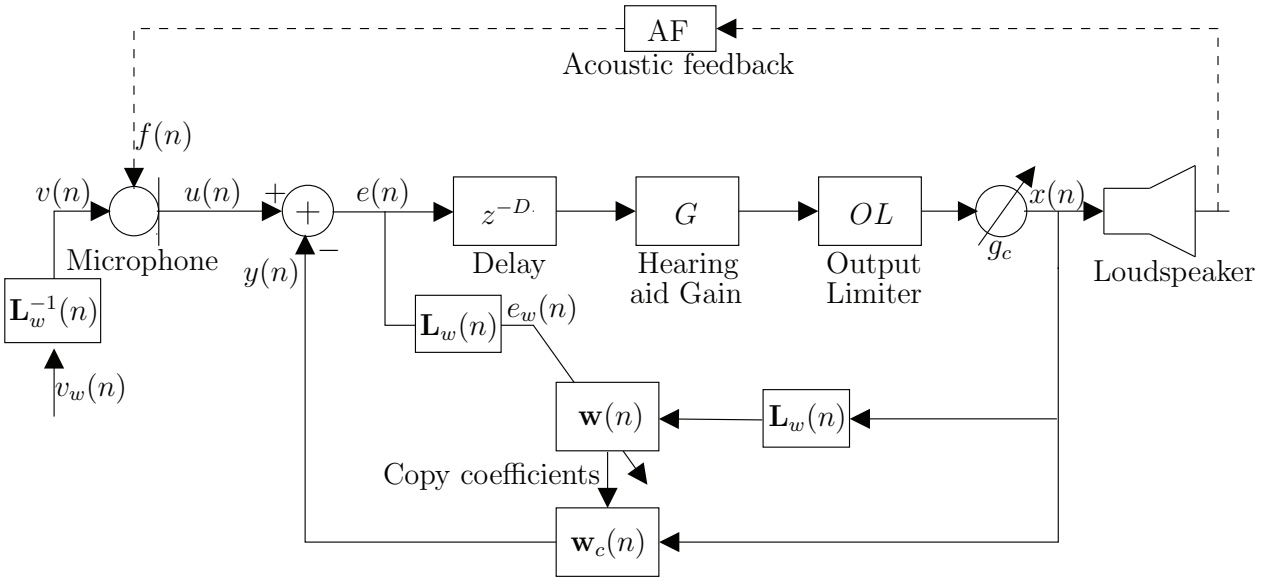

Figure 2.3: Block diagram adaptive feedback cancellation using a filtered-XLMS adaptive filter.

where $\mathbf{x}_t(n) = \left[\begin{array}{cccc} x(n) & x(n-1) & \cdots & x(n-N-M_a+2) \end{array} \right]^T$, $\mathbf{A}(n)$ is a column vector of length M_a, $\mathbf{u}_t(n) = \left[\begin{array}{cccc} u(n) & u(n-1) & \cdots & u(n-M_a+1) \end{array} \right]^T$, and $\mathbf{B}(n)$ is a column vector of length $N + M_a - 1$. A block diagram of the two-channel filtered-XLMS (TC-FXLMS) algorithm proposed by Spriet *et al.* is shown in Figure 2.4. Minimizing error $e_t(n)$ results in a nonlinear optimization. This dependency is effectively ignored by the authors by neglecting the second term in the gradient of the cost function [79]. Spriet *et al.* successfully reduced the bias of the

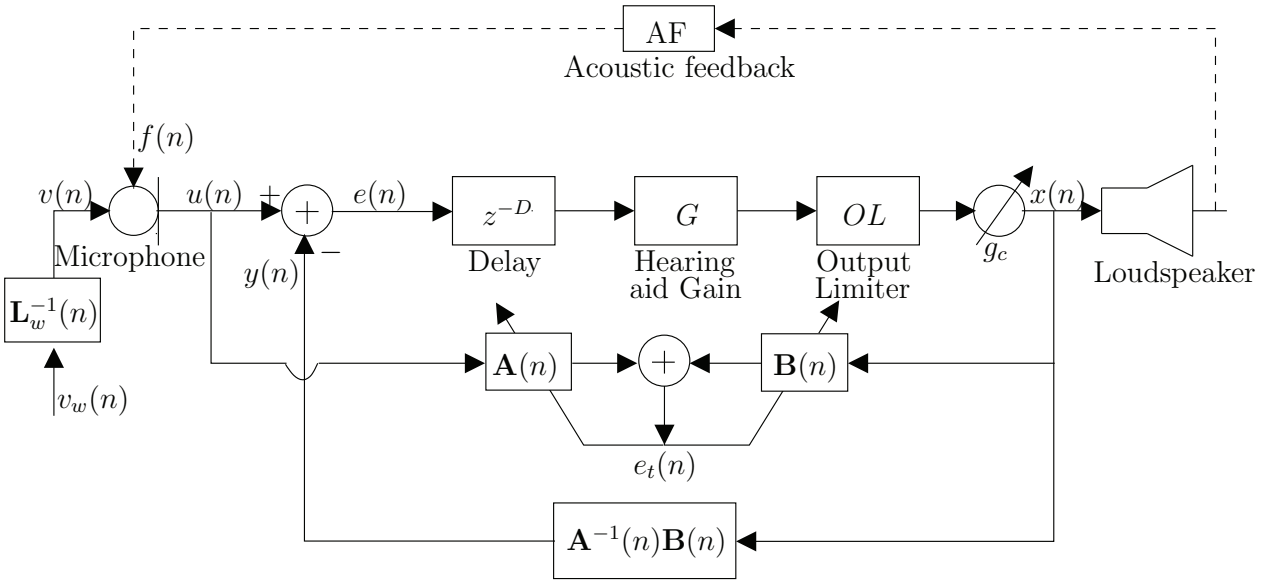

Figure 2.4: Block diagram of the adaptive feedback cancellation with the two-channel filtered-XLMS algorithm (TC-FXLMS).

adaptive filter for a given delay with the two-channel approach. However, the two-channel FXLMS algorithm approximates the feedback path transfer function $H(e^{j\omega})$ with an IIR transfer function whose poles are the zeros of the adaptive filter $A(e^{j\omega})$. Therefore, it is necessary for the stability of the system that the zeros of $A(e^{j\omega})$ are inside the unit circle. Ensuring this condition can be computationally complex for the higher order of the adaptive filter $A(e^{j\omega})$ [80].

2.2 Spectral gain shaping in hearing aids

In addition to acoustic feedback control, hearing aids provide frequency-dependent gain to hearing aid users. Furthermore, they modify frequency-dependent gain in the forward path of hearing aids to perform dynamic signal processing. In this section, we discuss some of the methods used in the literature for spectral gain shaping in hearing aids.

2.2.1 Frequency domain implementation

As stated earlier, hearing aids provide frequency-dependent hearing aid gain. Moreover, dynamic signal processing is done in the frequency domain. This makes frequency domain implementation a logical choice for hearing aids. Kaelin *et al.* [13, 81] have implemented hearing aids in the frequency domain that can perform necessary frequency-dependent hearing aid signal processing. In addition, they also investigated the use of the frequency domain block-based LMS (FBLMS) adaptive filters for feedback reduction in digital hearing aids based on the "overlap-save" method. The block diagram of the hearing aid structure in the frequency domain employing the FBLMS algorithm for adaptive feedback cancellation is shown in Figure 2.5. To better understand description of this algorithm, the following notation is used. Let $x(k,n)$ defined as

$$x(k,n) = x(n + k\Delta K) \quad n = 1, 2, \cdots, N_f \tag{2.5}$$

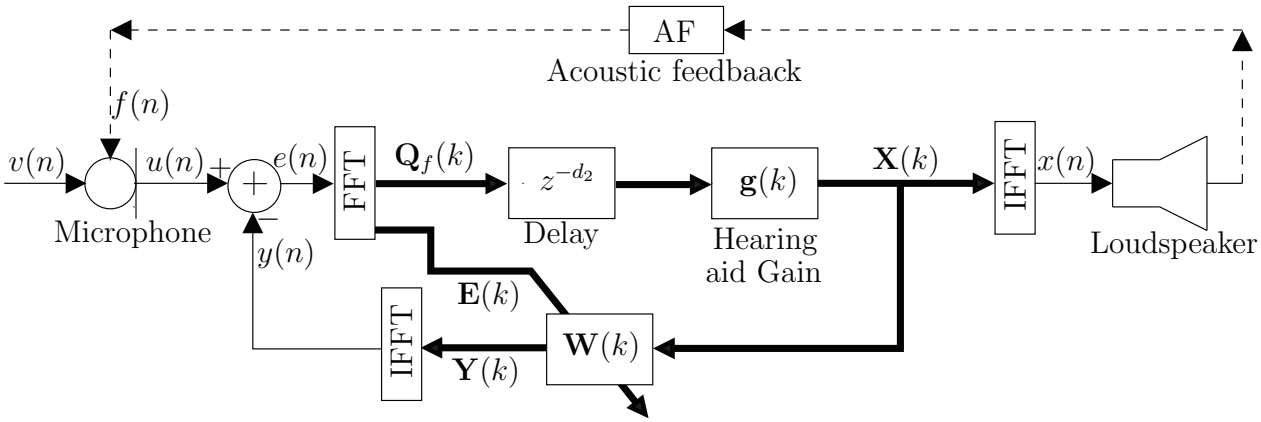

Figure 2.5: A block diagram of the hearing aid structure employing the FBLMS algorithm.

represents the k^{th} frame of the input signal $x(n)$. In (2.5), N_f is the frame size in number of samples and ΔK represents the shift between successive frames. Let the discrete fourier transform (DFT) of the signal $x(k,n)$ be $X(k,i)$ where i represents the frequency bin $\omega_i = \frac{2\pi i}{N_f}$ radians/sample. We denote the vector of all frequency components $X(k,i)$ in frame k by $\mathbf{X}(k)$. In the implementation of Kaelin *et al.* [13], the reference signal $x(n)$ and the desired signal $u(n)$ is segmented into $2N$ point vectors with N point overlap and used to update the adaptive filter coefficients in frequency domain. The hearing aid gain and dynamic signal processing can be performed by adjusting gain of frequency bins $g(k,i)$ of a forward path signal. The adaptive feedback cancellation algorithm at block k is summarized in Table 2.2. In Table 2.2, the variables $\mathbf{W}(k)$ and $\mathbf{g}(k)$ are the vector representations of the adaptive filter coefficients and the hearing aid gain in the frequency domain, respectively. The variable $d_2 = D/N$ is the normalized delay.

While the frequency domain implementation of hearing aids provides a computationally efficient implementation, it adds long delays in the forward path which is not acceptable for hearing

Table 2.2: Adaptive feedback cancellation with FBLMS adaptive filter.

Definitions

$\mathbf{S}(0)$	...	A vector of length $2N$ with small positive constant
$\mathbf{W}(0)$	...	A vector of length $2N$ with all zeros
μ_0	...	Suitable adaptation constant
β	...	An averaging constant close to 1

Update Difference Equations

$$\mathbf{u}(k) = \left[\begin{array}{cccc} u(kN) & u(kN+1) & \cdots & u((k+2)N+1) \end{array}\right]$$

$$\mathbf{Y}(k) = \mathbf{W}(k) \bigodot \mathbf{X}(k)$$

$$\mathbf{y}(k) = \text{the last N elements of IFFT}(\mathbf{Y}(k))$$

$$\mathbf{e}(k) = \mathbf{u}(k) - \mathbf{y}(k)$$

$$\mathbf{E}(k) = \text{FFT}\left(\left[\begin{array}{c} \mathbf{0} \\ \mathbf{e}(k) \end{array}\right]\right)$$

$$\mathbf{W}(k+1) = \mathbf{W}(k) + \mu_0 \mathbf{S}(k)\mathbf{X}(k)\mathbf{E}(k)$$

$$\mathbf{W}(k+1) = \text{FFT}\left(\left[\begin{array}{c} \text{the first N elements of IFFT}(\mathbf{W}(k+1)) \\ \mathbf{0} \end{array}\right]\right)$$

$$Q_f(k,i) = E(k,i) + (-1)^j E(k-1,i) \text{ for } i = 0, \cdots, 2N-1$$

$$X(k+1,i) = g(k,i) Q_f(k-d_2,i) \text{ for } i = 0, \cdots, 2N-1$$

$$\mathbf{S}(k+1) = \beta \mathbf{S}(k) + (1-\beta)\mathbf{U}(k+1) \bigodot \mathbf{U}^{\star}(k+1)$$

- Note: $\bigodot$ denotes element-by-element multiplication of vectors
- $\mathbf{0}$ denotes column vector of length N

aids [31]. The requirement of long delays in the forward path almost makes the above implementation unusable for practical purposes in hearing aids. The delay in the forward path for a frequency domain implementation can be reduced using partitioned FBLMS type algorithms [12]. An implementation of partitioned FBLMS adaptive filter for hearing aids is suggested in [82].

2.2.2 Subband domain implementation

The complete signal processing of hearing aids can also be implemented in subband domain as well [3, 36, 83]. Uniform or nonuniform subbands can be used [36, 84, 85]. Nonuniform subband whose bandwidths are equivalent to auditory filter bandwidths across frequency are believed to perform better noise reduction [86, 87]. However, often nonuniform subbands implementation requires additional complexity and processing delays [88]. Even though the low-delay implementation of the nonuniform subbands are available [88], uniform subbands are a more popular choice for hearing aid implementation due to their simplicity [3, 9].

In most subband structures, a block-based structure is used where first, samples are collected into a frame and then, a transformation is applied to convert them into subband signals. There are many transformations used in the literature such as Discrete Fourier Transform (DFT), Modulated Lapped Transform (MLT), Generalized DFT (GDFT), Discrete Hartley Transform (DHT) and Discrete Cosine Transform (DCT) [3, 36, 83]. These transformations differ in the implementation efficiency, side band attenuation and type of the output signal (real vs. complex valued). Any of the transformations is sufficient; however, the subband implementation with GDFT is a popular choice for hearing aids as it produces odd stacked complex valued subbands which can be efficiently implemented with the FFT algorithm and bandwidths are uniform across frequencies which are easier to visualize [9, 28, 89]. A subband-based system employing M subbands, which are created with oversampled Generalized Discrete Fourier Transform (GDFT) filter banks is shown in Figure 2.6.

Each subband component operates at $L \leq M$ times lower sampling rate than the full sam-

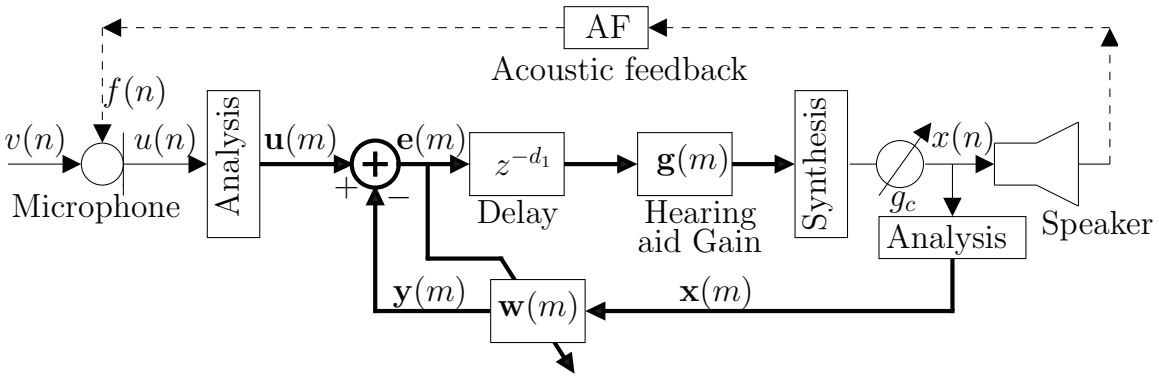

Figure 2.6: Block diagram showing the signal processing components of a typical digital hearing aid in the subband domain implementation.

pling rate of the system. The GDFT filter banks are known for their computationally efficient implementation via FFT [9, 83, 90]. Let $u_i(m)$ denote subband domain signal in band i at time m for the microphone, then, $\mathbf{u}(m)$ denotes a vector containing all subband domain signals such that $\mathbf{u}(m) = \begin{bmatrix} u_0(m) & u_1(m) & \cdots & u_{M-1}(m) \end{bmatrix}^T$. Other signals follow a similar notation in the subband domain for this dissertation. Gain compensation for hearing loss and adaptive feedback cancellation are done in the subband domain. Gain compensation is done by adjusting the subband gain values $g_i(m)$ based on a frequency dependent audiogram of the hearing-impaired listener. Finally, adaptive feedback cancellation is done with a normalized adaptive least-mean-squares (NLMS) algorithm in each subband. Subband adaptive filters together model a full band feedback path that is approximated with a linear impulse response with N coefficients. Let $\mathbf{w}_i(m)$ represent the adaptive filter coefficient vector for the i^{th} subband and contain $N_s = [N/L]$ coefficients, where the operation $[a]$ returns the integer part of the real number a. If N is not a multiple of L, modeling the adaptive filter with N_s coefficients in subband is not an exact but close approximation of the impulse response with N coefficients in full band. The update equations for the NLMS adaptation in the i^{th} subband for the m^{th} subband sample to estimate the feedback path are given in Table 2.3. In Table 2.3, α is a small positive constant that controls the adaptation speed of the system and ζ is another small positive constant designed to avoid a divide-by-zero [12, 91, 92].

2.2.3 Low-delay implementation

Researchers have recognized requirements for low-delay in various areas of audio signal processing and have proposed low-delay implementations for audio signal processing [36]. In the subband-based methods, long prototype filters are needed to achieve a sufficient stopband attenuation, which results in a high signal delay. One approach to achieve a reduced delay is to design the prototype lowpass filter of the DFT filter-bank by numerical optimization with the design target to reduce the aliasing distortions with constrained signal delay [93, 94]. A lower signal delay

Table 2.3: Update equations for a subband-based adaptive feedback cancellation system.

$$\mathbf{x}_i(m) = \begin{bmatrix} x_i(m) & x_i(m-1) & \cdots & x_i(m-N_s+1) \end{bmatrix}^T$$
$$\mathbf{w}_i(m) = \begin{bmatrix} w_i^0(m) & w_i^1(m) & \cdots & w_i^{N_s-1}(m) \end{bmatrix}^T$$
$$e_i(m) = u_i(m) - y_i(m) = u_i(m) - \mathbf{w}_i^T(m)\mathbf{x}_i(m)$$
$$\mu_i(m) = \frac{\alpha}{\|\mathbf{x}_i(m)\|^2 + \zeta}$$
$$\mathbf{w}_i(m+1) = \mathbf{w}_i(m) + \mu_i(m)e_i(m)\mathbf{x}_i(m)$$

can be achieved by the concept of the filter-bank equalizer (FBE) proposed in [95, 96]. In this method, the adaptation of the coefficients is performed in the (uniform or nonuniform) short-term frequency domain while the actual filtering is performed in the time domain. Smaller delays are obtained by approximating the time-domain filter of the FBE by a filter of lower degree. These methods reduce requirements of delay compared to the analysis-synthesis filter banks; however, they still possess broadband delays. In a related approach, Kates *et al.* [4] used frequency warping using an all-pass transformation[1] for dynamic range compression in hearing aids. Implementations with all-pass transformed elements need fewer frequency channels for the same low frequency resolution. However, these systems require a higher computational complexity in comparison to the corresponding uniform filterbank (with delay elements) [36].

2.3 Human auditory signal processing

The field of psychoacoustics has made significant progress toward characterizing human auditory perception. In many areas of signal processing, perceptually irrelevant signal information is used to improve the output sound quality [23, 97–99]. Research in psychoacoustics has shown that humans can have difficulty hearing weak signals that fall in the frequency (frequency masking) or time vicinity (temporal masking) of stronger signals [17, 24, 100]. Irrelevant information is identified during signal analysis by incorporating several psychoacoustic principles, including absolute hearing thresholds, critical band frequency analysis, simultaneous masking, the spread of masking along the basilar membrane, and temporal masking. This section reviews psychoacoustic fundamentals that are used in this research.

2.3.1 Absolute threshold of hearing

The absolute threshold of hearing at a frequency is the minimum amount of energy of a pure tone at that frequency that can be detected by a human ear in a noiseless environment. These thresholds $H_T(f)$ at various frequencies f are approximated by a nonlinear function construed based on the average of a few normal-hearing listeners thresholds. One such model [101] approximates the absolute threshold of hearing using the nonlinear function

$$H_T(f) = 3.64(f/1000)^{-0.8} - 6.5e^{-0.6(f/1000-3.3)^2} + 10^{-3}(f/1000)^4 \text{dB SPL} \qquad (2.6)$$

where f is the frequency in Hz.

[1] This transformation is achieved by substituting all delay elements of the discrete filters by all-pass filters $z^{-1} \rightarrow \frac{z^{-1}-\alpha_f}{1-\alpha_f z^{-1}}$, where α_f is a positive number that determines the amount of frequency warping.

2.3.2 Critical bands

Defining critical bands is an important step in perceptual modeling. A critical band is a band of frequencies that the human auditory system treats similarly. We describe a psychoacoustic experiment to illustrate this phenomenon. Researches have found that the perceived loudness of a narrow band noise source remains at a constant level as the bandwidth of the source is increased up to the critical bandwidth. Physiologically speaking, neurons associated with in band frequencies are tuned together more than neurons associated with the out of band frequencies.

A critical band is characterized by its center frequency and bandwidth that varies along the frequency axis. The width of critical bands increases as frequency increases. Center frequencies and bandwidths of various critical bands had been determined by many researchers with different psychoacoustic experiments [17, 24, 101, 102]. In this dissertation, we use Zwicker's data [102] for the center frequency and bandwidth of a critical band. These values are listed in Table 2.4.

Table 2.4: Parameters of critical bands.

Band No	Center frequency (Hz)	Bandwidth (Hz)
1	50	-100
2	150	100-200
3	250	200-300
4	350	300-400
5	450	400-510
6	570	510-630
7	700	630-770
8	840	770-920
9	1000	920-1080
10	1175	1080-1270
11	1370	1270-1480
12	1600	1480-1720
13	1850	1720-2000
14	2150	2000-2320
15	2500	2320-2700
16	2900	2700-3150
17	3400	3150-3700
18	4000	3700-4400
19	4800	4400-5300
20	5800	5300-6400
21	7000	6400-7700
22	8500	7700-9500
23	10500	9500-12000
24	13500	12000-15500
25	19500	15500-

It can be seen from Table 2.4 that width of critical bands increases progressively. For a normal listener, critical bandwidths can be conveniently approximated as a function of frequency f (Hz) [101] as

$$B_C(f) = 25 + 75\left[1 + 1.4(f/1000)^2\right]^{0.69} \text{ Hz} \tag{2.7}$$

Critical bands can also be treated as a nonuniform filter bank that is a set of band pass filters with bandwidths shown in Table 2.4. A band pass filter improves the signal-to-noise ratio by removing out-of-band noise. This improves hearing ability of listeners in noisy environments [17, 103]. A width of one critical band is commonly referred to as "one Bark" in the literature. The following equation is used to convert frequency f in Hz to frequency $H_B(f)$ Bark

$$H_B(f) = 13\text{arctan}(0.00076f) + 3.5\text{arctan}\left(\frac{f}{7500}\right) \text{ Bark} \tag{2.8}$$

2.3.3 Masking and spreading function

Masking is a phenomenon in which a sound renders another sound (usually weaker) inaudible. The sound that renders the maskee inaudible is known as the masker whereas the sound that is inaudible is known as the maskee. Masking can occur in time or in frequency. If a sound masks another sound that occurs at a different time, it is known as temporal masking. Temporal masking can be further categorized into forward and backward masking in which the maskee can occur before or after the masker, respectively. In frequency masking, a sound at a frequency masks sound at another frequency at softer levels than the masker. Frequency masking is used more often in audio signal processing than temporal masking due to the simplicity of its implementation [24, 39, 97].

For the purpose of calculating masking thresholds, it is helpful to distinguish between two types of masking, namely *tone-masking-noise* and *noise-masking-tone* [104, 105]. In the first case, a tone occurring at the center of a critical band masks noise of any subcritical[2] bandwidth if the noise spectrum is below a predictable threshold. In the second case, the nature of the masker and the maskee are reversed. From a psychophysical point of view, this phenomenon can be explained as follows. The presence of a strong noise or tone masker creates an excitation of sufficient strength on the basilar membrane at the critical band location to effectively block transmission of a weaker signal. In addition, interband masking has also been observed, *i.e.* a masker centered within one critical band has some predictable effect on detection thresholds in other critical bands. This effect,

[2]Within a critical band.

also known as the spread of masking, is often modeled by an approximately triangular spreading function which has slopes of $+25$ and -10 dB per Bark. A convenient analytical expression for the spread of masking is given by [24]:

$$S_F(x) = 15.81 + 7.5(x + 0.474) - 17.5\sqrt{1 + (x + 0.474)^2} \quad \text{dB} \tag{2.9}$$

where x has units of Barks and $S_F(x)$ is expressed in dB. After critical band analysis is done and the spread of masking has been accounted for, masking thresholds are established by the following relation [106]

$$T_H^N = E_T - 14.5 - B_C^N \tag{2.10}$$

$$T_H^T = E_N - K_C \tag{2.11}$$

where T_H^N and T_H^T, respectively, are the noise and tone masking thresholds due to tone-masking-noise and noise-masking-tone, E_N and E_T are the critical band noise and tone masker energy levels, and B_C^N is the critical band number. The parameter K_C, has typically been set between 3 and 5 [104]. Masking thresholds are commonly referred to as just noticeable distortion (JND). In Figure 2.7, we show the masked signal below the masking threshold in the shaded area. In Figure 2.7, we consider the case of a single masking tone occurring at the center of a critical band. Physiologically speaking, it can be said that the masking threshold shown in Figure 2.7 is hypothetically the excitation of the tone along the basilar membrane.

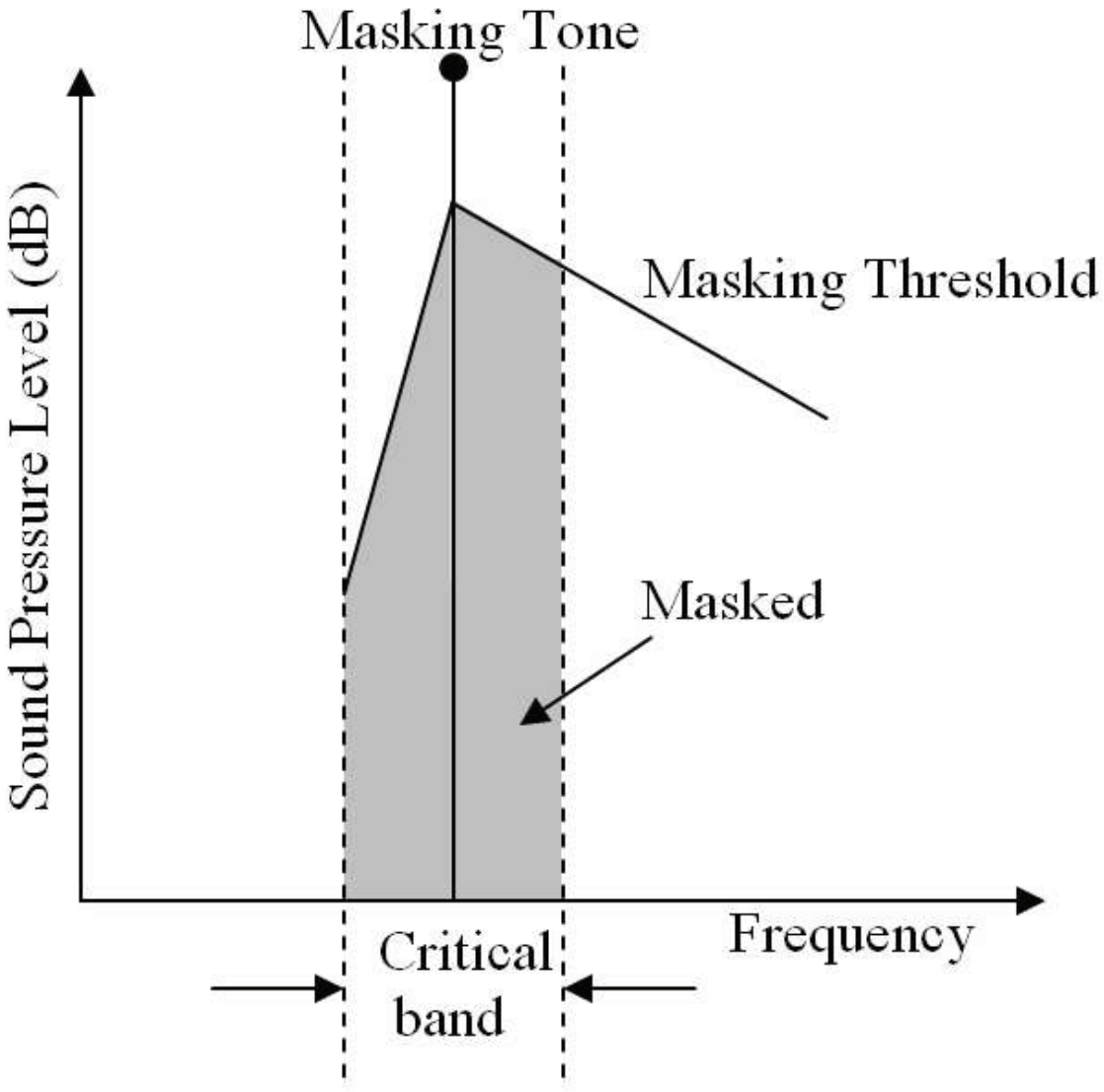

Figure 2.7: Schematic representation of in-band frequency masking due to a tone.

CHAPTER 3

EVALUATION OF VARIOUS DECORRELATORS

Due to the closed loop nature of the hearing aid system, a decorrelator D_c in the forward path, as shown in Figure 3.1, is used to decorrelate the reference signal $x(n)$ from the input signal $u(n)$. The use of a decorrelator can in general improve the adaptive filter estimate of the feedback path. Introducing a delay in the forward path is the most popular decorrelation method employed in hearing aids due to its simplicity [6, 7]. However, there are also several shortcomings to the use of delays as decorrelators. They include slower convergence with longer delays [7], smaller decorrelation of tonal signals in the input signal such as voiced segments in speech [10, 107] and coloration effects at the cochlea for longer delays (usually greater than 4 ms to 8 ms) [10]. Many researchers have proposed the use of additional decorrelators such as adding probe noise [6], frequency shifting [10] and continuous phase shifting [11] along with the delay in the forward path to alleviate some of the above difficulties.

Portions of this chapter are reprinted, with permission, from

- Ashutosh Pandey and V. John Mathews, "Improving adaptive feedback cancellation in digital hearing aids through offending frequency suppression," in *Proc. IEEE Intl. Conf. on Acoustics, Speech and Signal Processing*, vol. 5, Dallas, TX, March 2010, pp. 173-176. ©[2010] IEEE.

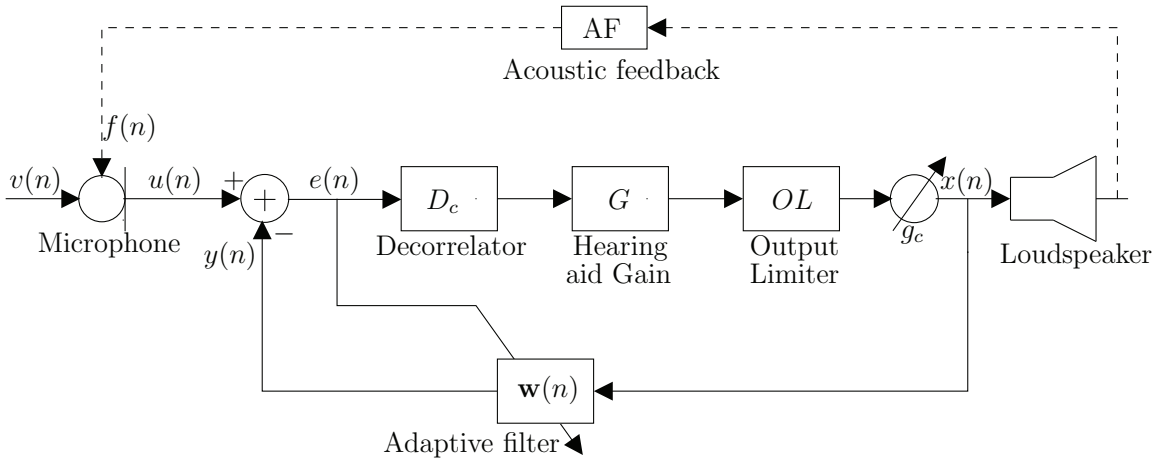

Figure 3.1: Simplified block diagram of a digital hearing aid with adaptive feedback cancellation employing a decorrelator in the forward path.

In this chapter, we present a thorough evaluation of the different methods for decorrelating the reference and primary inputs to the adaptive feedback canceller through MATLAB simulations and subjective tests. Decorrelators studied in this chapter for digital hearing aids are described in Section 3.1. Section 3.2 presents MATLAB simulations and results from subjective evaluations for some of the most popular decorrelators employed in hearing aid systems.

3.1 Decorrelators

Available decorrelators in the literature include adding probe-noise, constant frequency shift, continuous phase shifting, delay in the forward path and delay in the cancellation path [7]. Siqueria *et al.* [7] showed that delays in the forward path were more beneficial than delays in the cancellation path. Moreover, it was shown that power levels of probe noise needed to reasonably reduce the adaptive filter bias were high and degrade the output sound quality (reduced SNR) significantly [7, 11]. Therefore, we do not study the effects of the probe noise and decorrelation delay in the cancellation path in this chapter. Effect of forward path delay values, frequency shifting and phase shifting are explored in this chapter in terms of added stable gain and subjective quality of output sound. Delay in the forward path is implemented with a delay line on the error signal $e(n)$.

3.1.1 Frequency shifting

The frequency shift is employed in the forward path at the error signal $e(n)$ as shown Figure 3.2. In Figure 3.2, h_l is the Hilbert transform operation, N_l is the number of sample delays introduced into the lower path in Figure 3.2 by the Hilbert transform operator and ω_s is the desired frequency

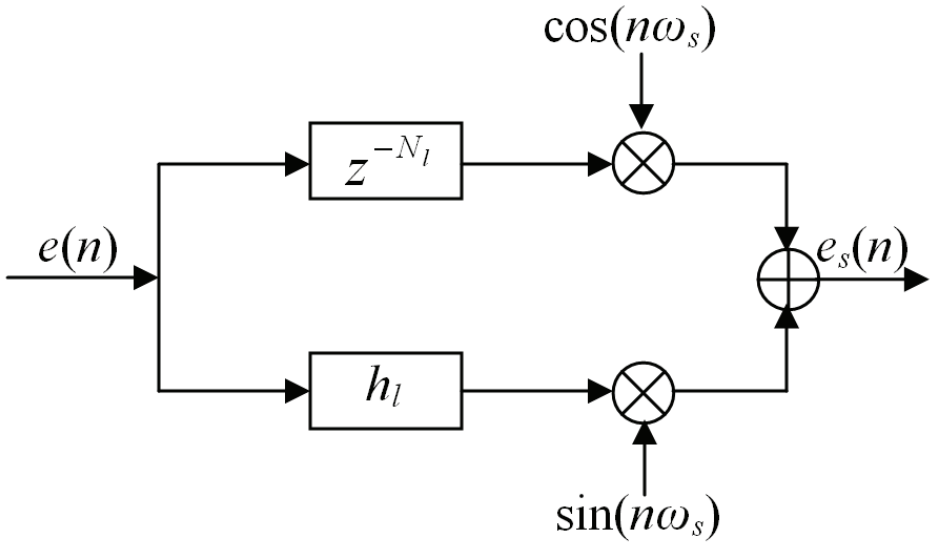

Figure 3.2: The frequency shifter employed in this dissertation.

shift in the spectrum of the error signal $e(n)$. Details can be found in Chapter 8 of [36]. The authors of [10] have argued that shifting the spectrum up to 5 Hz does produce audible artifacts.

3.1.2 Phase modulation

Phase shifting is implemented in the forward path of a hearing aid with a second-order all-pass filter $A_p(z)$ with transfer function

$$A_p(z) = \frac{-d + c(1-d)z^{-1} + z^{-2}}{1 + c(1-d)z^{-1} - dz^{-2}}, \tag{3.1}$$

$$d = \frac{\tan(\omega_d) - 1}{\tan(\omega_d) + 1}, c = -\cos(\omega_c) \tag{3.2}$$

where ω_c controls the center frequency of the phase change and ω_d controls the amount of delay across the center frequency. As ω_d becomes smaller, the transition width of the phase response becomes narrower. The parameters ω_c and ω_d were varied as suggested in [11] to implement the continuous phase shifting and to minimize audible artifacts in the output sound. Specifically, the process of coefficients variation included slow variation of the parameter ω_c between 0.25π and π radians/second and scaling of the parameter ω_d as $\omega_d = (\pi - \omega_c)/2$. The phase shifting was not implemented for the frequency region corresponding $\omega_c = 0 \sim 0.25\pi$ radians/second (low frequencies) to avoid audible artifacts. The scaling was done to reduce amount of delay towards low frequencies and vice versa.

3.2 Results and discussion

This section presents the results from MATLAB simulations of the hearing aid algorithms to demonstrate the performance of the adaptive feedback cancellation with different decorrelators. A subjective evaluation of the output sound quality for all methods from MATLAB simulations is also presented. The sampling frequency f_s used for all experiments was 16000 Hz. In the next set of experiments, the adaptive feedback cancellation (AFC) was performed in MATLAB for the phase modulation and frequency shifting decorrelator along with forward path delay values of 2 ms, 4 ms and 8 ms. Only the 2 ms delay was used with the frequency shifting and phase modulation decorrelators to evaluate additional benefits provided by these decorrelators.

The true feedback path was simulated using a 192-tap FIR filter in parallel with a homogeneous quadratic degree of nonlinearity. The nonlinearity simulates the nonlinear distortions in the loudspeakers and A/D converters in a hearing aid system. The harmonic signal strength was 40 dB below that of the output of the linear component. Coefficients for the linear component

of the feedback path were obtained from measurements of an inside-the-ear (ITE) hearing aid. The critical gain for the acoustic feedback model used in this chapter was 36.4 dB. The feedback canceller employed a linear FIR system model with 128 coefficients. This undermodeling attempts to capture the practical situation where it is very difficult to exactly model the feedback path in the system. Other parameters used in the adaptive filter were $\alpha = 0.001$ and $\epsilon = 10^{-3}$. The output signal $x(n)$ was clipped if the level became greater than 80 dBu.

A frequency shifting of -3 Hz was used for the frequency shift decorrelator. The frequency shifting was implemented using a 33-tap Hilbert transformer designed with the MATLAB filter design toolbox. For the phase shift decorrelator, the parameter ω_c was modulated by $0.0002 f_s$ as suggested in [11]. The input signals to the hearing aid were clean speech waveforms taken from the TIMIT database. Colored noise samples, with the power spectral density reducing at the rate of 3 dB per octave as frequency increases, were added to the input signal to create the signal-to-noise ratio of 40 dB. This noise model was chosen to represent the hardware noise due to circuits/sensors in the hearing aid.

To evaluate effectiveness of various decorrelators, adaptive feedback cancellation was performed at several different hearing aid gain values for all the decorrelators. The initial value of hearing aid gain was set to 20 dB below the target gain. Subsequently, the gain was slowly increased for 20 seconds at the rate of 1 dB/second to reach the target gain level. The adaptive feedback cancellation experiment ran for 80 seconds in each case. The last 10 seconds of the experiment were deemed as the steady state. The performance indicators from the steady state were used to judge performances of various schemes. The performance indicators are the average misalignment (MSL) in the adaptive filter estimates during the steady state, and subjective ratings of residual feedback components and loudness of the steady state output signal on a scale of $0 - 5$, as described in Table 3.1.

Loudness ratings refer to the volume of the words in each sentence. The misalignment in dB at time n is calculated from the estimated adaptive coefficients vector $\mathbf{w}(n)$ and the first N coefficients

Table 3.1: Description of user ratings for feedback and loudness.

Ratings	Feedback	Loudness
0	Loud howling	Inaudible
1	Loud continuous whisting	Soft
2	Soft continuous whistling	Somewhat soft
3	Soft intermittent whistling	Comfortable
4	No audible feedback, acceptable quality	Somewhat loud
5	No audible feedback, good quality	Extremely loud

of the linear component of the true feedback path coefficients vector $\mathbf{h}_p(n)$ as

$$\text{misalignment(dB)} = 20\log\frac{\|\mathbf{w}(n) - \mathbf{h}_p(n)\|_F}{\|\mathbf{h}_p(n)\|_F} \tag{3.3}$$

where $\|.\|_F$ is the Frobenius norm of a vector. Five subjects participated for subjective evaluations and they rated each system's output on 6 speech signals. During the test, the recorded speech signals were played in a random order through a loudspeaker in a quiet environment.

The performance indicators for all the schemes for 7 distinct gain values are summarized in Table 3.2. In Table 3.2, the misalignment value of 0, the feedback rating of 0 or the loudness rating of 5 indicate that the system went into instability for that hearing aid gain. The subjective ratings of residual feedback and loudness for the input signal to the hearing aid were 4.34 and 3.08, respectively. The following conclusions can be drawn based on performance indicators in Table 3.2. First, the adaptive filter estimate got better (misalignment reduced) as the hearing aid gain increased for all methods when the hearing aid system was stable. However, the output sound quality deteriorated as indicated by the feedback ratings for traditional methods. Moreover, at higher gains (greater than 47 dB), the misalignment increased for traditional decorrelation methods. This is because there were tonal signals due to residual feedback components in the forward path that deteriorated the performance of the adaptive filter.

The results of Table 3.2 also suggest that the adaptive filter estimate got better with increase in the forward path delay and with the use of the phase and frequency shifter. Nonetheless, this did not translate into additional hearing aid gains when compared to a 2 ms delay with no additional decorrelator employed. The frequency shifting was the most effective decorrelator in terms of reducing misalignment. The phase shifter provided higher gains than the use of forward path delay alone. This was possible because changing phase in the forward path reduced the buildup of some acoustical feedback components in successive iterations. However, the output sound quality at the higher gain values was rated below acceptable levels. The phase shifter yielded slightly better output sound quality at gain values of 45 dB, 47 dB and 49 dB than the other approaches.

Table 3.2: Performance indicators for different schemes.

Gain (dB)		45	47	49	51	53	55	57
Delay 2 ms	MSL	-13.3	-19.0	-22.7	-22.1	0	0	0
	Feedback	3.9	3.68	2.57	2.45	0	0	0
	Loudness	3.24	3.27	3.72	3.91	5	5	5
Delay 4 ms	MSL	-16.0	-22.3	-22.5	-21.4	0	0	0
	Feedback	3.88	3.55	2.23	1.98	0	0	0
	Loudness	3.23	3.21	3.69	4.02	5	5	5
Delay 8 ms	MSL	-23.7	-29.6	-27.9	0	0	0	0
	Feedback	3.85	3.62	2.16	0	0	0	0
	Loudness	3.19	3.24	3.92	5	5	5	5
Freq. shift	MSL	-24.5	-29.6	-28.0	0	0	0	0
	Feedback	3.95	3.56	2.81	0	0	0	0
	Loudness	3.21	3.13	3.73	5	5	5	5
Phase shift	MSL	-22.3	-27.5	-27.8	-25.8	0	0	0
	Feedback	4.04	3.78	3.04	2.19	0	0	0
	Loudness	3.14	3.12	3.46	3.78	5	5	5

CHAPTER 4

ADAPTIVE GAIN PROCESSING WITH OFFENDING FREQUENCY SUPPRESSION

This chapter presents algorithms to modify the forward path gain in digital hearing aids to provide additional amplification and better output sound quality. This approach employs a variable, frequency-dependent gain function that is lower at frequencies of the incoming signal where the information is perceptually insignificant. We refer to this as adaptive gain processing in this dissertation. In addition, this chapter presents a method that automatically identifies and suppresses residual acoustical feedback components at frequencies that have the potential to drive the system to instability. This is termed offending frequency suppression in this dissertation. The suppressed frequency components are monitored and the suppression is removed when such frequencies no longer pose a threat to drive the hearing aid system into instability.

Portions of this chapter are reprinted, with permission, from

- Ashutosh Pandey, V. John Mathews and Michael Nilsson, "Adaptive gain processing to improve feedback cancellation in digital hearing aids," in *Proc. IEEE Int. Conf. on Acoustics, Speech and Signal Processing*, vol. 5, Las Vegas, NV, April 2008, pp. 357-360.

- Ashutosh Pandey and V. John Mathews, "Improving adaptive feedback cancellation in digital hearing aids through offending frequency suppression," in *Proc. IEEE Int. Conf. on Acoustics, Speech and Signal Processing*, vol. 5, Dallas, TX, March 2010, pp. 173-176.

- Ashutosh Pandey and V. John Mathews, "Offending frequency suppression with a reset algorithm to improve feedback cancellation in digital hearing aids," in *Proc. IEEE Int. Conf. on Acoustics, Speech and Signal Processing*, vol. 5, Prague, Czech, May 2011.

- Ashutosh Pandey and V. John Mathews, "Adaptive gain processing with offending frequency suppression for digital hearing aids," submitted to *IEEE Trans. on Audio, Speech and Language Processing*, Dec. 2010.

The rest of the chapter is organized as follows. The gain processing methods - adaptive gain processing and offending frequency suppression with the reset algorithm to remove offending frequency suppression filters are presented and discussed in Section 4.1. In Section 4.2, the performance of both gain processing algorithms is evaluated and compared in MATLAB as well as from real time implementations.

4.1 Hearing aid gain processing methods

In the traditional system described in Section 2.2.2, the hearing aid gain in the forward path does not change over time. The methods of this chapter alter the hearing aid gain in the forward path with the hearing aid gain values and parametric EQ filters. A block diagram of the new scheme employing the gain processing methods of this chapter is shown in Figure 4.1. First, the system applies adaptive gain processing (AGP) by calculating the masking thresholds from the target amplified signal $\mathbf{Q}(m)$, and uses that to modify the gain values in the each subband. The modified gain values are referred to as $\mathbf{g}^a(m)$. The modified gain values $\mathbf{g}^a(m)$ and prescribed gain values $\mathbf{g}(m)$ are also used to modify step size for NLMS adaptation. The details of modifying gain values $\mathbf{g}^a(m)$ and step size control are presented in Section 4.1.1.

Second, the new scheme identifies potential offending frequencies from the microphone signal. The forward path gain is reduced in narrowband frequency bands at those frequencies using parametric EQ filters, as shown in Figure 4.1. The change in offending frequencies is monitored with a reset algorithm that uses subband adaptive filter coefficients $w_i(m)$. The offending frequency suppression (OFS) and the reset methods are described in Section 4.1.2.

4.1.1 Adaptive gain processing

The adaptive gain processing (AGP) utilizes the information about masking thresholds in the target amplified signal. We describe the steps involved in finding the masking thresholds in Section 4.1.1.1. Gain and step size control schemes that result in low artifacts and low distortions in the output signals are discussed later in the section.

4.1.1.1 Calculation of masking thresholds

Masked signal components are considered as "'irrelevant information" and it is shown in literature that even well trained human ears do not hear these components. In this chapter, we do not consider the contribution of temporal masking because it is usually difficult to quantify [17]. Spectrally masked components used in this chapter are identified with psychoacoustic principles such as absolute hearing thresholds, critical band frequency analysis and the spreading function.

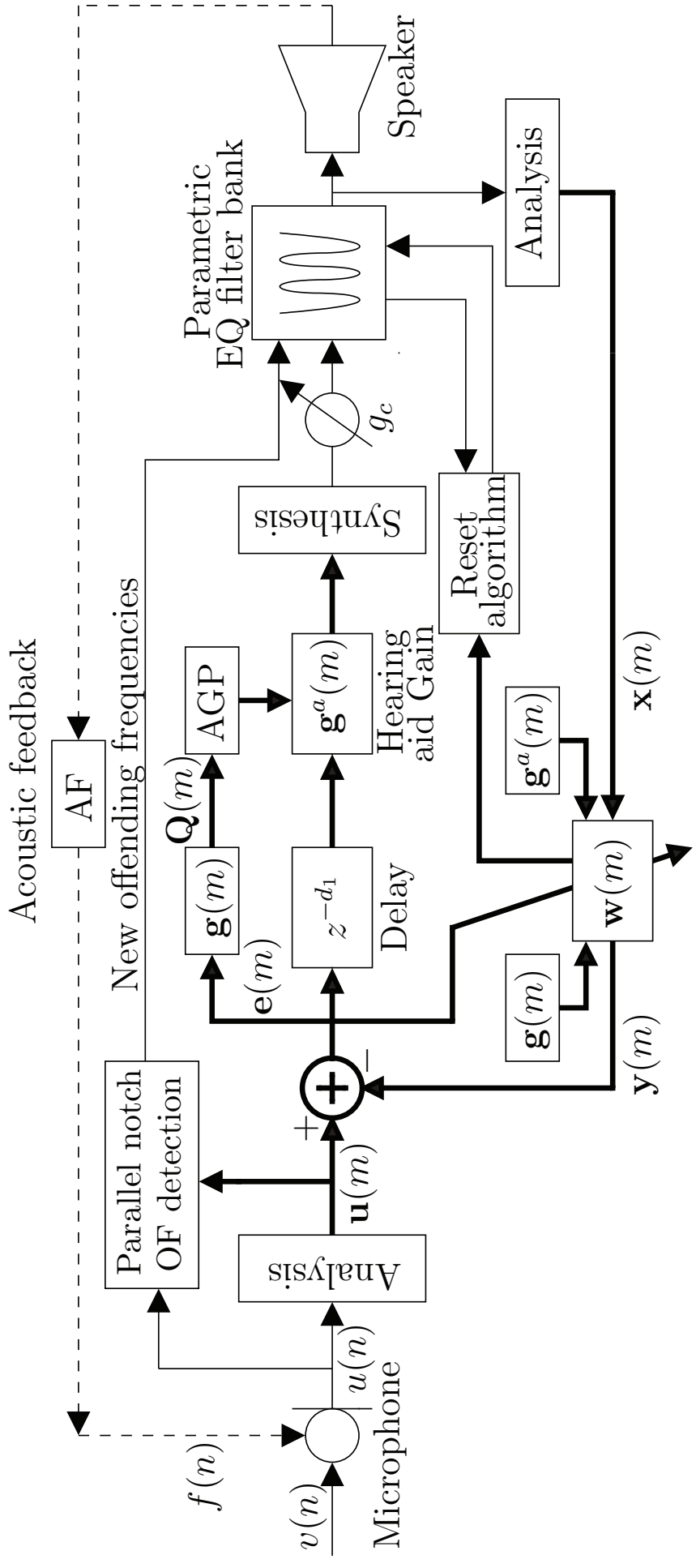

Figure 4.1: Simplified block diagram of a digital hearing aid employing AGP and OFS along with adaptive feedback cancellation.

Calculation of the masking thresholds $T_i(m)$ for the m^{th} frame and i^{th} subband involves defining critical bands on the power spectrum $P_i(m)$ of the speech signal. The power spectrum is calculated from the spectrum of the target amplified signal $Q_i(m)$ using speech pressure level (SPL) normalization [24]. Subsequently, tonal and noise maskers are identified in each critical band which are above the hearing threshold [17, 24, 102]. If two or more maskers are close to each other in a critical band, only the strongest masker is kept and others are discarded. Details of the masking model and estimation of the maskers can be found in [24, 108]. After identifying the maskers, the masking effects due to these maskers are calculated using a spreading function [102]. Finally, the global masking threshold $T_i(m)$ is calculated for each subband by combining the individual masking thresholds of all the maskers identified in the previous steps.

4.1.1.2 Gain adjustment with $T_i(m)$

The adaptive gain processing algorithm reduces the hearing aid gain at subbands where the instantaneous signal energy ($|Q_i(m)|^2$) is below the global masking threshold $T_i(m)$. However, a large reduction in the gain may produce artifacts due to aliasing [13]. Consequently, the algorithm reduces the gain by no more than some preselected fraction η, where $0 < \eta < 1$ from frame to frame. Similarly, we also limit the minimum gain at a frequency to avoid unnatural artifacts in the output. The adaptive gain processing maintains the gain to prescribed levels as soon as the signal strength is above the masking threshold. It must be mentioned that the AGP increases the hearing aid gain to prescribed levels as soon as the signal strength is above the masking threshold in the current frame irrespective of the gain value in the previous frame. We have not experienced any artifacts due to sudden changes; however, a gradual increase in gain similar to what is employed for reducing the hearing aid gain can be used if needed. The algorithm for varying the gain $g_i^a(m)$ is summarized in Table 4.1.

Table 4.1: Adaptive gain processing

Initialization

$g_i^a(0) = g_i(0)$ ... for each subband i

Gain update

$$p_i^r(m) = \begin{cases} 0 & \text{if } |Q_i(m)|^2 < T_i(m) \\ 1 & \text{else} \end{cases}$$

$$g_i^a(m) = p_i^r(m) g_i(m) + (1 - p_i^r(m)) \eta g_i^a(m-1)$$

$$g_i^a(m) = \max[g_i^a(m), \eta_m g_i(m)]$$

In Table 4.1, $\eta_m < 1$ is a positive constant that determines the minimum permissible gain based on the prescribed gain value $g_i(m)$ for the i^{th} subband.

4.1.1.3 Step size control for adaptive gain processing

It is intuitive to see that the better the adaptive filter estimates the feedback path, the more stable is the hearing aid system. Interestingly, for fixed step size α, the error between the adaptive filter estimate and the true feedback path in a hearing aid system shown in Figure 2.6 depends on the hearing aid gain [3, 13]. Let us define the coefficient error vector in the adaptive filter estimate for band i at time m as

$$\widetilde{\mathbf{w}}_i(m) = \mathbf{h}_i - \mathbf{w}_i(m) \tag{4.1}$$

where $\mathbf{h}_i = \begin{bmatrix} h_i^0 & h_i^1 & \cdots & h_i^{N_s-1} \end{bmatrix}^T$ represents true feedback path coefficient vector for band i. For the derivations, we assume the feedback path is time-invariant. The steady state misalignment $E[|\tilde{w}_i|^2]$ is approximated by $\frac{\alpha}{2g_i^2(m)}$ as shown in [3]. In fixed gain systems, the gain value $g_i(m)$ is constant over time. Consequently, the steady state misalignment does not change. However, the adaptive gain processing varies the subband gain values $g_i^a(m)$ depending on the input signal. If the hearing aid gain is reduced in a band, the error in the adaptive filter estimate (misalignment) will increase. Subsequently, if the gain is increased suddenly in that band, the adaptive filter will take sometime to adapt to the new (better) estimate. In order to avoid the readaptation of adaptive filter, we vary the adaptation parameter to keep the misalignment independent of the hearing aid gain change due to the adaptive gain processing. The variable adaptation parameter $\alpha_i^a(m)$ is based on the current hearing aid gain value $g_i^a(m)$ and prescribed hearing aid gain value $g_i(m)$. This scheme will avoid additional error in the adaptive filter coefficients when hearing aid gain is reduced for a short period of time. Based on the above two gain values, the adaptation parameter $\alpha_i^a(m)$ and the NLMS update for band i at time m for the adaptive gain processing is done as shown in Table 4.2.

Table 4.2: Update equations for a subband-based adaptive feedback cancellation system employing the adaptive gain processing.

$$\alpha_i^a(m) = \alpha \left(\frac{g_i^a(m)}{g_i(m)} \right)^2$$
$$\mu_i^a(m) = \frac{\alpha_i^a}{\|\mathbf{x}_i(m)\|^2 + \zeta}$$
$$\mathbf{w}_i(m+1) = \mathbf{w}_i(m) + \mu_i^a(m) e_i(m) \mathbf{x}_i(m)$$

4.1.2 Offending frequency suppression

The offending frequency suppression method presented in this chapter identifies offending frequencies that are likely to drive the hearing aid system into instability and uses parametric EQ filters [27, 109] to reduce gain at those frequencies. The acoustic feedback components are known to grow steadily in successive time intervals whereas the audio components behave otherwise. Therefore, if energy in a subband is increasing in successive time intervals, it is likely that there exists an offending frequency within the frequency range of that subband. The offending frequency within that subband is accurately estimated with an adaptive notch filter whose center frequency is constrained to the frequency range of the subband. Adaptive notch filters can identify offending frequencies because they behave like tonal signals [25, 110–113].

At high gains, as the hearing aid system nears unstable behavior, the energy in the signal components at and around the offending frequencies increases in the forward path of the hearing aid and creates spectral peaks. The adaptive notch filter (ANF) tracks and identifies such spectral peaks. In the presence of such spectral peaks, the ANFs will converge to the offending frequencies and stay in their vicinities till the energy in such spectral components reduces. The variability of the coefficients of the ANF will be smaller when the system is tracking a strong frequency component than when the input signal does not contain strong spectral peaks.

The adaptive notch filters can also be implemented in the subband without loss of performance. However, we chose to implement the ANFs in the fullband. M adaptive notch filters are used to monitor frequency ranges for M subbands. Similarly, M energy growth monitoring values, one from each subband, are used for detection of an offending frequency. The detection method immediately starts to look for another offending frequency after detection of an offending frequency in a subband. More details are provided in Section 4.1.2.1. Upon detection of an offending frequency, a parametric EQ filter is used to suppress it. The parametric EQ filter employed in this work is a second-order IIR filter that is specified by three parameters - the center frequency f_p, the depth of suppression $p < 1$ and the quality factor q [114, 115]. The parameters p and q are fixed in our implementation whereas the parameter f_p is derived from the adaptive notch filter. Coefficients of the parametric EQ filter in the discrete-time domain with the transfer function

$$H_{EQ}(z) = \frac{b_0 + b_1 z^{-1} + b_2 z^{-2}}{a_0 + a_1 z^{-1} + a_2 z^{-2}} \tag{4.2}$$

can be calculated from the parameters p, q and f_p as given in Table 4.3. The variable f_s in Table 4.3 represents the sampling frequency.

Table 4.3: Calculation of the coefficients of the EQ filters.

$$K = \tan(\frac{2\pi f_p}{f_s}),\ \beta = 1 + K/q + K^2$$
$$b_0 = \frac{1 + pK/q + K^2}{\beta},\ b_1 = \frac{2(K^2 - 1)}{\beta},\ b_2 = \frac{1 - pK/q + K^2}{\beta}$$
$$a_0 = 1.0,\ a_1 = \frac{2(K^2 - 1)}{\beta},\ a_2 = \frac{1 - K/q + K^2}{\beta_i}$$

4.1.2.1 Detection of offending frequencies

As stated earlier, the offending frequencies are detected independently for each subband. In this section, we explain offending frequency detection in the ideal frequency range of the i^{th} subband - [f_i^l, f_u^l], where $f_i^l = \frac{2\pi i}{M}$ is the lower frequency and $f_i^u = \frac{2\pi(i+1)}{M}$ is the upper frequency of the band $i, i = 0 \cdots M-1$. By monitoring frequency ranges associated with all subbands, we can detect any offending frequency occurring in the operating frequency range of the hearing aid.

The energy growth monitoring and ANF tracking for the i^{th} frequency range (f_i^l to f_i^u) work independently in the subband and fullband, respectively. The energy growth monitoring is performed for each subband microphone signal $u_i(m)$ whereas the adaptive notch filter works with the fullband microphone signal $u(n)$. Let the microphone signal energy in band i at time m be $P_i^u(m) = \mathbf{u}^T(m)\mathbf{u}(m)$, where $\mathbf{u}_i(m) = \begin{bmatrix} u_i(m) & u_i(m-1) & \cdots & u_i(m-N_s+1) \end{bmatrix}^T$. The relative change in the microphone energy between two successive time intervals $P_i^{\Delta}(m)$ defined as

$$P_i^{\Delta}(m) = \frac{P_i^u(m) - P_i^u(m-1)}{P_i^u(m-1)}$$

along with the estimated microphone signal energy $P_i^u(m)$ and the estimated background noise signal power $P_i^b(m)$ are used by the counter $\gamma_i^r(m)$ to monitor the energy growth for the i^{th} subband at time m. Larger values of the counter $\gamma_i^r(m)$ makes the band i more probable to contain an offending frequency.

The counter is incremented if the microphone signal $P_i^u(m)$ is at least T_b times larger than the background noise power[1] $P_i^b(m)$ for band i. Otherwise, it is reset to 0 to indicate that the system is stable. If the energy in the microphone signal is higher than the predetermined multiple of the the background noise power and the energy in the microphone signal at time m is greater than

[1]In this chapter, the background noise is estimated with the minimum statistics method according to [116]. In Table 4.4, the constant $\delta_b > 1$ is the slow rising constant, λ_u is an averaging constant and $\overline{P_i^u}(m)$ is the average microphone signal for band i at time m. These quantities are required in the minimum statistics method.

the energy at time $m-1$, *i.e.* the relative change in the energy $P_i^{\Delta}(m)$ is positive, the energy growth counter value is incremented by $\Gamma_u > 0$. On the other hand, the energy growth counter $\gamma_i^r(m)$ is reduced by an amount $\Gamma_l < 0$, if the relative change is smaller than a predetermined negative constant ν_l. This is because sudden decrease in the energy is not a characteristics of the acoustic feedback components at the onset of instability. Additionally, if the relative change in energy $P_i^{\Delta}(m)$ is negative, however the change is small, say $\nu_u < 0$, the energy growth counter is still increased by Γ_u. This is because a small change in energy may indicate early stages of howling [117]. In other situations, where the relative change in energy $P_i^{\Delta}(m)$ lies between ν_l and ν_u, the energy growth counter is modified with a number that is linear interpolation between Γ_l and Γ_u. The amount of change in the energy growth counter at time m for a given $P_i^{\Delta}(m)$ is defined by a function $\Phi(P_i^{\Delta}(m))$ as

$$\Phi(P_i^{\Delta}(m)) = \begin{cases} \Gamma_u & ;\ P_i^{\Delta}(m) > \nu_u \\ \Gamma_l & ;\ P_i^{\Delta}(m) < \nu_l \\ \frac{\Gamma_u - \Gamma_l}{\nu_u - \nu_l}(P_i^{\Delta}(m) - \nu_l) + \Gamma_l & ;\text{otherwise} \end{cases}$$

The complete energy growth calculation is described in Table 4.4. It is easy to see from Table 4.4 that if the microphone signal $P_i^u(m)$ is sufficiently above (T_b times) the noise floor $P_i^b(m)$ and the relative change in energy is positive or close to zero in successive time indexes, the energy growth counter $\gamma_i^r(m)$ grows. On the other hand, if it is relatively negative ($< \nu_u$), the energy growth counter will tend to a minimum value γ_m^r. If the energy growth counter $\gamma_i^r(m)$ exceeds a predetermined threshold T_r, one of the two criteria for band i to have an offending frequency is fulfilled. The other criterion is determined using adaptive notch filters as described in the following text.

The microphone signal $u(n)$ in Figure 4.1 is used as the input signal to the adaptive notch filter for calculating the center frequency for each parametric EQ filter employed to suppress an offending frequency. In addition, the adaptive notch filters are also used to detect onset of instability along with the energy growth counters. We employ a second-order notch filter with input-output relationship of the form

$$H_a(z) = \frac{1 - a(n)z^{-1} + z^{-2}}{1 - \rho a(n)z^{-1} + \rho^2 z^{-2}} \tag{4.3}$$

to suppress the offending frequencies for band i. The ANF adjusts to the center frequency of the notch filter by adjusting parameter $a_i(n)$ such that at time n, the output power of the notch filter $z_i(n)$ is reduced [25]. The parameter $a_i(n)$ is constrained to adapt between $[2\cos(2\pi f_i^u), 2\cos(2\pi f_i^l)]$ to track the frequency range of the i^{th} subband - $[f_i^l, f_i^u]$. The update equations for the

Table 4.4: Adaptive notch filtering and detection for frequencies in the i^{th} band.

Adaptive notch filter update

$$s_i(n) = u(n) + \rho a_i(n-1)s_i(n-1) - \rho^2 s_i(n-2)$$

$$z_i(n) = s_i(n) - a_i(n-1)s_i(n-1) + s_i(n-2)$$

$$P_i(n) = \lambda_s P_i(n-1) + (1-\lambda_s)s_i^2(n-1)$$

$$a_i(n) = a_i(n-1) + \frac{\alpha_a}{P_i(n)+\epsilon_a} s_i(n-1)z_i(n)$$

$$a_i(n) = \begin{cases} 2\cos(2\pi f_i^l) & ; a_i(n) > 2\cos(2\pi f_i^l) \\ 2\cos(2\pi f_i^u) & ; a_i(n) < 2\cos(2\pi f_i^u) \\ a_i(n) & ;\text{otherwise} \end{cases}$$

ANF tracking monitor

$$a_i^m(n) = \lambda_m a_i^m(n-1) + (1-\lambda_m)a_i(n)$$

$$\gamma_i^a(n) = \begin{cases} \gamma_i^a(n-1)+1 & ; |a_i(n) - a_i^m(n)| < \delta_q \\ 0 & ;\text{otherwise} \end{cases}$$

Energy growth monitor

$$P_i^u(m) = \mathbf{u}^T(m)\mathbf{u}(m)$$

$$\overline{P_i^u}(m) = \lambda_u \overline{P_i^u}(m-1) + (1-\lambda_u)P_i^u(m)$$

$$P_i^b(m) = \min(\delta_b P_i^b(m-1), \overline{P_i^u}(m))$$

$$\gamma_i^r(m) = \begin{cases} \gamma_i^r(m-1) + \Phi(P_i^\Delta(m)) & ; P_i^u(m) > T_b P_i^b(m) \\ 0 & ;\text{otherwise} \end{cases}$$

$$\gamma_i^r(m) = \max(\gamma_i^r(m), \gamma_m^r)$$

Offending frequency detection (when $n = Lm$)

if$\gamma_i^a(n) > T_a$ and $\gamma_i^r(m) > T_r$

$\Rightarrow$ Offending frequency detected

$\Rightarrow$ Add a parametric EQ at $\frac{1}{2\pi}\cos^{-1}(a(n)/2)$

$\Rightarrow \gamma_i^a(n) = 0, \gamma_i^r(m) = \gamma_m^r$

adaptive notch filter realized in direct-form II are summarized in Table 4.4. In Table 4.4, λ_s is a suitable averaging constant, α_a is the step size for adaptation and ϵ_a is a small positive constant to prevent singularities. The second parameter we employ to detect onset of instability is the variability of the coefficients of the notch filter. It has been observed [117] that the adaptive filters coefficients show little variability in the presence of the strong tonal signals. The variability of the parameter $a_i(n)$ from the mean of its past values $a_i^m(n)$ is monitored with a counter $\gamma_i^a(n)$.

The mean $a_i^m(n)$ is estimated by averaging past values of $a_i(n)$ with a single pole IIR filter with an averaging constant λ_m. If the parameter $a_i(n)$ does not vary significantly from its mean as determined by a preselected threshold δ_q, the counter $\gamma_i^a(n)$ grows; otherwise it is reset to

0. If the counter $\gamma_i^a(n)$ gets larger than a predetermined threshold T_a, and the energy growth counter $\gamma_i^r(m)$ becomes larger than a predetermined threshold T_r, the system determines that the hearing aid may go unstable (howl) at or around the notch frequency. When both thresholds are exceeded, a parametric EQ filter whose center frequency is derived from the current value of $a_i^m(n)$ as $\frac{1}{2\pi}\cos^{-1}(a_i^m(n)/2)$ is applied to the output signal and the counters $\gamma_i^a(n)$, $\gamma_i^r(m)$ are reset to 0.

4.1.2.2 Resetting offending frequency suppression filters

The offending frequency suppression method places parametric EQ filters to suppress offending frequencies when they are detected. In practice, new offending frequencies appear because the acoustic feedback path of the hearing aid and the signal characteristics change [41]. The feedback path of the hearing aid changes if a person moves closer to a reflective surface, brings a telephone receiver close to the face plate of a hearing aid, wears a hat *etc.* While new offending frequencies will appear inevitably during the operation of a hearing aid, it is possible that some of the old offending frequencies are no longer problematic. In other words, if parametric EQ filters at those old frequencies are removed from the loop, the system will not go into instability.

Traditionally, commercial offending frequency suppression methods in PA systems employ periodic reset of offending frequencies to remove unnecessary parametric EQ filters. In this chapter, we use analysis of the adaptive filter coefficients to reset offending frequencies - remove the parametric EQ filters. Furthermore, we monitor each subband independently to track the changes in different frequency regions. The reset method calculates relative change in the current adaptive filter estimate from its older estimates. If the relative change between the current and old estimates is small, we assume no change in the feedback path. Therefore, offending frequencies are not modified. On the other hand, if the change is larger than a predetermined threshold, the offending frequencies are reset - parametric EQ filters are removed.

The reset algorithm uses two measurements of the adaptive filter coefficients $\mathbf{w}_i(m)$. First, a long-term average $\mathbf{L}_i(m)$ of the coefficients for the i^{th} band at time m is estimated using a single pole IIR filter with averaging constant $\lambda_l, 0 < \lambda_l < 1$. This is treated as a measure of the past stable path of the feedback path at time m. A short-term average $\mathbf{M}_i(m)$ of the adaptive filter coefficients for the i^{th} band at time m is also estimated with an averaging constant λ_h where the averaging constant is such that $0 < \lambda_h < \lambda_l < 1$. The short-term average is treated as a measure of the current state of the feedback path. If the distance between the short-term average differs significantly from the long-term average for a few iterations, say T_o, the system assumes that the feedback path has changed for that band. In this event, any parametric EQ filters that fall in the frequency range of that band are removed. The reset algorithm for the i^{th} band at time m is listed in

Table 4.5: Monitoring i^{th} band to estimate change in the feedback path.

Initialization

$\mathbf{L}_i(0)$ ... A column vector of length N_s with all zeros
$\mathbf{M}_i(0)$ ... A column vector of length N_s with all zeros
$\gamma_i^o(0)$ ... 0

Reset algorithm

$$\mathbf{L}_i(m) = \lambda_l \mathbf{L}_i(m-1) + (1-\lambda_l)\mathbf{w}_i(m)$$
$$\mathbf{M}_i(m) = \lambda_h \mathbf{M}_i(m-1) + (1-\lambda_h)\mathbf{w}_i(m)$$
$$\mathbf{D}_i(m) = \mathbf{L}_i(m) - \mathbf{M}_i(m)$$
$$\kappa_i(m) = \frac{\mathbf{D}_i^T(m)\mathbf{D}_i(m)}{\mathbf{L}_i^T(m))\mathbf{L}_i(m) + \epsilon_r}$$
$$\gamma_i^o(m) = \begin{cases} \gamma_i^o(m-1)+1 & ; \kappa_i(m) > \delta_o \\ 0 & ;\text{otherwise} \end{cases}$$

Detection

if $\gamma_i^o(n) > T_o$
$\Rightarrow$ Remove all parametric EQs between frequencies f_i^l and f_i^u

Table 4.5. In Table 4.5, $\mathbf{D}_i(m)$ is the distance vector and $\kappa_i(m)$ is the normalized distance between the long-term and short-term average measurements. The normalized distance $\kappa_i(m)$ remains close to 0 if the feedback path is relatively stationary and increases in magnitude when there are changes in the feedback path. The variable $\gamma_i^o(m)$ counts the number of times the normalized distance has been more than a predetermined threshold δ_o to trigger reset process.

4.2 Results and discussion

This section presents the results from MATLAB simulations and real time implementations of the hearing aid algorithms to demonstrate the performance of the chapter's gain processing approaches and the classical scheme described in Section 2.2.2 with fixed gain function. Both methods were evaluated in terms of output sound quality and added stable gain. The true feedback path was simulated using a 192-tap FIR filter in parallel with a homogeneous quadratic nonlinearity. The nonlinearity simulates the nonlinear distortions in the loudspeakers and A/D converters in a hearing aid system. The harmonic signal strength was 40 dB below that of the output of the linear component. Coefficients for the linear component of the feedback paths were obtained from measurements of an inside-the-ear (ITE) hearing aid.

The ITE hearing aid consisted of two FG-3653 omni-directional microphones and a receiver. The output of the microphones and input to the receiver were available at the face plate of the

hearing aid as CS44 plugs. We used a standard EXPRESSfit hearing aid programming cable to drive and access microphones and the speaker of the hearing aid. The programming cable was connected to an interface board through an 8-pin mini-DIN plug that provided the required power to the programming cable and amplified the signals. Two feedback paths were used in the experiments. In estimating the feedback paths, the ITE hearing aid was fitted into the earpiece of a Knowles Electronic Manikin for Acoustic Research (KEMAR) that was placed in a quiet location. A large white board on a stand was placed parallel to the face plate of the ITE hearing aid at different distances to create different feedback paths. The white board worked as a reflective surface and was chosen to see the effect of reflective surfaces on the hearing aid feedback paths. The reflective surface was 100 cm and 5 cm away for the first and second feedback path, respectively. Impulse and magnitude responses of the two feedback paths are shown in Figure 4.2.

The feedback canceller employed a linear FIR system model with 128 coefficients. This undermodeling and the model mismatch attempt to capture the practical situation where it is very difficult to exactly model the feedback path in the system. Our prior work has indicated similar levels of performance during simulation and real-time implementations of other hearing aids. The signal processing was done at a sampling rate of $f_s = 16000$ Hz in all experiments in this section.

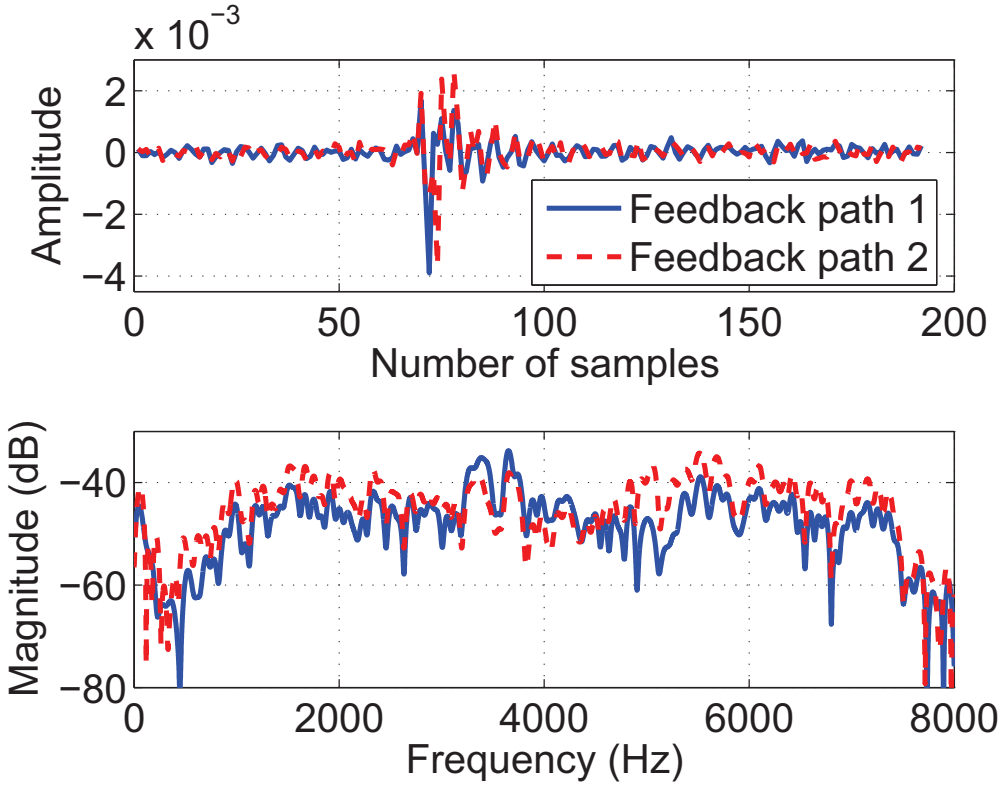

Figure 4.2: Impulse and magnitude responses of the two feedback path models used in the simulations.

Parameters of the subband design were $M = 128, L = 16$ and $L_p = 128$. Parameters for the adaptive feedback cancellation were $\alpha = 0.001$, $d_1 = 0$, $g_c = 1$ and $\zeta = 10^{-7}$. Parameters for the hearing aid gain processing were $\eta = 0.95$ and $\eta_m = 0.1$.

The speech input signals to the hearing aid in experiments were 6 clean speech waveforms of length 80 seconds taken from the TIMIT database. The peak value of the speech input signals used in experiments was approximately -6 dBu. In experiments where music signals were used, 6 music waveforms of length 80 seconds from the album "18 till I die" by Bryan Adam were chosen. The music signals were resampled at 16000 Hz for the experiments in this chapter. The gain of each music file was adjusted so that the peak value is no more than -6 dBu for the input music signals. Colored noise samples, with the power spectral density reducing at the rate of 3 dB per octave as the frequency increases, were added to simulate a noisy signal with 40 dB signal-to-noise ratio. This noise model was chosen to represent the hardware noise due to circuits/sensors in the hearing aid. The maximum hearing aid gain value used in the experiments was 61 dB. The output was clipped if the output signal became greater than 80 dBu.

To assess performance of the fixed gain system and the method of this chapter, four hearing aid profiles - mild-gently sloping loss[2], moderate-flat loss, moderate-steeply sloping loss and profound-gently sloping loss – as shown in Figures 4.3a - 4.3d were used. The hearing loss thresholds across various frequency ranges are determined at the time of hearing aid fitting with the pure tone audiogram, commonly at frequencies 125, 250, 500, 1000, 1500, 2000, 3000, 4000, 6000 and 8000 Hz [3]. A digital hearing aid attempts to provide the insertion gain for a hearing aid patient for a given hearing loss profile. The shape of the insertion gain does not necessarily follow the shape of the hearing aid loss profile and depends on the prescription method. The insertion gains for the hearing loss profiles used in this chapter were obtained with the NAL-RP prescription [118] and are shown in Figures 4.3a - 4.3d. In addition, we also used many flat[3] insertion gain values to find added stable gains for all methods.

Unless stated otherwise, the initial value of hearing aid gain was set to 20 dB below the target gain. Subsequently, the gain was slowly increased for 20 seconds at the rate of 1 dB/second to reach the target gain level. The adaptive feedback cancellation experiment ran for 80 seconds in each case. The last 10 seconds of the experiment were deemed as the steady state. Psychoacoustic measures were obtained from the steady state signals to judge the performances of various schemes. In some cases, we also employed the perceptual evaluation of speech quality (PESQ) measure [119]

[2]In the definition of a hearing loss profile, the first word suggests the degree of hearing loss and the second hyphenated word suggests the hearing loss shape across frequency [52].

[3]Same gain at all frequencies.

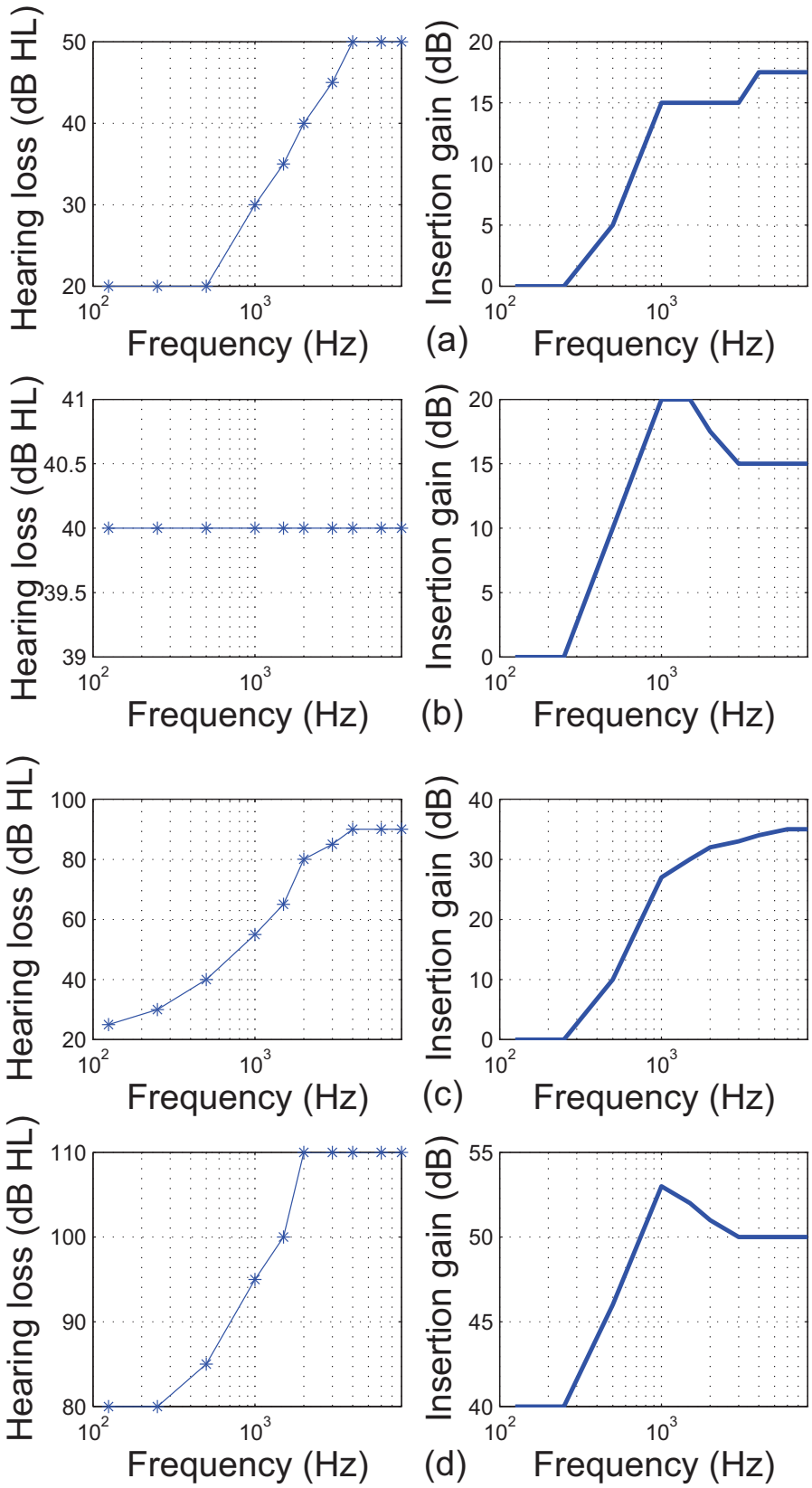

Figure 4.3: Hearing loss profile and insertion gain of, (a) mild-gently sloping hearing loss (b) moderately-flat hearing loss (c) moderate-steeply sloping hearing loss (d) profound-gently sloping hearing loss.

to obtain an easy-to-compute quantitative measure of perceptual quality of the signals. PESQ is an objective measure that analyzes a test speech signal after temporal alignment with a corresponding reference signal based on psychoacoustic principles. PESQ provides perceptual quality rating of a speech segment between -0.5 and 4.5 and can be interpreted as follows. The highest score indicates that the speech signal contains no audible distortions and it is virtually identical to the clean speech segment. The PESQ scores between -0.5 and 1 indicate that the distortions and residual noise in the speech signal are very high and the segment sound unacceptably annoying. The ratings of 4, 3, 2 can be interpreted as "good quality," "slightly annoying" and "annoying" respectively.

We also performed an informal subjective evaluation of the steady state data. The subjects evaluated the feedback canceled audio for the amount of residual feedback components and loudness perception as outlined in Section 3.2 of Chapter 3. To obtain psychoacoustic measures, six normal-hearing listeners participated in the listening test. In order to work with normal-hearing listeners, the output of the hearing aid system was further processed with long linear-phase filters that equalized for the effects of the insertion gain of the hearing aid. The processed sounds were presented to subjects in both ears with a pair of headphones in a quiet place. Before the subjects started the experiment, they were provided with an example of the clean sound as well as example sounds of various types of artifacts for listening. The subjects always had access to the clean audio while rating the processed sounds.

The global masking thresholds $\mathbf{T}(m)$ for different subbands for one signal frame from a MATLAB simulation are shown in Figure 4.4. The feedback path model 1 was used in this experiment. The hearing aid gain was flat 5 dB above the critical gain. It can be seen from Figure 4.4 that there were many frequency components below the masking threshold in this simulation. This indicates that the algorithm is able to reduce the gain for a large number of input signal components without reducing the perceptual quality of the output of the hearing aid.

In the first experiment, we demonstrate the ability of the system to detect and suppress offending frequencies. We disabled the adaptive feedback canceller to evaluate the behavior of the offending frequency detection algorithm. Feedback path 1 was used for this experiment and the hearing aid gain was set flat at 36.1 dB which is 0.5 dB above the critical gain for the feedback path. The parameters for detection of offending frequencies with adaptive notch filters and energy growth monitoring were $\rho = 0.95$, $\alpha_a = 0.005$, $\lambda_s = 0.99$, $\epsilon_a = 10^{-5}$, $\lambda_m = 0.99$, $\delta_q = 0.05$, $T_a = 750$, $\nu_u = -0.01$, $\nu_l = -0.1$, $\Gamma_u = 1$, $\Gamma_l = -4$, $\gamma_m^r = -20$, $T_r = 75$, $\delta_b = 1.0003$, $\lambda_u = 0.99$ and $T_b = 6$. Parameters of the parametric EQ filters to suppress offending frequencies upon detection were $p = 0.5012$ (-6 dB) and $q = 5$. The maximum number of parametric EQ filters were set to 12 in order to limit perceptual distortions in the output sound. Figures 4.5a - 4.5c show signals with

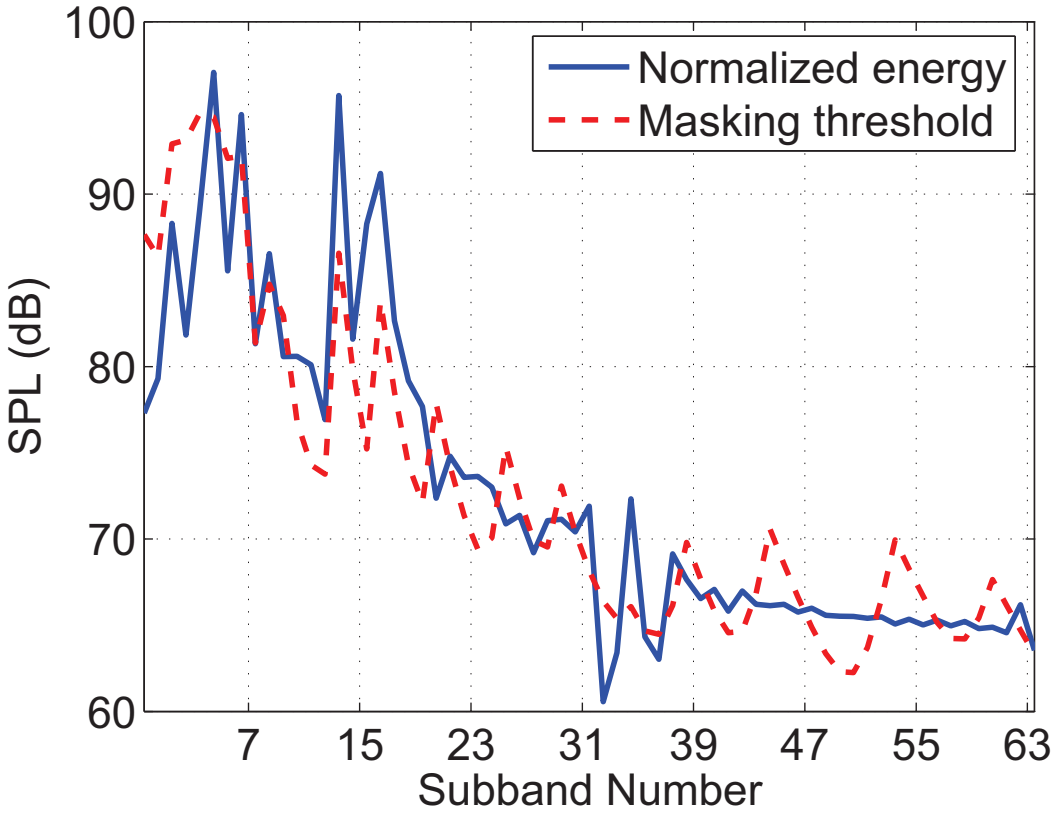

Figure 4.4: Masking thresholds at various subbands.

and without suppression against the desired signal. Clearly, the offending frequency suppression method quickly stopped the system from going into instability. Figure 4.5d shows the adaptive notch filter tracking during the operation for the subband where an offending frequency occurred. It can be seen that, once howling started, the adaptive notch filter converged to the offending frequency and tracking became less variable. During instability, both the energy monitoring counter and the ANF tracking counter grew, as shown in Figure 4.5e. In Figure 4.5e, scaled down values of the ANF tracking counter are shown for better presentation of both counters (γ_i^a and γ_i^r) on one axis. However, this does not affect the performance. In fact, the energy monitoring criterion was fulfilled before the the ANF tracking criterion was met. However, the offending frequency was not detected until the ANF variance became smaller, as indicated by the ANF tracking counters.

In the next experiment, we evaluate the offending frequency suppression scheme in terms of speed of detection and output sound quality. The output sound quality was judged with the PESQ measure from the steady state output sound. The speed of the offending frequency suppression method was calculated with the maximum time to recover from instability (mTRI) measure. The mTRI is an estimate of the duration of the longest howling occurrence. Howling occurrences were manually identified according to the method described in [120]. Let the duration of the j^{th} howling

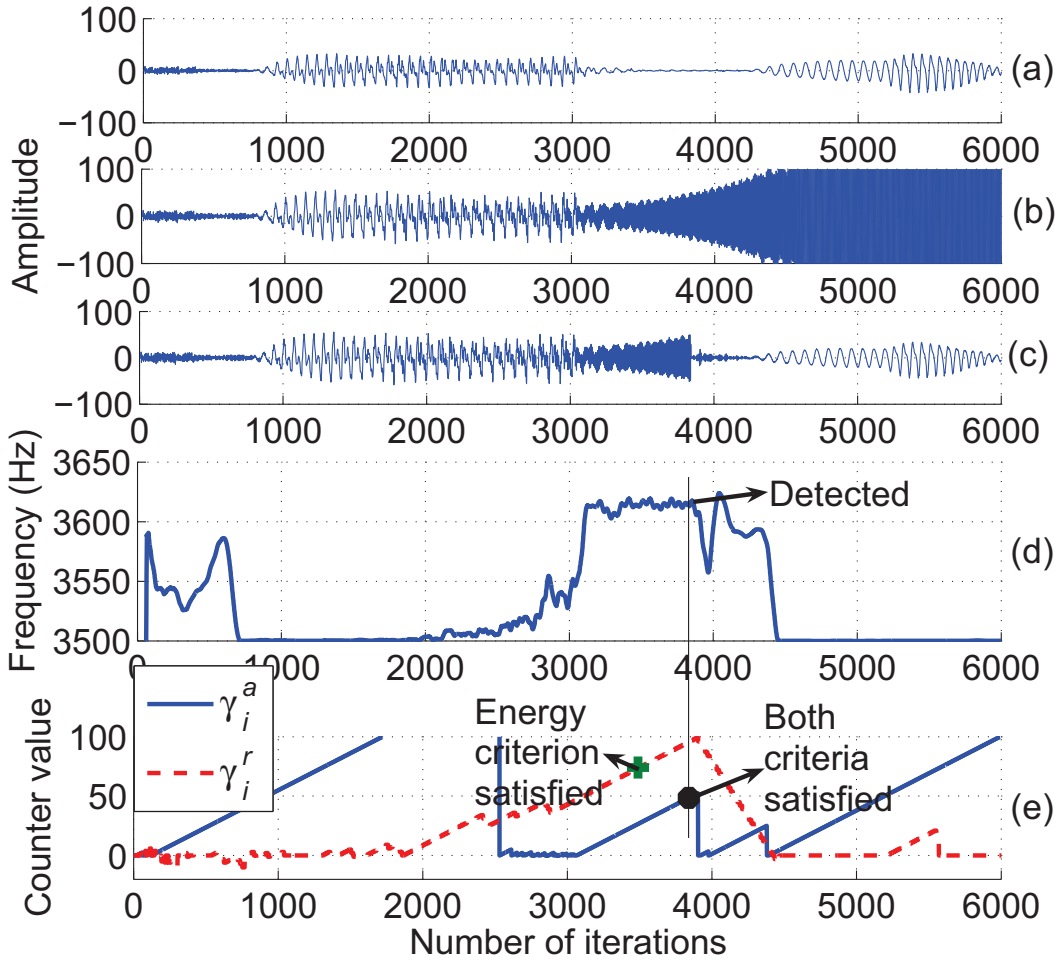

Figure 4.5: Signals and counters demonstrating ability of the offending frequency suppression method - (a) desired signal (b) signal without suppression (c) signal with offending frequency (d) ANF tracking (e) energy monitoring and ANF tracking counters in band 28.

segment be Δt_j, then the mTRI is calculated as

$$\text{mTRI} = \max_{\forall j \in [1\ N_h]} (\Delta t_j) \tag{4.4}$$

where N_h is the number of offending frequencies detected. The parameters for the reset algorithm were $\lambda_l = 0.999$, $\lambda_h = 0.7$, $\epsilon_r = 10^{-12}$, $\delta_o = 0.1$ and $T_o = 10$. In this simulation, profile 4 and the six speech input signals of 80 seconds were used. Three acoustic feedback cases were studied. In the first case, feedback path 1 was used for the whole 80 seconds. Feedback path 2 was used for the whole experiment in the second case. In the third case, the experiment started with feedback path 1 and after 40 seconds, it was switched to feedback path 2. For the three feedback cases discussed above, Table 4.6 lists the total number of howling occurrences (N_h), mTRI and mean PESQ values. Table 4.6 also lists the average number of offending frequencies per experiment that

Table 4.6: Measures for the OFS with and without reset algorithm.

Measures	With reset			Without reset		
	Case 1	Case 2	Case 3	Case 1	Case 2	Case 3
N_h^s	1	3	3	3	5	8
N_h	19	30	48	18	30	44
mTRI (s)	0.2	0.2	0.4	0.1	0.2	0.4
PESQ	3.8	3.8	3.8	3.7	3.7	3.5

remained for the different feedback cases in the steady state (N_h^s) with and without the use of the reset algorithm. Clearly, the number of steady state offending frequencies are typically smaller than the total number of howling occurrences (N_h) during the experiment for the reset algorithm because some of the offending frequencies get reset.

The howling occurrences (N_h) in Table 4.6 indicate that ramping up gain to the target gain in the beginning and the feedback path change created several instances of howling. The number of howling occurrences were the most for the feedback case 3 because of the feedback path change. The effects of such occurrences were mitigated by the OFS method. The instability was detected in less than 0.5 second in all the experiments. The use of the reset algorithm yielded fewer number of parametric EQ filters in the steady state (N_h^s) than without the reset algorithm. However, this did not compromise the output sound quality as indicated by the PESQ values. On the contrary, use of the reset algorithm yielded slightly better output sound quality.

The number of offending frequencies (OFs) and the output signal during the experiment for the feedback situation 3 and profile 4 are shown in Figures 4.6a and 4.6b, respectively. Figure 4.6a also shows a zoomed in view of two half a second long intervals - one at the beginning of the experiment and the other when the feedback path changed, to better understand the changes in the number of offending frequencies. It can be seen that two offending frequencies were detected in the beginning when the hearing aid gain was ramping up to the desired value. These frequencies were reset later on. The third offending frequency that was detected later and was not reset during the course of the simulations as the adaptive filter was close to the steady state behavior at that time. When the feedback path changed, offending frequencies were detected, suppressed and reset several times. Finally, the output signal in Figure 4.6b suggests that the offending frequency detection during the gain increase was quick enough to keep the system stable. However, the feedback path change sent the system into instability for a short period of time, as shown in the 0.5 second long inset plot in Figure 4.6b.

In the next experiment, we explore added stable gains for various schemes - adaptive gain processing (AGP), offending frequency suppression (OFS), combined gain processing that includes

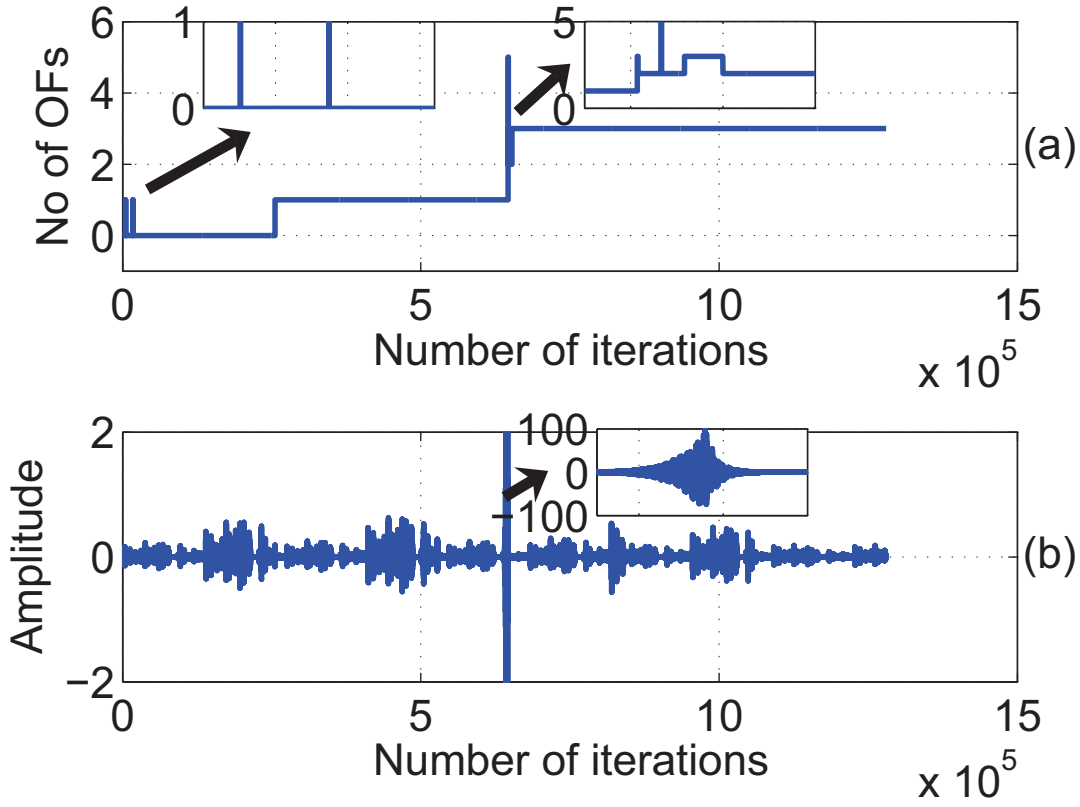

Figure 4.6: With the OFS method - (a) number of offending frequencies and (b) the output signal.

adaptive gain processing with offending frequency suppression (AGP+OFS), and the fixed gain processing (FGP) method. The gain processing methods - AGP, OFS and (AGP+OFS) - modified the forward path hearing aid gain along with the adaptive feedback cancellation. On the other hand, the hearing aid gain was fixed during the course of the experiment for the fixed gain processing method. The fixed gain processing method incorporated adaptive feedback cancellation for canceling the acoustic feedback. The feedback path 1 was used for this evaluation. The psychoacoustic measures, feedback and loudness ratings, for all the schemes at various flat hearing aid gain values are summarized in Figure 4.7. In Figure 4.7, the feedback rating (FR) of 0 or the loudness rating (LR) of 5 indicate that the system went into howling for that hearing aid gain. The subjective ratings of residual feedback and loudness for the input signal to the hearing aid were 4.1 and 3.1, respectively. The following conclusions can be drawn from psychoacoustic measures in Figure 4.7. The output sound quality deteriorated as indicated by the feedback ratings for fixed gain methods as the hearing aid gain was increased. The gain processing methods of this chapter, individually and combined, maintained the output sound quality at higher hearing aid gains than the fixed gain method by suppressing unwanted acoustical feedback components. According to the feedback ratings in Figure 4.7, it can be said that the fixed gain processing provided approximately 11 dB

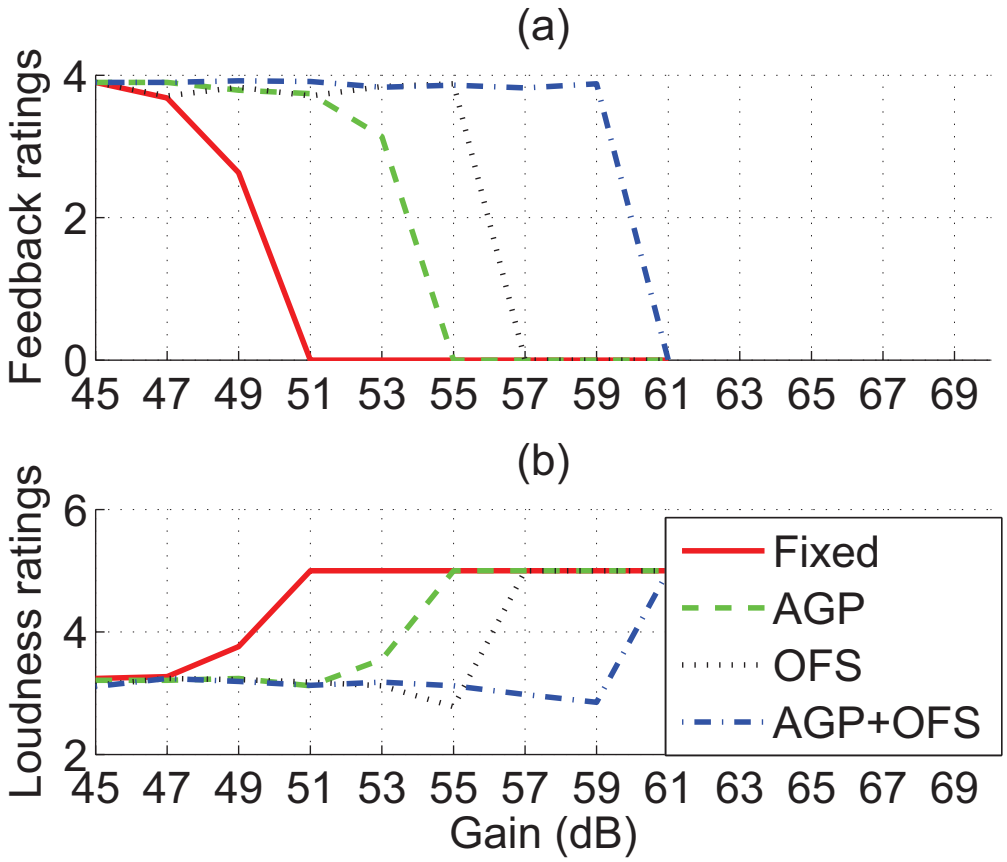

Figure 4.7: Subjective ratings for various methods - (a) feedback ratings (b) loudness ratings.

of added stable gain, the adaptive gain processing (AGP) provided 15 dB of added stable gain, the offending frequency suppression provided up to 19 dB of added stable gain and the combined gain processing (AGP+OFS) could provide 23 dB of added stable gain without deteriorating the sound quality due to the residual acoustic feedback. Furthermore, according to the loudness ratings in Figure 4.7, the adaptive gain processing did not reduce loudness for all stable hearing aid gains, whereas the OFS and the combined gain processing (AGP+OFS) had slightly lower loudness ratings at higher gains before becoming unstable. The reduction in loudness in the OFS and AGP+OFS was due to use parametric EQ filters. Our studies indicate that the use of $6-8$ parametric EQ filters did not affect loudness of the output sound. Comparing the ratings for the combined gain processing (AGP+OFS) at hearing aid gain values of 55 - 59 dB with the fixed gain processing at the hearing aid gain of 47 dB, it can be said that the combined gain processing presented in this chapter provided 8 to 12 dB additional gain over traditional fixed gain processing with good output sound quality.

To better understand the gain processing methods of the chapter, we compare the power spectra of the output produced with the fixed gain method and with the adaptive gain processing (AGP) method for a flat hearing aid gain of 49 dB, as shown in Figure 4.8. At this gain value, the

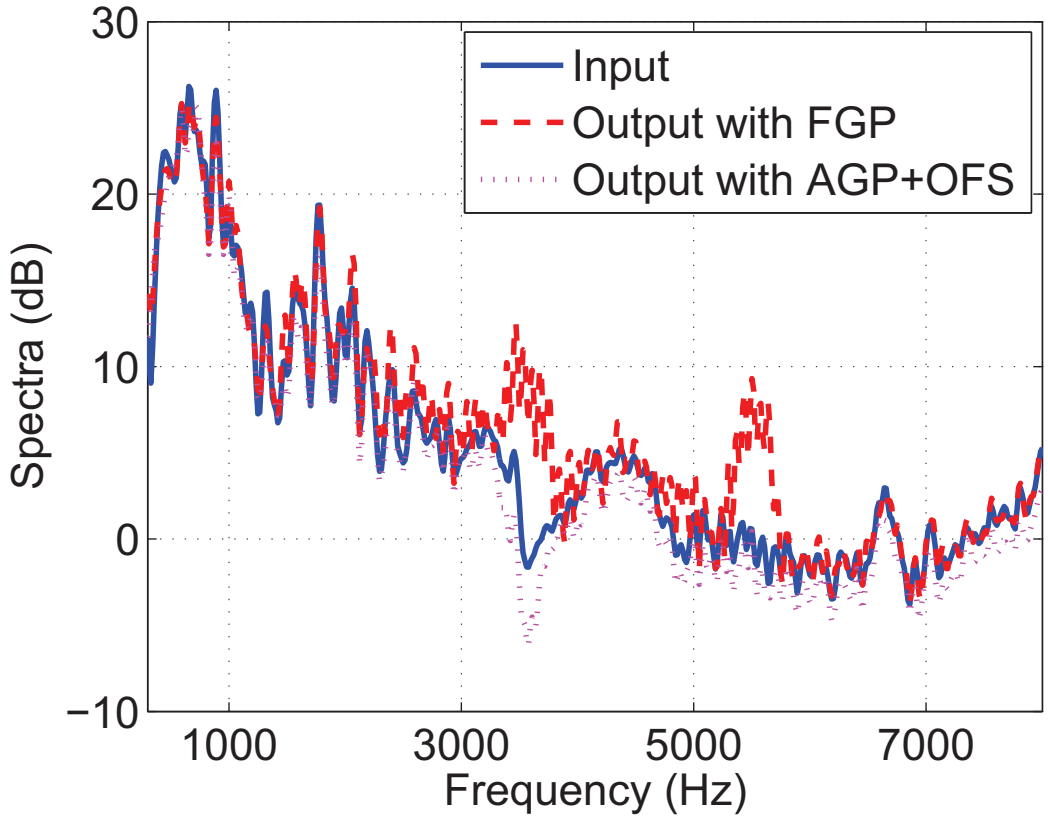

Figure 4.8: Comparison of the output spectra of the two methods.

fixed gain system was close to instability. The spectra were estimated using the Welch method by dividing data into frames of 512 samples with 256 sample overlap. There are noticeable differences between the spectra of the output of the fixed gain system and the input speech, especially at frequencies near 3500 and 5500 Hz. These differences were due to residual feedback components that caused ringing/howling behavior in the output signal. The output of the combined gain processing scheme (AGP+OFS) did not exhibit residual feedback or howling effects. Specifically, the build-up near 5500 Hz frequencies was reduced just with the adaptive gain processing and with no use of parametric EQ filters. On the other hand, parametric EQ filters were used to reduce gain near 3500 Hz frequencies along with adaptive gain processing to eliminate the ringing/howling effects. Together, the combined gain processing (AGP+OFS) completely eliminated the residual feedback components, as indicated by the feedback rating in Figure 4.7. The gain processing resulted in slightly lower spectra than the input signal spectra, especially at higher frequencies. However, these reductions did not reduce loudness according to loudness ratings in Figure 4.7.

In the next experiment, the fixed gain system was evaluated against the adaptive gain processing (AGP), offending frequency suppression (OFS) and combined gain processing (AGP+OFS) on four hearing aid gain profiles using speech and music signals. Feedback path 2 was used for this

experiment. The average subjective ratings for various profiles with all methods are summarized in Table 4.7. In Table 4.7, all methods provided good output sound quality for profiles 1 and 2 for both types (speech and music) of input signals. The fixed gain processing provided good output sound quality for profile 3 with speech signals; however, there were soft whisting sounds in the output signal when music signals were input to the hearing aid system. On the other hand, all gain processing methods (AGP, OFS and AGP+OFS) yielded good output sound quality for both types of input signals with hearing aid gain profile 3.

Finally, the fixed gain processing had significant residual feedback components in the the output sound for the hearing aid profile 4, as indicated by the feedback ratings in Table 4.7. Use of the gain processing methods improved the output sound quality in every situation. Specifically, the gain processing methods suppressed the residual feedback components for it to be inaudible with every gain processing method except with the adaptive gain processing for music signals. The adaptive gain processing (AGP) produced output sound with intermittent residual feedback components in it when the input to the hearing aid system was the music signal and gain profile 4 was used.

It is interesting to note that the traditional fixed gain system could not provide enough feedback cancellation in the case of profound hearing loss gain profile (profile 4) for an ITE hearing aid[4] used in the experiment. Often, audiologists suggest the use of behind-the-ear hearing aids for patients with profound hearing loss [52]. The results in Table 4.7 indicate that the method of this chapter

[4]The feedback path was derived from an ITE.

Table 4.7: Performance measures for various schemes.

Profile	Signal	Measures	Fixed	AGP	OFS	AGP+OFS
1	SPEECH	FR	3.9	3.9	3.9	3.9
		LR	3.3	3.2	3.2	3.2
	MUSIC	FR	3.9	3.9	3.9	3.9
		LR	3.2	3.2	3.3	3.2
2	SPEECH	FR	3.9	3.9	3.9	3.9
		LR	3.2	3.3	3.2	3.2
	MUSIC	FR	3.9	3.9	3.9	3.9
		LR	3.2	3.2	3.2	3.2
3	SPEECH	FR	3.9	3.9	3.9	3.9
		LR	3.2	3.2	3.2	3.2
	MUSIC	FR	3.1	4.0	3.9	3.9
		LR	3.3	3.2	3.2	3.2
4	SPEECH	FR	2.2	3.9	3.7	4.0
		LR	3.9	3.2	3.3	3.2
	MUSIC	FR	0	2.9	3.8	3.9
		LR	5	3.4	3.2	3.2

will enable a patient with profound hearing loss to use an ITE hearing aid which is not possible otherwise. Consequently, the methods of this chapter not only provide additional added stable gain but also enable patients to use more comfortable style hearing aids which is a big concern for many patients [52].

In the next experiment, the combined gain processing (AGP+OFS) was evaluated against the classical fixed gain processing method with a real-time feedback path. The experimental setup used to obtain coefficients of the feedback paths, as described earlier in this section, was used for this experiment. The white board was placed parallel to the face plate of the ITE hearing aid at 100 cm in this experiment. The gain processing methods of this chapter and the feedback cancellation algorithm with the fixed gain were implemented using an ADSP-21364 processor. With the above setup, output of the hearing aid system was recorded with a sound card for both schemes.

Residual feedback ratings and loudness ratings of the recorded data with both schemes were obtained with subjective evaluations. The average subjective ratings for both methods at different flat hearing gain values are summarized in Table 4.8. As can be seen from the table, the ratings for the feedback and the loudness obtained from the test for combined gain processing at 18 dB above the critical gain (CG) is approximately the same as those for the fixed gain at 10 dB above the CG. The output sound had significant residual acoustic feedback components for the fixed gain method at 12 dB above the CG. On the other hand, the good output sound quality was obtained with the combined gain processing (AGP+OFS) for gain values of 18 dB above the critical gain (CG). The output sound at 20 dB above the CG for the combined gain processing (AGP+OFS) exhibited intermittent ringing. The output sound quality was unacceptable due to substantial acoustic feedback components for the combined gain processing at 22 dB above the CG. The low perceptual ratings for the fixed gain processing at gain values 12 dB and higher along with the acceptable performance of the gain processing methods (AGP+OFS) for hearing aid gain values 18 dB and lower indicates the viability of the hearing aid system presented in this chapter.

Table 4.8: Average ratings for the two schemes.

Gain above CG (dB)		8	10	12	14	16	18	20	22	24
Fixed gain processing	Feedback	4.0	4.0	2.2	0	0	0	0	0	0
	Loudness	3.2	3.1	3.6	5	5	5	5	5	5
AGP+OFS	Feedback	4.0	3.9	4.1	3.8	4.0	3.8	3.2	2.3	0
	Loudness	3.1	3.1	3.0	3.2	3.1	3.2	3.2	3.7	5

CHAPTER 5

LOW-DELAY SIGNAL PROCESSING FOR DIGITAL HEARING AIDS

In this chapter, we present the low-delay structure to reduce the delay requirement in the forward path. The low-delay structure provides frequency-dependent amplification for hearing loss compensation with low forward path delays and performs dynamic signal processing such as noise suppression and dynamic range compression. In addition, the low-delay structure also employs an off-the-forward-path, frequency domain adaptive filter to perform acoustic feedback cancellation.

Portions of this chapter are reprinted, with permission, from

- Ashutosh Pandey and V. John Mathews, "Low-delay signal processing for digital hearing aids," in *IEEE Trans. on Audio, Speech and Language Processing*, vol. 19, no. 4, May 2011, pp. 699-710. ©[2011] IEEE.

The rest of the chapter is organized as follows. The low-delay structure is described in Section 5.1. In Section 5.2, the performance of the hearing aid system of this chapter is evaluated and compared with the structure described in Section 2.2.2 using MATLAB simulations. This section also contains design discussions and the results of subjective evaluations of the two systems.

5.1 Low-delay hearing aid structure

The block diagram of the low-delay digital hearing aid system is shown in Figure 5.1 where vector quantities are drawn in thicker lines. In the low-delay structure, an optional delay d_m is included in the forward path. The extra delay may help increase the added stable gain for a hearing-aid patient if needed. The low-delay structure performs some of the signal processing in the time domain on a sample-by-sample basis and others in the frequency domain on a block-by-block basis. In particular, the spectral gain shaping and estimation of the whitening filter coefficients $\mathbf{L}_w(n)$ are done on a sample-by-sample basis. The low-delay spectral gain shaping incorporates both dynamic signal processing and hearing loss compensation. The feedback cancellation is performed using an off-the-forward-path, filtered-XLMS adaptive filter [14] in the frequency domain. The notations used in this chapter for the frequency domain block-based signal processing algorithm are adopted from Section 2.2.1 of Chapter 2. This notation is used to present the details about the

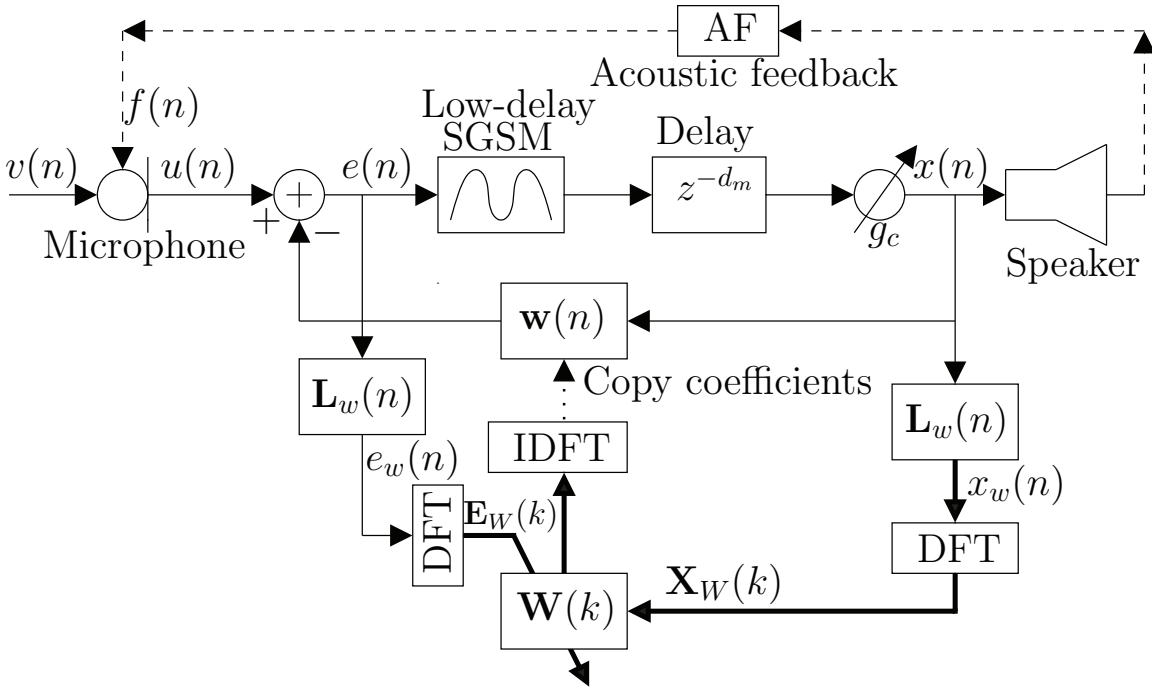

Figure 5.1: Block diagram of the low-delay structure.

low-delay hearing aid signal processing in the following sections. Section 5.1.1 provides details of the low-delay spectral gain shaping method. The adaptive feedback cancellation associated with the low-delay structure is described in Section 5.1.2.

5.1.1 Low-delay spectral gain shaping

Even though the estimated hearing loss profile measured at the time of hearing aid fitting does not change at least until the patient is evaluated again, our system performs spectral gain shaping on a block-by-block basis. This is because, in addition to hearing loss compensation, the spectral gain shaping system also incorporates noise suppression and dynamic range compression. Let $T(e^{j\omega})$ represent the magnitude of the desired spectral gain shaping function in any given block of the input signal. If $W_n(e^{j\omega})$ is the noise suppression response, $T(e^{j\omega})$ is given by

$$T(e^{j\omega}) = O\left(B_l(e^{j\omega})W_n(e^{j\omega})\right) \tag{5.1}$$

$O(.)$ represents the dynamic compression operation and $B_l(e^{j\omega})$ is the desired hearing loss compensation. Given $T(e^{j\omega})$ at $N_l + 1$ different frequencies $\omega_i, i = 0 \cdots N_l$, the spectral gain shaping system consists of J equalization filters, as shown in Figure 5.2. The coefficients $c_i^{eq}, i = 0 \cdots J$ are selected as a least-squares approximation of the desired overall spectral characteristics of the hearing aid. That is, the system selects the coefficients such that the cost function

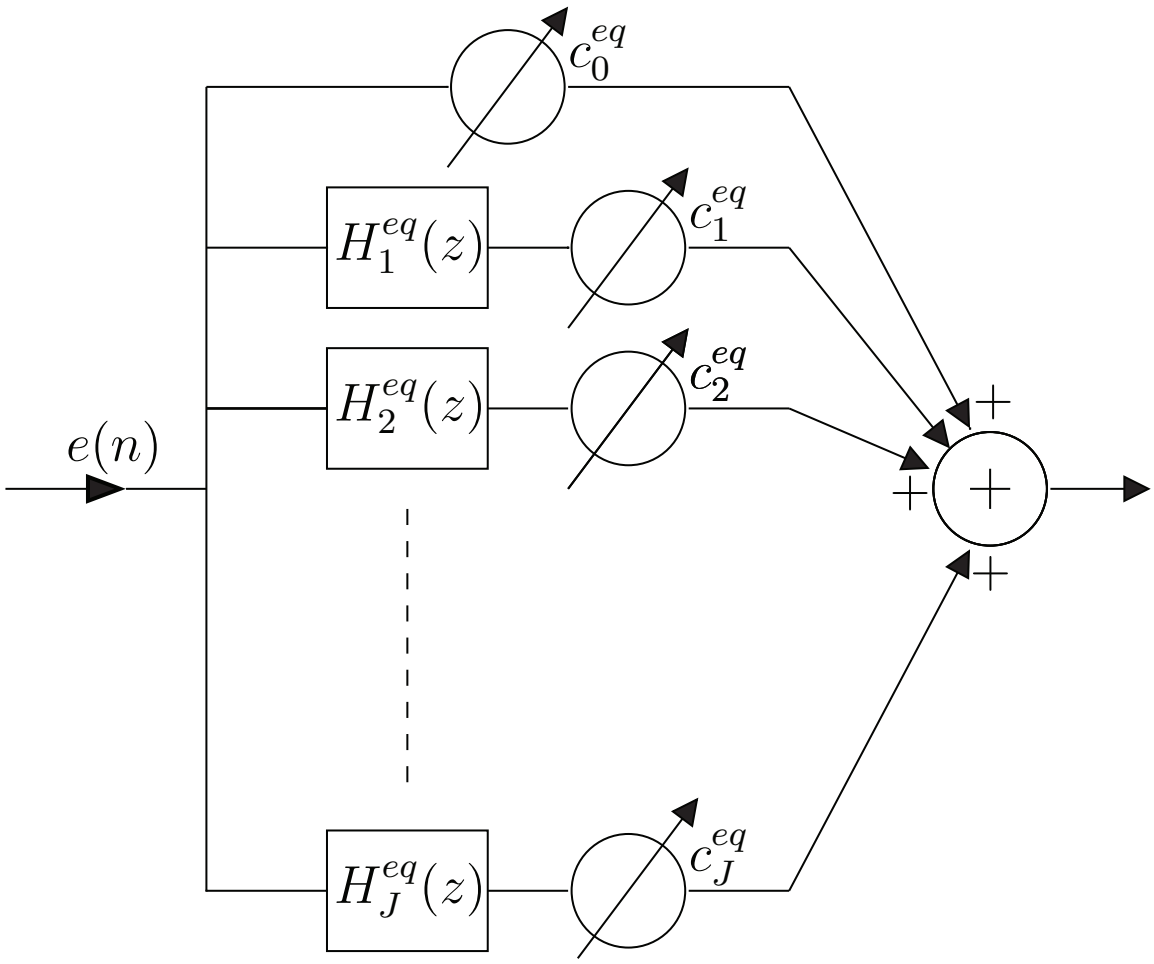

Figure 5.2: The low-delay spectral gain shaping method with parallel equalization filters.

$$\Lambda_l = \sum_{i=-N_l}^{N_l} \left\| T_m(e^{j\omega_i}) - \left(c_0^{eq} + \sum_{k=1}^{J} c_k^{eq} H_k^{eq}(e^{j\omega_i}) \right) \right\|^2 \tag{5.2}$$

is minimized, where $H_k^{eq}(e^{j\omega_i})$ is the frequency response of the k^{th} EQ filter in the parallel structure, $\omega_{-i} = -\omega_i$, $H_k^{eq}(e^{-j\omega_i}) = (H_k^{eq}(e^{j\omega_i}))^*$ for $k = 1 \cdots J$ and $T_m(e^{-j\omega_i}) = (T_m(e^{j\omega_i}))^*$. In the above equation, $T_m(e^{j\omega})$ is a minimum phase system whose magnitude response is the same as $T(e^{j\omega})$. This particular transfer function can be obtained by a spectral factorization of $T(e^{j\omega})$. Our implementation utilizes a computationally efficient algorithm employing the discrete Hilbert transform as described in [121, 122]. It is known that for all causal and stable systems that have the same magnitude response, the minimum phase system has the minimum group delay [123]. Therefore, matching to a minimum phase transfer function reduces the overall group delay of the low-delay spectral gain shaping filter block shown in Figure 5.2. In (5.2) c_0^{eq} adjusts the average frequency response to match the desired spectral response. The least-squares solutions to the above problem are given by

$$\mathbf{c_{eq}} = (\mathbf{H_{eq}^H H_{eq}})^{-1}\mathbf{H_{eq}^H T_{eq}} \tag{5.3}$$

where the solution vector $\mathbf{c_{eq}}$ is made up of the coefficients c_0^{eq}, c_1^{eq}, $\cdots$, c_J^{eq} shown in Figure 5.2,

$$\mathbf{T}_{eq} = [\ T_m(e^{-j\omega_{N_l}}) \quad \cdots \quad T_m(e^{j\omega_{N_l}})\ ]^T$$

and

$$\mathbf{H}_{eq} = \begin{bmatrix} 1 & H_1^{eq}(e^{-j\omega_{N_l}}) & H_2^{eq}(e^{-j\omega_{N_l}}) & \cdots & H_J^{eq}(e^{-j\omega_{N_l}}) \\ 1 & H_1^{eq}(e^{-j\omega_{(N_l-1)}}) & H_2^{eq}(e^{-j\omega_{(N_l-1)}}) & \cdots & H_J^{eq}(e^{-j\omega_{(N_l-1)}}) \\ \vdots & \vdots & \vdots & \vdots & \vdots \\ 1 & H_1^{eq}(e^{-j\omega_0}) & H_2^{eq}(e^{-j\omega_0}) & \cdots & H_J^{eq}(e^{-j\omega_0}) \\ \vdots & \vdots & \vdots & \vdots & \vdots \\ 1 & H_1^{eq}(e^{j\omega_{(N_l-1)}}) & H_2^{eq}(e^{j\omega_{(N_l-1)}}) & \cdots & H_J^{eq}(e^{j\omega_{(N_l-1)}}) \\ 1 & H_1^{eq}(e^{j\omega_{N_l}}) & H_2^{eq}(e^{j\omega_{N_l}}) & \cdots & H_J^{eq}(e^{j\omega_{N_l}}) \end{bmatrix}$$

The matrix $(\mathbf{H_{eq}^H H_{eq}})^{-1}\mathbf{H_{eq}^H}$ in (5.3) can be determined off-line once the parametric filters and the frequencies $\omega_0, \omega_1 \cdots \omega_{N_l}$ are known. These parameters are typically specified at the time of hearing aid fitting.

While a variety of equalization filters can be used for spectral gain shaping, this work employs second order peaking filters derived from analog peaking filters with transfer function [114, 124]

$$H(s) = \frac{s^2 + p_e q s + 1}{s^2 + qs + 1} \tag{5.4}$$

where q represents the quality factor and p_e is the filter gain at the center frequency $\Omega = 1$ rad/s. This filter has gain close to 1 at most frequencies and shows a boost or attenuation at frequencies in the vicinity of its center frequency. The maximum gain (when $p_e > 1$) occurs at the center frequency and is given by p_e. Table 4.3 displays the computations involved in calculating the coefficients of the equivalent discrete-time filter when the center frequency is specified in the analog domain [34]. Here, discrete-time transfer function has the form

$$H(z) = \frac{b_0 + b_1 z^{-1} + b_2 z^{-2}}{a_0 + a_1 z^{-1} + a_2 z^{-2}} \tag{5.5}$$

and f_s denotes the sampling frequency and the conversion from analog to discrete-time was performed using the bilinear transformation.

In this work, we designed the EQ filters in the spectral gain shaping system to match the auditory filters in the ear. An auditory filter refers to a band of frequencies that the human auditory system treats similarly during sound processing [3, 39]. The frequency band associated with each auditory filter is referred to as the critical band of that filter. Psychoacoustic research has indicated that there are approximately 25 auditory filters in the audible frequency range. Each equalization filter was selected with the center frequency to match the center of a critical band. Similarly, the quality factor q_i for the i^{th} filter was selected according to

$$q_i = \frac{f_{c,i}}{\Delta f_{cr,i}} \tag{5.6}$$

where $f_{c,i}$ is the center frequency of the i^{th} critical band and $\Delta f_{cr,i}$ is the bandwidth of the i^{th} critical band. The value of p_e is chosen heuristically to keep the overall forward-path delay small and reasonably accurately match the spectral response with the gain values $c_i^{eq}, i = 1 \cdots J$. In the experimental results presented later in the chapter, the EQ filters were selected to match the auditory filters and center frequencies were selected to match the auditory filters of a human with normal hearing. The design can be extended to match the auditory filters of hearing-impaired patients in a similar manner; however, the auditory filter shapes must be estimated separately for each patient.

5.1.2 Adaptive feedback cancellation

In this section, we describe the adaptive feedback cancellation algorithm employed in the hearing aid for the low-delay structure. The adaptive feedback cancellation is performed in the frequency domain with the filtered signals $e_w(n)$ and $x_w(n)$ shown in Figure 5.1. The filtered signals are used in the adaptation process to reduce the bias in the estimate of an adaptive filter as suggested by Hellgren [14]. The filtered signals are created by filtering the full band signals with the whitening filter $\mathbf{L}_w(n)$ [125, 126]. The whitening filter coefficients are estimated with the one-step forward linear predictor filter $\mathbf{p}(n)$ as shown in Figure 5.3. In the z-domain, the whitening filter $L_w(z)$ can be related to the predictor filter $p(z)$ as $L_w(z) = 1 - z^{-1}p(z)$ [12]. The linear predictor filter $\mathbf{p}(n)$ is an FIR filter of order M_a, whose coefficients are estimated by minimizing the forward prediction error of the error signal $e(n)$.

The linear predictor filter attempts to estimate the time-varying auto-regressive model for the input signal of a hearing aid [127]. The input signals in hearing aids are audio signals such as speech/music that are highly nonstationary. Therefore, it is imperative that the linear predictor filter quickly adapt to the correct model as the input signal is varying. In this research, we use recursive least-squares type algorithms which are known for their faster convergence compared to the gradient-based methods at the cost of additional computational complexity. However, in

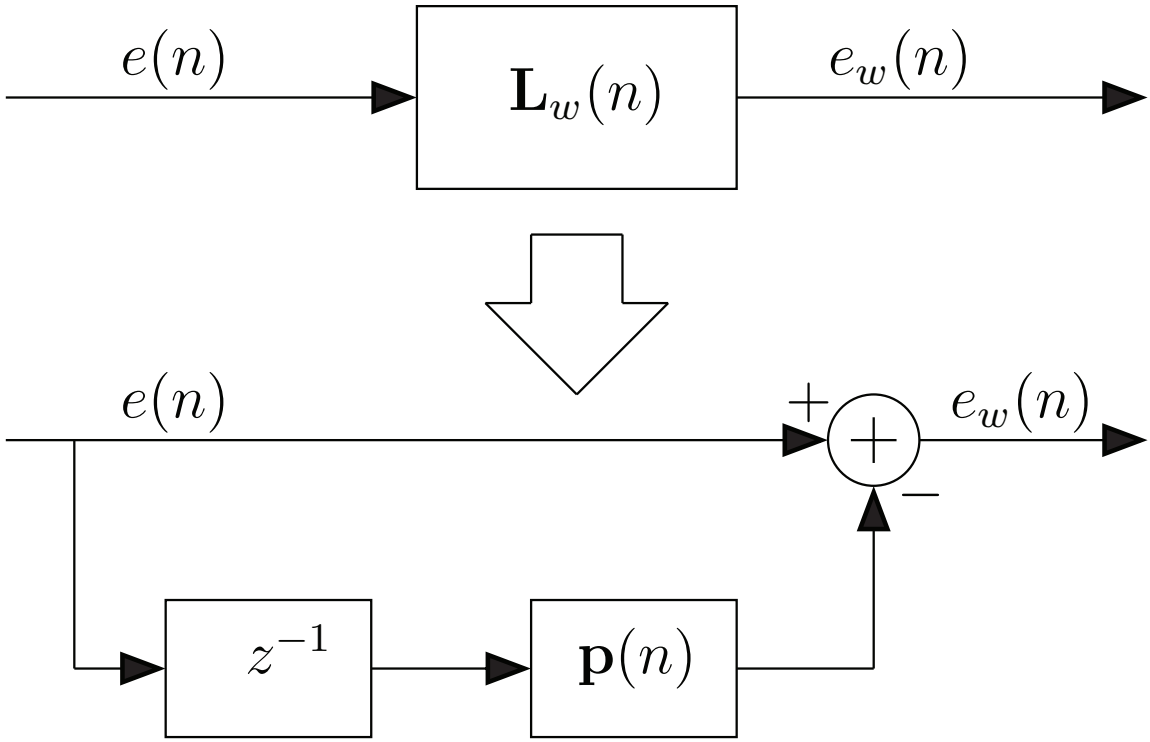

Figure 5.3: Obtaining the whitening filter coefficients with a forward linear predictor.

this case, the additional computational complexity in obtaining the predictor coefficients is smaller compared to the overall computational complexity in implementing the hearing aid system because the order of the predictor filter M_a is usually small in practice. Specifically, the linear predictor coefficients are obtained using the weighted recursive least-squares (WRLS) algorithm with a variable forgetting factor as suggested by Milosavljevic *et al.* [126, 128, 129].

The variable forgetting factor (VFF) is used to improve the tracking capability of the WRLS algorithm which is in particular helpful for nonstationary signals such as speech/music. The forgetting factor is adjusted depending on the signal stationarity, using the modified generalized likelihood ratio algorithm (MGLR) [126]. The MGLR algorithm provides information about the signal stationarity by computing a discrimination function $D_s(n)$. The discrimination function signifies the speed and the amount of change in the signal. At time n, the discrimination function $D_s(n)$ uses the last $2I$ samples of a signal, I being an integer, to indicate the signal stationarity as

$$\begin{aligned} D_s(n) = L_s(n-2I+1, n) - L_s(n-2I+1, n-I) \\ -L_s(n-I+1, n) \end{aligned} \tag{5.7}$$

where $L_s(c, d)$ is the logarithmic function for the interval $[c, d]$ defined as

$$L_s(c,d) = (d-c+1)\ln\left\{\frac{1}{d-c+1}\sum_{n=c}^{d} e_w^2(n)\right\} \tag{5.8}$$

In (5.8), the variable $e_w(n)$ is defined in Table 5.1. If the value of $D_s(n)$ calculated by equation (5.7) becomes smaller than a value D_{min}, it is set to D_{min}. Similarly, if the value of $D_s(n)$ becomes larger than a value D_{max}, it is set to D_{max}. Subsequently, the forgetting factor $\lambda(n)$ is chosen so that $\lambda(n) = \lambda_{min}$ when $D_s(n) = D_{min}$; $\lambda(n) = \lambda_{max}$ when $D_s(n) = D_{max}$ and linear interpolation between them if $D_{min} < D_s(n) < D_{max}$. The limits on the forgetting factor values are such that $0 < \lambda_{min} \leq \lambda(n) \leq \lambda_{max} < 1$. The complete algorithm for determining the linear predictor coefficients with the VFF-WRLS at time n is summarized in Table 5.1.

In Table 5.1, $\mathbf{\Psi}(n)$ is a $M_a \times M_a$ matrix which is recursively updated. The whitened signals $e_w(n)$ and $x_w(n)$ are used to estimate the feedback path with an adaptive filter in the frequency domain using a block-based-least-mean-squares algorithm (FBLMS) [12]. The adaptive filter models the feedback path with an FIR filter containing N coefficients. Furthermore, signals are segmented into N_f point vectors with $N-1$ point overlap for adaptive filtering. The FBLMS algorithm for the k^{th} block is summarized in Table 5.2. In Table 5.2, μ_0 is a step-size parameter and the $S(k,m)$s are the power estimates of the samples of the reference signal, $X_W(k,m)$s, for the adaptive filter in the frequency domain. Table 5.2 also lists the sample-by-sample processing done in the forward path based on the adaptive filter update obtained from the block processing. We denote the adaptive filter coefficient vector in time domain at time n as $\mathbf{w}(n)$. The variable $\mathbf{W}(k)$ is the vector representations of the adaptive filter coefficients in the frequency domain.

Table 5.1: Finding linear predictor coefficients using WRLS with VFF.

$$\mathbf{z}(n) = \left[\begin{array}{cccc} e(n-1) & e(n-2) & \cdots & e(n-M_a) \end{array}\right]^T$$

$$e_w(n) = e(n) - \mathbf{z}^T(n)\mathbf{p}(n)$$

Calculate $D_s(n)$ according to (5.7)

$$\lambda(n) = \frac{\lambda_{max} - \lambda_{min}}{D_{max} - D_{min}}(D_s(n) - D_{min}) + \lambda_{min}$$

$$\mathbf{r}(n) = \frac{\mathbf{\Psi}(n)\mathbf{z}(n)}{\lambda(n) + \mathbf{z}^T(n)\mathbf{\Psi}(n)\mathbf{z}(n)}$$

$$\mathbf{p}(n+1) = \mathbf{p}(n) + \mathbf{r}(n)e_w(n)$$

$$\mathbf{\Psi}(n) = \frac{1}{\lambda(n)}(\mathbf{\Psi}(n) - \mathbf{r}(n)\mathbf{z}^T(n)\mathbf{\Psi}(n))$$

Table 5.2: Delayless adaptive feedback cancellation.

Initialization

$\mathbf{S}(0)$ ... A vector with small positive constant

$\mathbf{W}(0)$ ... A vector with all zeros

Sample Processing Iterations (for $n = 1, 2 \cdots$)

$$\mathbf{x}(n) = \left[\begin{array}{cccc} x(n) & x(n-1) & \cdots & x(n-N+1) \end{array} \right]^T$$

$$e(n) = u(n) - \mathbf{w}^T(n)\mathbf{x}(n)$$

$$e_w(n) = \mathbf{L_w}(n) \left[\begin{array}{cccc} e(n) & e(n-1) & \cdots & e(n-M_a) \end{array} \right]^T$$

$$x_w(n) = \mathbf{L_w}(n) \left[\begin{array}{cccc} x(n) & x(n-1) & \cdots & x(n-M_a) \end{array} \right]^T$$

Block Processing Iterations (for $n = R, 2R, \cdots$ where $k = n/R$)

$$\mathbf{e}_w(k) = \left[\begin{array}{cccc} e_w(kR) & e_w(kR+1) & \cdots & e_w((kR+R-1) \end{array} \right]^T$$

$$\mathbf{E}_W(k) = \text{FFT} \left(\left[\begin{array}{c} \mathbf{0} \\ \mathbf{e}_w(k) \end{array} \right] \right)$$

$$W(k+1, i) = W(k, i) + \frac{\mu_0}{S(k, i)} X_W(k, i) E_W^*(k, i) \text{ for } i = 0, \cdots, N_f - 1$$

$$\mathbf{W}(k+1) = \text{FFT} \left(\left[\begin{array}{c} \text{the first N elements of IFFT}(\mathbf{W}(k+1)) \\ \mathbf{0} \end{array} \right] \right)$$

$$\mathbf{S}(k+1) = \beta \mathbf{S}(k) + (1-\beta) \mathbf{X}_W(k+1) \bigodot \mathbf{X}_W^*(k+1)$$

- $\bigodot$ denotes element-by-element multiplication
- $\mathbf{0}$ denotes column vector of length $N - 1$

5.2 Results and discussion

This section presents results from MATLAB simulations of the hearing aid algorithms to demonstrate the performance of the low-delay approach and the subband-based algorithm described in Section 2.2.2. Both methods were evaluated in terms of processing delays and output sound quality. The true feedback path was simulated using a 192-tap FIR filter in parallel with a homogeneous quadratic nonlinearity. The nonlinearity simulates the nonlinear distortions in the loudspeakers and A/D converters in a hearing aid system. The harmonic signal strength was 40 dB below that of the output of the linear component. Coefficients for the linear component of the feedback path were obtained from measurements of an inside-the-ear (ITE) hearing aid. The ITE hearing aid consisted of two FG-3653 omni-directional microphones and a receiver. The output of the microphones and

input to the receiver were available at the face plate of the hearing aid as CS44 plugs. We used a standard EXPRESSfit hearing aid programming cable to drive and access microphones and the speaker of the hearing aid. The programming cable was connected to an interface board through an 8-pin mini-DIN plug that provided required power to the programming cable and amplified the signals. The critical gain[1] for the acoustic feedback model used in this chapter was 36.4 dB. The feedback canceller employed a linear FIR system model with 128 coefficients. This undermodeling attempts to capture the practical situation where it is very difficult to exactly model the feedback path in the system. The signal processing was done at a sampling rate of $f_s = 16000$ Hz in all experiments in this section.

The subband-based system performs various signal processing in a hearing aid system with a fixed delay known as the analysis-synthesis filter bank (AS-FB) delay [83]. The AS-FB delay depends on the prototype filter length L_p, spectral resolution for the filter bank M and decimation ratio L. Generally, for linear-phase prototype filters commonly used in hearing aids and employed in this chapter, the AS-FB delay increases as spectral resolution increases, *i.e.* M increases. In this chapter, four subband designs S1, S2, S3 and S4 with spectral resolutions of 500, 250, 125 and 62.5 Hz were used to compare performance against the low-delay method. Parameters of the subband designs S1, S2, S3 and S4 were $M = 32, L = 4, L_p = 32$ (S1); $M = 64, L = 8, L_p = 64$ (S2); $M = 128, L = 16, L_p = 128$ (S3); and $M = 256, L = 32, L_p = 256$ (S4), respectively. A relatively low down-sampling ratio L was used in all designs to avoid aliasing and keep the analysis-synthesis delay as small as possible for the subband designs. The prototype filter coefficients were generated with the least-squares design given in [28]. The AS-FB delays for S1, S2, S3 and S4 were 2, 4, 8 and 16 ms, respectively.

Unlike the subband method, delay $d_t(\omega)$ in the low-delay system for a frame depends on the frequency-dependent group delay $d_g(\omega)$ [2] as

$$d_t(\omega) = \int_0^{\omega} \frac{d_g(\omega)}{\omega} d\omega$$

In the above equation, we assume without loss of generality that the phase of the low delay system at $\omega = 0$ is 0. Moreover, for the low delay method, group delay in a frame depends on the magnitude of the spectral gain shaping function $T(e^{j\omega})$ and is different for each frame. Since the maximum group delay d_g^m in a frame is always larger than or equal to $d_t(\omega)$ for that frame, we used

[1] Critical gain refers to the maximum amplification for which the output signal quality is acceptable without feedback cancellation.

[2] The group delay $d_g(\omega)$ of a system is related to its phase response $\phi(\omega)$ as $d_g(\omega) = -\frac{d\phi(\omega)}{d\omega}$.

the maximum of all d_g^m values in an experiment from different frames to characterize delay in the low-delay method. We refer to the maximum of all group delay values in an experiment as d_{max}. In the simulations, we explored d_{max} values that provided comparable or better performance than the four subband designs S1, S2, S3 and S4. Different components of the hearing aid system were evaluated separately prior to evaluation of the complete system.

For every experiment in this section, four hearing aid profiles - mild-gently sloping loss,[3] moderate-flat loss, moderate-steeply sloping loss and profound-gently sloping loss – as shown in Figures 5.4a - 5.4d, were used. The hearing loss thresholds across various frequency ranges are determined at the time of hearing aid fitting with the pure tone audiogram, commonly at frequencies 125, 250, 500, 1000, 1500, 2000, 3000, 4000, 6000 and 8000 Hz [3]. A digital hearing aid attempts to provide the insertion gain for a hearing aid patient for a given hearing loss profile. The shape of the insertion gain does not necessarily follow the shape of the hearing aid loss profile and depends on a prescription method. The insertion gains for the hearing loss profiles used in this chapter were obtained with the NAL-RP prescription [118] and are shown in Figures 5.4a - 5.4d.

The perceptual quality of the output speech was measured in each simulation using the perceptual evaluation of speech quality (PESQ) measures [119]. PESQ is an objective measure that analyzes a test speech signal after temporal alignment with corresponding reference signal based on psychoacoustic principles. PESQ uses differences in the loudness spectra of the reference and test signal to calculate perceptual quality of the test signal. PESQ provides perceptual quality rating of a speech segment between -0.5 and 4.5 and can be interpreted as follows. The highest score indicates that the speech signal contains no audible distortions and it is virtually identical to the clean speech segment. The PESQ scores between -0.5 and 1 indicate that the distortions and residual noise in the speech signal are very high and the segment sound unacceptably annoying. The ratings of 4, 3, 2 can be interpreted as "good quality," "slightly annoying" and "annoying," respectively. Besides PESQ measures, the output sound quality of the complete system for all methods was also evaluated subjectively by normal-hearing listeners.

5.2.1 Low-delay spectral gain shaping method

In the first experiment, we demonstrate the spectral gain shaping capability of the low-delay hearing aid system and study the effect of the frequency dependent delay of the low-delay system. Specifically, we simulated the coloration effect in hearing aids due to the hearing aid signal processing and studied the effectiveness of the low-delay method to reduce the coloration effect with

[3] In the definition of a hearing loss profile, the first word suggests the degree of hearing loss and the second hyphenated word suggests the hearing loss shape across frequency [52].

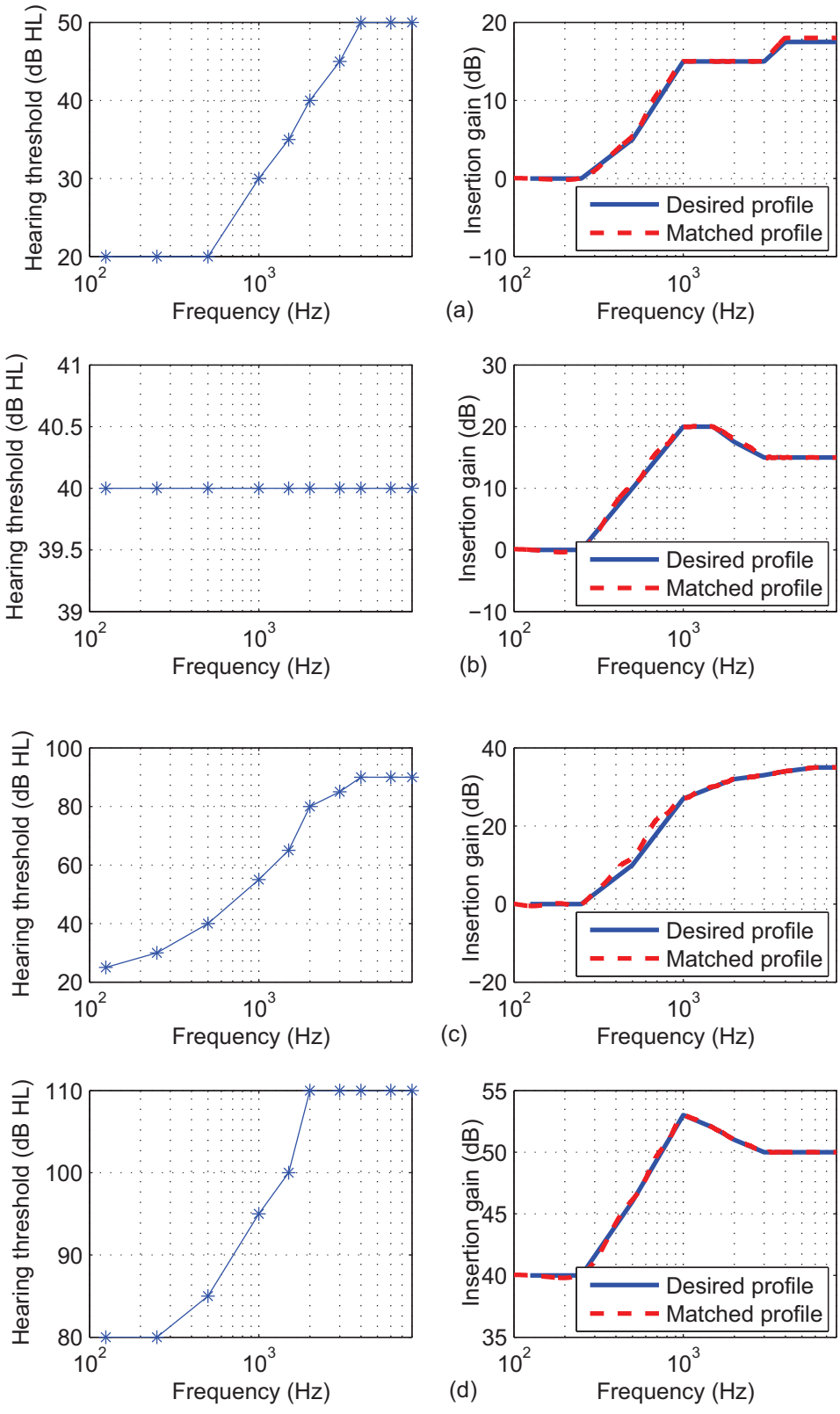

Figure 5.4: Hearing loss profile and insertion gain of, (a) mild-gently sloping hearing loss (b) moderately-flat hearing loss (c) moderate-steeply sloping hearing loss (d) profound-gently sloping hearing loss, matched with the low-delay SGSM.

a psychophysical experiment. Additionally, we also evaluated the low-delay method in a binaural listening situation.

For all the experiments in this section, we used auditory parameters for normal-hearing listeners because these data are well known and documented. Auditory parameters for hearing-impaired listeners, on the other hand, must be measured for each patient individually. We employed 21 filters to model the auditory system based on the critical band models for a healthy human as described in [39]. The center frequencies and quality factors for the equalization filters in each parallel section of our system were selected as illustrated in Section 5.1. The parameter p_e was set to 20 dB for all filters. This choice provided good magnitude match and small group delays for the hearing loss profiles used in the experiments.

Spectral gain shaping was accomplished using the least-squares method by minimizing the sum of errors over 63 equally spaced frequencies in the operating frequency range ($0 - 8000$ Hz). The resulting insertion gains are plotted against the desired gains in Figure 5.4. It can be seen that the spectral gain shaping achieved by the method closely matches the desired frequency response for all four hearing aid gain profiles. The group delays associated with the low-delay SGSM in the forward path across frequencies are shown in Figure 5.5.

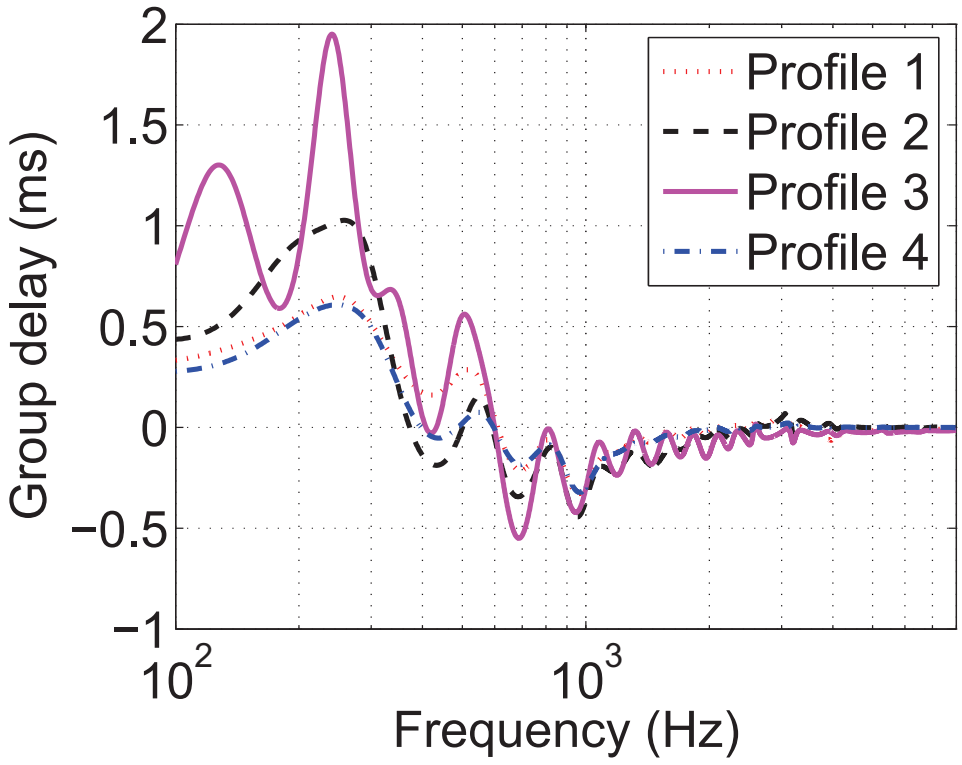

Figure 5.5: Group delay of the low-delay system for four different hearing aid gain profiles used in the simulations.

It can be seen from Figure 5.5 that the maximum group delay d_g^m among the four hearing aid gain profiles over all frequencies is less than 2.0 ms. While the low-delay method produces substantially smaller delays across frequency compared to the broadband analysis-synthesis delay, the delay is variable across frequency for the low-delay method. It is not clear if this will mitigate coloration effects in hearing aids. We performed a psychophysical experiment on normal-hearing (NH) listeners to evaluate the effect of nonlinear phase in the low-delay method and broadband delays in the subband methods in terms of the coloration effect. Degradation in the sound quality due to the coloration effect depends on the amount of the unprocessed sound combining with the processed. This in turn depends on several factors such as the hearing aid gain profile, type of hearing aid fitting [130, 131] *etc.* In order to get various degrees of the coloration effect, we simulated the coloration effect by adding two sounds - processed and unprocessed, where the attenuation in the unprocessed sound was controlled, as shown in Figure 5.6.

The unprocessed signal was simply an attenuated original sound where the attenuation modeled loss in the original sound while traveling through bones and a hearing aid earmold. In creating the processed sound, the hearing aid gain was provided with either the low-delay method or with the subband methods. The magnitude response of the gain function in the hearing aid was compensated with a long linear-phase filter because the subjects for the experiment were normal-hearing listeners. We call this the inverse HA gain filter. The delay due to the inverse HA gain filter was compensated in the unprocessed sound so that only delays due to amplification methods under evaluation remained in the combined signal. The combined sounds were created from six 5 seconds long speech files at 3 attenuation levels 0 dB, -5 dB and -20 dB. The combined sounds were presented in a random order to 6 normal-hearing listeners through a pair of headphones in both ears at a quiet place. The subjects were asked to rate the combined sound on a scale of 1 to 5 for the coloration effect according to Table 5.3. They were provided with example sounds for various types

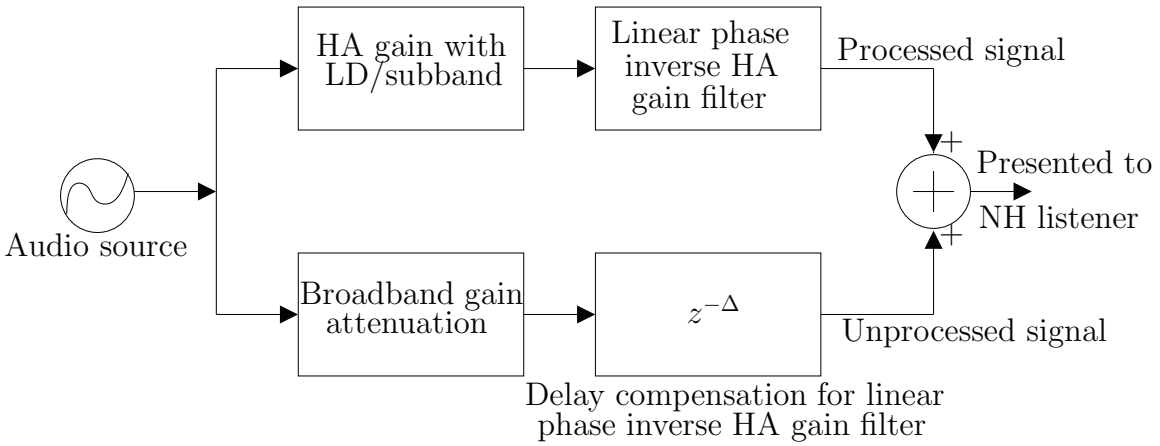

Figure 5.6: Block diagram to simulate coloring effects.

Table 5.3: Description of coloration ratings to the subject.

Ratings	Processed sound quality
1	Sounds different from original with strong echo
2	Sounds different from original, with weak echo
3	Sounds different from original with tonal shifts
4	Sounds different from original but acceptable
5	Sounds same as original, no perceptible change

of degradation due to the coloration effect before starting the test. The subjects had access to the original sound at all times while rating the corresponding combined sound and were encouraged to listen to both before rating the combined sound.

The coloration ratings with 95% confidence intervals for the low-delay (LD) method and the subband methods S1, S2, S3 and S4 at different attenuation levels are listed in Table 5.4. As expected, the coloration effect reduced as the attenuation increased for all systems. The coloration effect was the smallest for the subband design S1 among all the subband methods, indicating that the coloration effect increased with delay. This is in agreement with other findings [32,33,130,131]. Furthermore, the coloration effect for the low-delay method was the least for all attenuation levels. This confirms that the low-delay method mitigates the problem of coloration effects in hearing aids.

Based on the above experiment, it can be said that the nonlinear phase with the low-delay method does not degrade audio quality in monaural listening situations or if the phase responses are the same in both ears. However in practice, a hearing aid patient may wear a hearing aid in only one ear or can have binaural hearing aid fittings with different hearing aid gain profiles in each ear. In

Table 5.4: Ratings for coloration effects for various methods at different attenuation levels in the unprocessed path.

Profile	Attenuation levels (dB)	Method				
		S1	S2	S3	S4	LD
1	0	3.4±0.3	2.5±0.4	1.9±0.6	1.4±0.1	4.9±0.1
	-5	4.0±0.4	3.6±0.4	2.4±0.6	1.5±0.2	4.8±0.1
	-20	4.8±0.1	4.8±0.2	4.9±0.2	4.6±0.2	4.9±0.1
2	0	3.5±0.4	2.6±0.5	1.8±0.5	1.2±0.1	4.8±0.1
	-5	4.2±0.4	3.5±0.5	2.3±0.5	1.4±0.2	4.8±0.1
	-20	4.8±0.1	4.8±0.2	4.9±0.1	4.5±0.3	4.9±0.1
3	0	3.4±0.3	2.4±0.3	1.8±0.4	1.3±0.2	4.5±0.3
	-5	3.4±0.4	2.4±0.3	1.8±0.4	1.3±0.3	4.9±0.2
	-20	4.9±0.1	4.8±0.2	4.9±0.1	4.6±0.2	4.9±0.1
4	0	3.4±0.3	2.5±0.4	1.9±0.5	1.4±0.2	4.9±0.1
	-5	4.1±0.4	3.5±0.6	2.6±0.5	1.4±0.2	4.8±0.2
	-20	4.8±0.1	4.8±0.2	4.9±0.1	4.5±0.2	4.9±0.1

these situations, the hearing aid patient will have different phase responses if the low-delay method is employed. The human auditory system uses phase difference cues between two ears along with other cues to localize sound in space [132]. Therefore, it is important to understand the effect of different phase responses in both ears on the sound quality and localization abilities.

We performed a psychophysical experiment to assess effects of different phase responses in both ears due to the subband method and the low-delay method. The assessment was done in terms of the output sound quality and sound source localization abilities in the binaural listening situation. For this experiment, stereophonic sounds were used that appeared to come from a certain direction in space. A directional stereophonic sound was created by filtering a monophonic sound through head-related-transfer-functions (HRTFs) for the left and right channel corresponding to a direction in space. The head-related-transfer-functions were obtained from the MIT Media Labs HRTF set [133]. Five such stereophonic sounds were created that represented sounds coming from directions (0,0), (0,45), (0,90), (0,-45) and (0,-90).[4] Subsequently, phase responses corresponding to different subband methods or the low-delay method for various hearing aid profiles were added to simulate phase distortions due to these methods.

All subjects were first trained with the unprocessed stereophonic sounds (without additional phase response, just with the HRTFs) to localize sounds until they became comfortable. Subsequently, stereophonic sounds with additional phase responses corresponding to various methods were presented randomly to subjects through a pair of headphones binaurally in a quiet place. Six subjects participated in the experiment. The subjects were asked to guess the location of the sound among the five locations after listening the stereophonic sound. They were also asked to rate the sound quality according to the description in Table 5.3. The subjects were asked to ignore the directionality when rating the sound quality. Many combinations of the processing between the left and the right channels were tested. For each case, the mean values with 95% confidence intervals of the percentage of correct responses in the sound direction localization, the maximum error in the sound direction localization and the output sound quality are listed in Table 5.5.

In Table 5.5, LD profile 1 stands for the phase response corresponding to the hearing aid gain profile 1 for the low-delay method. Similar names have been used for the other profiles also. For the subband methods, only profile 1 was used because the phase distortion should be the same regardless of the hearing aid gain profile. It can be seen that the errors in localization for all hearing aid profiles in any combination for the low-delay method were comparable to the error in localization with the unprocessed sound. Audio quality ratings for the low-delay method suggest

[4]The first number is the elevation angle in degrees and the second number is the azimuth angle in degrees.

Table 5.5: User ratings in the binaural listening situation.

Phase distortions		Percentage correct	Maximum Error (degrees)	Stereo audio ratings
Left	Right			
Unprocessed	Unprocessed	88±6	45	4.8±0.1
S1 (2 ms)	Unprocessed	26±12	180	4.6±0.2
S2 (4 ms)	Unprocessed	23±12	180	4.4±0.2
S3 (8 ms)	Unprocessed	26±15	180	1.9±0.3
S4 (16 ms)	Unprocessed	26±15	180	1.3±0.1
S1 (2 ms)	S1 (2 ms)	90±6	45	4.8±0.1
S2 (4 ms)	S2 (4 ms)	88±6	45	4.7±0.2
S3 (8 ms)	S3 (8 ms)	93±5	45	4.8±0.1
S4 (16 ms)	S4 (16 ms)	88±6	45	4.8±0.1
LD Profile 1	Unprocessed	92±6	45	4.8±0.1
LD Profile 2	Unprocessed	88±6	45	4.7±0.2
LD Profile 3	Unprocessed	93±5	45	4.7±0.1
LD Profile 4	Unprocessed	90±6	45	4.8±0.1
LD Profile 2	LD Profile 1	88±6	45	4.8±0.1
LD Profile 3	LD Profile 1	88±6	45	4.8±0.1
LD Profile 4	LD Profile 1	90±6	45	4.7±0.1
LD Profile 3	LD Profile 2	88±5	45	4.8±0.1
LD Profile 4	LD Profile 2	93±5	45	4.8±0.1
LD Profile 4	LD Profile 3	88±5	45	4.8±0.1

that the added phase response due to the low-delay spectral gain shaping did not produce any unpleasant artifacts and the overall audio quality in the binaural listening situation was good. For the subband methods, the error in localization was small when the same subband method was used in both ears. However, if the subband method was used in one ear, the localization errors were very large. Even for the subband method S1 with the smallest delay, the localization error was as much as 180 degrees in some cases. The audio quality was acceptable for the subband methods S1 and S2, but the audio quality degraded significantly for the subband methods S3 and S4 where subjects perceived echo in the sound. Comparing the subjective ratings and the localization errors of the low-delay method with the subband methods with the broadband analysis-synthesis delay at all frequencies used in most hearing aids [9, 12] indicates that the low-delay method accomplishes the goal of reducing the forward path delay without sacrificing the ability to achieve desired gain profiles.

5.2.2 Noise suppression

In this section, we study the noise suppression capability of the low-delay method and compare the results with those of subband designs. In order to study the effect of noise suppression only, we disabled the adaptive feedback cancellation in this set of simulations, *i.e.* $f(n) = y(n) = 0$,

and $e(n) = v(n)$. Three male and three female speech segments of length 20 seconds were used as input signals in this experiment. Car noise segments taken from the noisy speech corpus (NOIZEUS) [134] at 3 different signal-to-noise ratios were added to the input signals to create the noisy signals. Postfilter weights were calculated according to the method given in the Appendix B and the gain was applied with the subband method and the low-delay spectral gain shaping method. Parameters for the noise suppression postfilter weights calculations were $\alpha_p = 0.8$ and $\epsilon_n = 1.00055$. PESQ measures were obtained for the noise suppressed speech segments. PESQ values from the noise suppressed speech segments for the low-delay method and all subband designs for the four hearing aid gain profiles are listed in Table 5.6. Table 5.6 also lists d_{max} for the low-delay method and the AS-FB delay for the subband designs S1, S2, S3 and S4.

The AS-FB delay only depends on the filter-bank while group delays in the low-delay method depend on the hearing aid gain profile as well as postfilter weights for noise suppression. The results in Table 5.6 indicate that all methods improved the output sound quality. PESQ values in Table 5.6 suggest that better noise suppression was achieved as spectral resolution increased for the subband method. However, improvements became less noticeable with the increase in spectral resolution. Perceptual quality ratings of the output sound for designs S3 and S4 were very similar. The output sound quality with the subband design S2 was slightly poorer than the subband designs S3 and S4 but was acceptable in most cases. This difference was more prominent for lower input signal-to-noise ratios. The subband design S1 yielded the worst output sound quality among all subband designs. If we consider the AS-FB delay and the noise suppression capability for various subband designs, the subband designs S2 and S3 are more practical choices than designs S1 and

Table 5.6: Measures of speech enhancement from noise suppression.

Input		Output										
SNR	PESQ	Profile	PESQ					d_{max}(ms)				
			S1	S2	S3	S4	LD	S1	S2	S3	S4	LD
0	1.9	1	2.0	2.4	2.8	2.9	2.7	2	4	8	16	1.7
		2	2.0	2.5	2.8	2.9	2.8	2	4	8	16	1.6
		3	1.9	2.4	2.8	2.8	2.8	2	4	8	16	2.0
		4	1.9	2.4	2.8	2.8	2.7	2	4	8	16	1.6
10	2.80	1	2.9	3.6	3.8	3.8	3.9	2	4	8	16	1.7
		2	3.0	3.6	3.8	3.9	3.9	2	4	8	16	1.7
		3	3.0	3.5	3.8	3.9	3.9	2	4	8	16	2.0
		4	3.0	3.5	3.8	3.9	3.8	2	4	8	16	1.6
20	3.5	1	3.6	3.9	4.0	4.0	4.1	2	4	8	16	1.9
		2	3.6	3.9	4.0	4.0	4.0	2	4	8	16	2.0
		3	3.6	3.8	4.1	4.1	4.1	2	4	8	16	2.1
		4	3.6	3.8	4.0	4.0	4.0	2	4	8	16	1.7

S4 for a hearing aid system. This is because the subband design S4 requires long delay with little improvement over the subband design S3 whereas the noise suppression performance for the subband design S1 falls below acceptable levels in many cases evaluated here.

PESQ ratings in Table 5.6 also indicate that the low-delay method produced similar perceptual output speech quality as the subband designs with high spectral resolution such as S3 and S4. Nonetheless, the low-delay method required much smaller delays than the subband designs S3 and S4, as indicated by the d_{max} values in Table 5.6. It can be concluded from these results that even the maximum delay at any frequency for the low-delay method is smaller than the broadband delays introduced by the conventional subband based methods while exhibiting noise suppression capabilities comparable to the subband systems with longer AS-FB delays.

5.2.3 Adaptive feedback cancellation

Adaptive feedback cancellation was implemented in MATLAB for the low-delay structure and the subband-based structure. Noise suppression was disabled for this experiment to assess only the feedback cancellation capability of both structures. Parameters for the frequency domain adaptive feedback cancellation used in the low-delay structure were $N = 128$, $\Delta K = 128$, $\beta = 0.98$, $\mu_0 = 0.02$ and $N_f = 256$. Parameters for the subband-based method were $\alpha_{sub} = 0.001$ and $\zeta = 10^{-7}$. Finally, parameters for the forward linear predictor to estimate the whitening filter were $M_a = 5$, $\lambda_{min} = 0.99$, $\lambda_{max} = 0.999$, $D_{min} = 200$, $D_{max} = 1000$ and $I = 256$. The broadband gain was set to unity, *i.e.* $g_c = 1$.

The input signals to the hearing aid were 6 clean speech waveforms of length 80 seconds taken from the TIMIT database. Colored noise samples, with the power spectral density reducing at the rate of 3 dB per octave as the frequency increases, were added to simulate a noisy signal with 40 dB signal-to-noise ratio. This noise model was chosen to represent the hardware noise due to circuits/sensors in the hearing aid. The initial value of the hearing aid gain was set to 20 dB below the target gain at all frequencies. Subsequently, the gain was slowly increased for 20 seconds at the rate of 1 dB/second to reach the target gain level. The adaptive feedback cancellation experiment ran for 80 seconds in each case. The last 10 seconds of the experiment were deemed as the steady state. PESQ measures from the steady state were used to judge performance of adaptive feedback cancellation capability for all methods in this section.

Figure 5.7 shows the PESQ values for all methods considered as a function of the processing delay in the system. The forward path delays were adjusted with parameters d_m for the low-delay method and d_1 for the subband method in addition to the minimum delay produced by these methods for spectral gain shaping. Figure 5.7 shows that all subband designs yielded similar perceptual

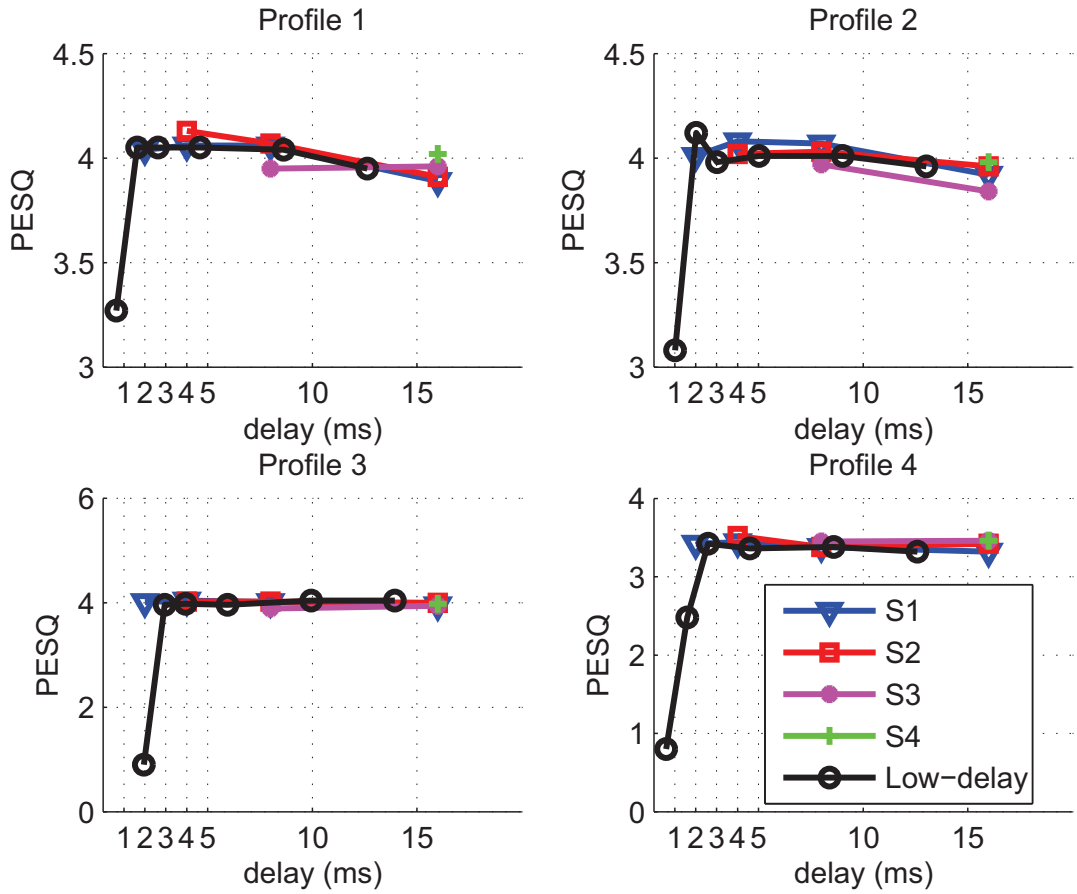

Figure 5.7: Misalignment (dB) as function of forward path delays for the subband and low-delay methods.

output sound quality for all profiles irrespective of the forward path delay values. Increase in the forward path delay did not increase the perceptual quality of the output sound. The output sound quality for profiles 1 to 3 was very good for all subband designs. On the other hand, the output sound quality for profile 4 was degraded for all subband designs. This is because the strength of the residual feedback components in the processed signal is larger for profile 4 than that for other profiles due to its higher gain requirements.

In case of the low-delay method, the output sound quality was unacceptable if the broadband delay was set to 0, as shown by the low PESQ values for the first data point in the low-delay method graph of Figure 5.7 for all profiles. The low-delay structure required at least 1 ms of the broadband delay for profiles 1 to 3 and at least 2 ms of delay for profile 4 to perform satisfactory adaptive feedback cancellation with good output sound quality. With these broadband delay values, total maximum processing delay d_{max} for the low-delay method during these experiments was less than 3 ms. We used the minimum acceptable broadband delay values for the low-delay method obtained from the simulations in this subsection for evaluating the complete system in the next section. We

used no additional broadband delay in the subband designs for the complete system evaluation. Without additional delay in the subband designs, the overall delay is equal to the AS-FB delay.

5.2.4 Evaluation of the complete system

In earlier sections, we evaluated the individual components of the hearing aid system. This process also helped us identify parameter values that resulted in acceptable performance in practical situations for these components. In this section, we evaluate the complete system that includes amplification, adaptive feedback cancellation and dynamic signal processing. Six 80 seconds long input speech signals described in the previous section were used in this experiment. Additionally, car noise was added to the speech signals to create signal-to-noise of 10 dB. The output sound quality in the steady state was subjectively evaluated for all methods. The perceived output sound quality of the hearing aid system for both structures was assessed with normal-hearing listeners as well as with the PESQ measure. In order to work with normal-hearing listeners, the output of the low-delay system was further processed with long linear-phase filters that equalized for the effects of the insertion gain of the hearing aid.

To assess sound quality, six subjects participated in the listening test. The processed sounds were presented to them in both ears with a pair of headphones in a quiet place. Subjects rated each system under test on a scale from 1 to 5, where 5 corresponded to listening directly to clean speech, and 1 corresponded to a signal of such poor quality that it was deemed unacceptable. Specifically, a rating of 1 indicates continuous loud artifacts, a rating of 2 indicates continuous low-level artifacts, 3 indicates intermittent low-level noticeable artifacts, and ratings of 4-5 indicate very good to excellent speech quality. Artifacts were explained to subjects as degradations in the speech signals. The output speech signals suffered from a variety of degradations such as the presence of residual background noise, ringing due to residual feedback and waterfall sounds.[5] Roughly speaking, ratings in the range 0-2 indicate unacceptable quality and ratings of 3-4 indicate tolerable degradations. Subjects could switch between the input and the processed output for a direct comparison to perfect quality. Before the subjects started the experiment, they were provided with an example of the clean sound as well as example sounds of various types of artifacts for listening. The subjects always had access to the clean audio while rating processed sounds.

The total maximum forward path delay at any time during an experiment was used to characterize the delay in the system. In case of the low-delay method, the maximum forward path delay is the addition of the broadband delay and d_{max} required for dynamic signal processing. On the other

[5] An artifact due to short term spectral changes in noise suppression systems. It is also sometimes referred to as swirling.

hand, the maximum forward path delay for the subband method is the addition of the broadband delay and the AS-FB delay.

The mean values with 95% confidence intervals of the user ratings, PESQ values and processing delays for all methods are listed in Table 5.7. PESQ values reported here exhibit similar trends as the user ratings for all hearing aid profiles and methods. This validates the use of PESQ values for earlier experiments and for the selection of the parameters of the hearing aids algorithms. Results in Table 5.7 indicate that the subband designs S2, S3 and S4 yielded good output sound quality for profiles 1 to 3. The output sound quality with the subband designs S3 and S4 was rated better than with the subband design S2 for the above profiles. Output sound quality ratings for the subband design S1 indicated more artifacts than any other method for profiles 1 to 3. This is mostly due to the lower spectral resolution in the subband design S1. The low-delay method also yielded good output sound quality that was comparable to the subband designs S2, S3 and S4. However, the low-delay method resulted in lower delay values compared to subband designs S2, S3 and S4. The processing delay for the subband design S1 is comparable to that of the low-delay method. However, the subband design S1 produced considerably more artifacts in the output than compared to the low-delay method.

For profile 4, the output sound quality was more degraded compared to other profiles for all methods. This is because profile 4 has higher insertion gain that leads to additional residual acoustical feedback components in the output sound. The hearing aid signal processing is limited in suppressing the acoustic feedback components to provide a better output sound quality for the feedback path used in this chapter. A hearing aid that has higher critical gain than the feedback

Table 5.7: Output sound quality for the combined system for both methods.

Profile	Measures	Method				
		S1	S2	S3	S4	LD
1	User ratings	3.2±0.3	3.8±0.4	4.1±0.4	4.1±0.3	4.1±0.4
	PESQ	2.9	3.6	3.8	3.8	3.8
	Max delay(ms)	2	4	8	16	2.0
2	User ratings	3.3±0.3	3.7±0.3	4.0±0.4	4.1±0.3	4.1±0.4
	PESQ	3.0	3.6	3.8	3.9	3.9
	Max delay(ms)	2	4	8	16	1.7
3	User ratings	3.3±0.2	3.7±0.5	4.0±0.4	4.1±0.3	4.0±0.3
	PESQ	3.0	3.5	3.8	3.9	3.9
	Max delay(ms)	2	4	8	16	2.3
4	User ratings	2.7±0.4	3.3±0.3	3.4±0.4	3.3±0.4	3.3±0.3
	PESQ	2.6	3.1	3.3	3.3	3.3
	Max delay(ms)	2	4	8	16	3.9

path used in this chapter may provide better output sound quality for profile 4. Audiologist often attempt to alter the feedback path response to improve audio quality for patients who require high levels of amplification [52]. This discussion is out of the scope of this chapter. Based on the above discussion, it can be said that the low-delay method performed as good as subband designs with high spectral resolutions with much lower processing delays. The work in this chapter paves the way for an alternative solution to the widely used subband method for implementing hearing aid signal processing algorithms and reducing the unwanted effects of the long and broadband forward path delays.

CHAPTER 6

HOWLING CONTROL WITH LEAST-SQUARES ESTIMATION AND PERCEPTUALLY MOTIVATED GAIN CONTROL

This chapter presents the howling suppression algorithm that adapts to the altered feedback path quickly and allows the patient to not lose perceivable information. A howling detection method is used to detect the onset of howling and the howling suppression method is employed. The howling suppression method changes the hearing aid gain function immediately after howling detection in such a way that the system operates in a stable manner and the distortions caused are not perceived because of temporal masking.

Portions of this chapter are reprinted, with permission, from

- Ashutosh Pandey and V. John Mathews, "Howling suppression in hearing aids using least-squares estimation and perceptually motivated gain control ," in *Proc. IEEE Int. Conf. on Acoustics, Speech and Signal Processing*, vol. 5, Toulouse, France, May 2006, pp. 149-152.

The rest of the chapter is organized as follows. Section 6.1 describes a howling detection algorithm. The new howling suppression algorithm is detailed in Section 6.2. In Section 6.3, the performance for the new algorithm is evaluated and compared with a competing structure using MATLAB simulations.

6.1 Howling detection

The design of the howling detector used in this chapter referring to Figure 2.1 in Chapter 2 is based on a simple correlation analysis of the error signal $e(n)$ and its delayed version $e(n-D)$. If the adaptive filter matches the feedback path closely, we expect the error signal $e(n)$ and its delayed version $e(n-D)$ to be relatively uncorrelated. When the feedback path is suddenly changed or the adaptive filter is unable to track the feedback path, the feedback signal $f(n)$ is not cancelled, implying that the feedback signal $f(n)$ is present in the error signal $e(n)$. When howling occurs, $f(n)$ typically has dominant sinusoidal components, making $e(n)$ and $e(n-D)$ relatively more

correlated. Consequently, the cross-correlation between $e(n)$ and $e(n-D)$ may be used as a marker to detect the onset of howling. We use a correlation factor defined as

$$\rho = \frac{\left| \sum_{i=0}^{L_h} e(n-i)e(n-D-i) \right|}{\sum_{i=0}^{L_h} |e(n-i)e(n-D-i)|} \tag{6.1}$$

and computed over a segment of length L_h for this purpose.

6.2 Howling suppression algorithm

The basic idea of howling suppression is as follows. The hearing aid employs an NLMS adaptive filter for estimating and canceling the feedback path. The system is also equipped with the howling detector described in Section 6.1. The adaptive filter coefficients stops adapting and coefficients are reset to zero as soon as howling is detected. For N samples after howling detection, we do not update the coefficients of the filter so that the dominant spectral components created by the howling activity do not affect the new updates. The least-squares algorithm described in the next subsection is employed to adapt the coefficients for the next $N + d - 1$ samples, where $d << N$. The gain function of the hearing aid is varied during the transition period in a manner that would allow the overall system to behave in a stable manner and at the same time allow the patient to mask the distortion caused by the variations. This process is described in Section 6.2.2. After the transition period of $2N + d - 1$ samples after howling detection, the coefficients obtained using the LS estimate are copied to the adaptive filter coefficients and the NLMS adaptation is resumed.

6.2.1 Least-squares estimation after howling detection

Let the data matrix $\mathbf{X}(n)$ and the desired response vector $\mathbf{d}(n)$ be defined as

$$\mathbf{X}(n) = \left[\begin{array}{cccc} \mathbf{x}(1) & \mathbf{x}(2) & \cdots & \mathbf{x}(n) \end{array} \right] \tag{6.2}$$

$$\mathbf{d}(n) = \left[\begin{array}{cccc} d(1) & d(2) & \cdots & d(n) \end{array} \right]^T \tag{6.3}$$

where $\mathbf{x}(n)$ is defined in (2.4). It is well known that the optimal least-squares coefficients vector $\hat{\mathbf{w}}(n)$ that minimizes $\| \mathbf{d}(n) - \mathbf{X}^T(n)\hat{\mathbf{w}}(n) \|^2$ is given by

$$\hat{\mathbf{w}}(n) = \mathbf{\Psi}^{-1}(n)\theta(n) \tag{6.4}$$

where $\mathbf{\Psi}(n) = \mathbf{X}(n)\mathbf{X^T}(n)$ and $\theta(n) = \mathbf{X}(n)\mathbf{d}(n)$. In what follows, we assume that $\mathbf{\Psi}(n)$ is invertible when $n = N$. The data matrix $\mathbf{X}(N)$ is a square matrix that will also be invertible in this

case. The extension of the results to the case when $\mathbf{\Psi}(n)$ is a singular matrix is not difficult. At time $n = N$, we can write

$$\begin{aligned}\hat{\mathbf{w}}(n) &= \mathbf{\Psi}^{-1}(n)\theta(n) \\ &= (\mathbf{X}(n)\mathbf{X}^T(n))^{-1}\mathbf{X}(n)\mathbf{d}(n) \\ &= (\mathbf{X}^T(n))^{-1}\mathbf{X}^{-1}(n)\mathbf{X}(n)\mathbf{d}(n) \\ &= (\mathbf{X}^T(n))^{-1}\mathbf{d}(n) \end{aligned} \tag{6.5}$$

Since $\mathbf{X}^T(n)$ is a Toeplitz matrix, (6.5) can be solved in $2N^2 + 8Nlog_2(N) - N$ arithmetic operations as shown in the Appendix A [45]. These many operations are expensive to implement in one iteration. Fortunately, we can solve a large portion of the algorithm in $N-1$ iterations as we get successive samples with a maximum $4N$ operations during any iteration, as shown in step 2 of the Appendix A. After N iterations, $8Nlog_2N + N$ operations are left to complete the computations in (6.5). We complete these operations in the next d iterations where d is a number of the order of $2log_2N$ so that approximately $4N$ operations are completed during each iteration. Therefore, we can obtain the initial estimate of the altered feedback path with the least-squares method in $2N + d - 1$ iterations with linear complexity.

6.2.2 Gain processing

The gain function of the hearing is reduced by a constant β for the first N samples after howling is detected to reduce the effect of the dominant spectral components created in the signal by the howling action. In all the simulations presented in the next section, we used $\beta = 0.01$. The gain is increased and kept at the prescribed level for the patient in the next $N + d$ samples. Maintaining a high gain at these samples helps to obtain a better estimate of the altered feedback path with the least-squares method [12, 13]. The gain is reduced for the next D samples because these samples were generated during the transition period with no feedback cancellation and a high gain and therefore may contain many unwanted spectral components of the feedback. Alternating low and high gain values for short periods of times allows stable operation of the system. Furthermore, since gain values are altered for short periods, the distortions may not be perceivable because of the temporal masking effect of the human auditory system [39].

6.3 Results and discussion

This section presents the results from MATLAB simulations of the hearing aid algorithms to demonstrate the performance of the chapter's howling suppression algorithm and the classical scheme described in Section 2.1.3 with delay in the forward path as the decorrelator. Simulations

were conducted in MATLAB with the feedback path obtained from an in-the-ear hearing aid. The impulse response of the feedback path was modeled using a FIR filter with 256 coefficients. The critical gain of the feedback path was 37 dB. An FIR adaptive filter with 256 taps was used to estimate the feedback path. The gain and delay used for simulations were set to 50 dB and 128 samples, respectively, in all simulations presented here. The howling detector declared the onset of howling whenever the correlation factor in (6.1) exceeded 0.9.

In the simulations, we introduced a sudden change in the feedback path by negating all coefficients of the feedback path sometime after the adaptive filter has reached the steady state. The howling detector sensed howling in about 652 samples (approximately 40 ms) after this change. The classical method reduces the gain as soon as howling is detected by 40 dB and increases it slowly back to the prescribed gain over the subsequent 50000 iterations. In simulations involving the method of this chapter, the gain is reduced by 40 dB intermittently during the transition period, as explained in Section 6.2.2. The parameter d was chosen to be 16. Figure 6.1 shows the output waveforms (normalized to have similar amplitude ranges for the three subplots) after the onset of howling for both schemes. It is clear that the classical scheme does not provide sufficient

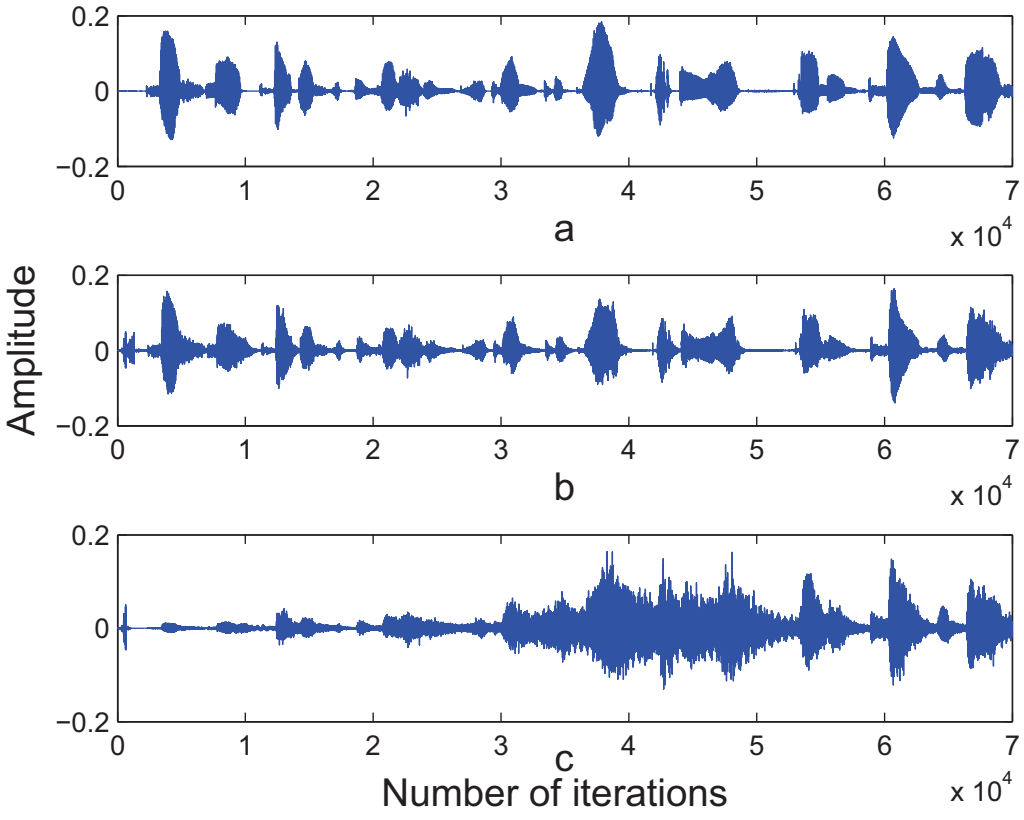

Figure 6.1: Scaled output signals after howling detection: (a) the desired output (b) with the new scheme (c) with slowly increasing gain.

amplification. The method of this chapter appears to reproduce the input signal reasonably faithfully at the output. We can see that the effect of the delay in howling detection in both Figures (6.1b) and (6.1c) for a very short duration at the beginning of the plots. There are slight differences between the signals in Figures (6.1a) and (6.1b). This is due to build up of uncancelled feedback during the transition period. However, these differences are not perceptually bothersome because they occur over very short durations. As can be expected, the classical scheme produced relatively faint output during the transition period, leading to some lack of intelligibility. The classical method attained the maximum gain in about 50000 iterations (3.125 sec) whereas the transient period for the new scheme was less than 657 iterations (0.0375 sec) for $N = 256$.

The outputs of the two schemes are compared in the frequency domain in Figure 6.2. The spectrum was calculated for the signals shown in Figure 6.1. The new scheme matches the desired response closely whereas the conventional scheme produces a significant amount of distortions in the process of ramping up the gain. These distortions occur because of the slow convergence of the classical scheme. On the other hand, the new scheme adapts to the altered feedback path quickly and therefore cancels out most of the undesired spectral components of the feedback. Figure 6.3 displays the misalignment between the true feedback path and the estimated feedback path just prior

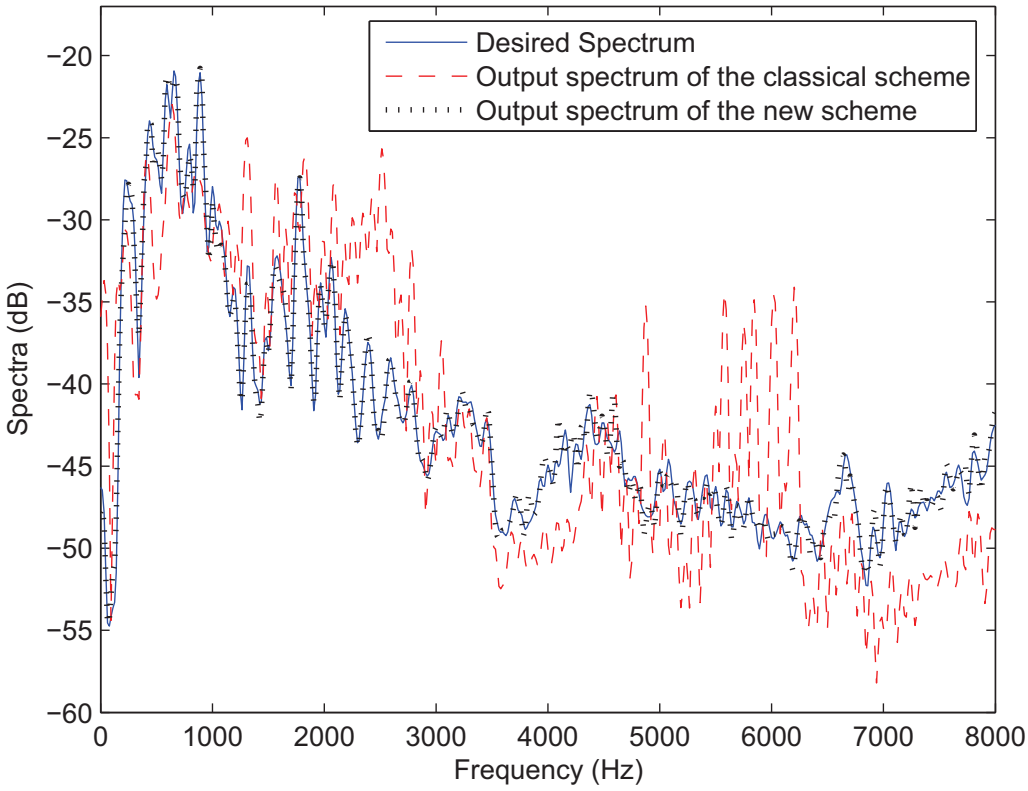

Figure 6.2: Comparision of the output spectra of the two schemes.

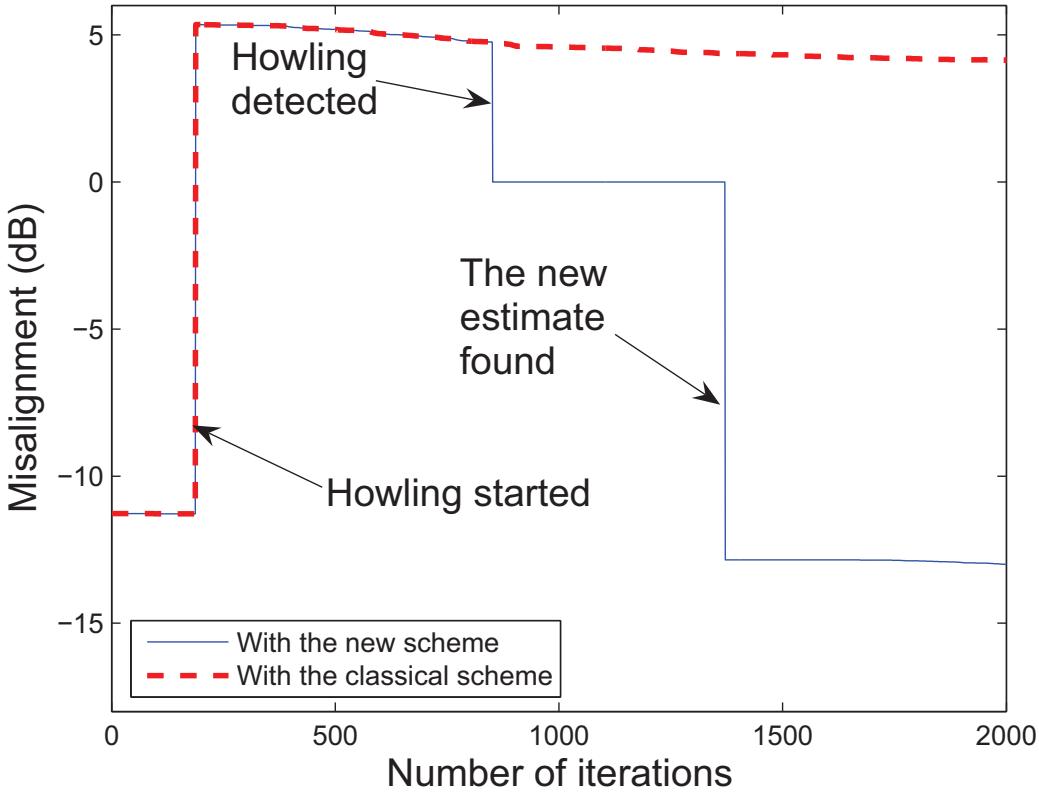

Figure 6.3: Misalignment around the onset of howling for the two schemes.

and just after the onset of howling. The misalignment was calculated as

$$\text{misalignment(dB)} = 20\log\frac{\|\mathbf{w}(n) - \mathbf{h}(n)\|}{\|\mathbf{h}(n)\|} \tag{6.6}$$

At the beginning of the plot, the system was adapted to the feedback path and the misalignment was low. The misalignment increased suddenly when the feedback path changed. With the first method, convergence was quite slow, as can be seen from the dashed line curve in Figure 6.3. With the new scheme, the misalignment did not change during the transition period because the adaptive filter was not updated. The new scheme accurately estimated the altered feedback path during the transition period and updated the adaptive filter at the end of the transition period, thus suddenly reducing the misalignment in a very short time (approximately 32 ms).

CHAPTER 7

PERCEPTUALLY MOTIVATED LOW-DELAY HEARING AID GAIN PROCESSING WITH HOWLING SUPPRESSION

In this chapter, we combine algorithms in Chapters 4, 5 and 6 to present the low-delay perceptually motivated signal processing (PMSP) method for digital hearing aids. A block diagram for the perceptually motivated signal processing (PMSP) for digital hearing aids with a microphone and a loudspeaker is shown in Figure 7.1. The PMSP can perform necessary signal processing for digital hearing aids with low-delay requirements and can provide higher hearing aid gains than possible with the state-of-the-art methods. The PMSP method is capable of handling sudden or rapid feedback path changes with low distortions in the output sound.

The rest of this chapter is organized as follows. The perceptually motivated signal processing (PMSP) method developed in this research is described in Section 7.1. Section 7.2 presents results and discussions from evaluations of the PMSP method.

7.1 Perceptually motivated signal processing

The perceptually motivated signal processing (PMSP) uses the low delay spectral gain shaping method (SGSM) to reduce delay requirements in the forward path. The adaptive feedback cancellation with the filtered-XLMS algorithm is performed as described in Table 5.1 and Table 5.2. Furthermore, the spectral analysis is performed on the error signal $e(n)$ and the microphone signal $u(n)$ to obtain spectrally distributed signal vectors $\mathbf{E}(k')$ and $\mathbf{U}(k')$, respectively. The spectral data follow the frequency domain block-based notations described in Section 5.1 of Chapter 5. The spectral analysis obtains new values every r samples at N_g frequencies in the operating frequency range, with k' denoting the time indices for signals after spectral analysis. The band i, $i = 0 \cdots N_g - 1$, of N_g bands represent frequency range of $\left[\frac{2\pi(i-1/2)}{N_g}, \frac{2\pi(i+1/2)}{N_g}\right]$. Among various available choices for the spectral analysis, we chose parallel-polyphase-network (PPN) based methods [95, 96, 135]. The PPN-based method uses DFT and polyphase implementation for the computational efficiency.

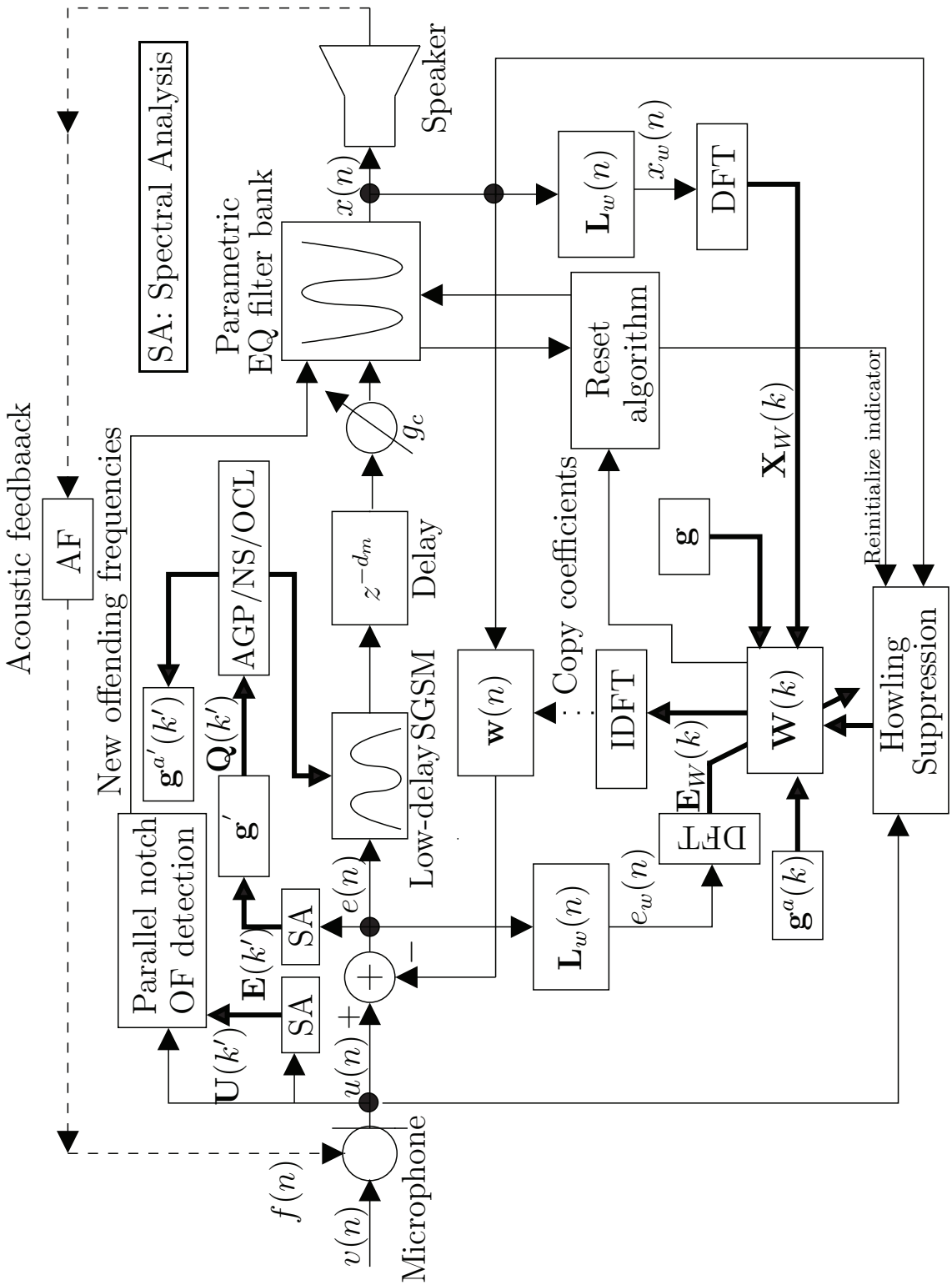

Figure 7.1: Simplified block diagram of the perceptually motivated signal processing.

This type of spectral analysis has been used by other researchers for similar structures where spectral weights are calculated offline and filtering is done in the time domain [95]. The spectrally distributed signal vectors $\mathbf{E}(k')$ and $\mathbf{U}(k')$ are used to find masking thresholds, the noise suppression filter and parameters of the output compression limiter. The noise suppression filter is calculated as described in Appendix B. The masking thresholds $T(k', i), i = 0 \cdots N_g - 1$ are calculated from the target amplified signal values $Q(k', i), i = 0 \cdots N_g - 1$, as shown in Figure 7.1. Subsequently, the masking threshold for the i^{th} frequency bin $T(k', i)$ is used to calculate the modified hearing aid gain value $g^{a'}(k', i)$ for this frequency bin. With the knowledge of the noise suppression filter values, the modified prescribed gain values and the output compression values, the desired spectral gain response $T(e^{j\omega})$ is given by

$$T(e^{j\omega}) = O\left(B_l(e^{j\omega})W_n(e^{j\omega})g^{a'}(e^{j\omega})\right) \tag{7.1}$$

$O(.)$ represents the dynamic compression operation and $B_l(e^{j\omega})$ is the desired hearing loss compensation and $g^{a'}(e^{j\omega})$ is the modified hearing aid gain function due to the adaptive gain processing. The modified hearing aid gain function $g^{a'}(e^{j\omega})$ can be derived from the modified hearing aid gain values $g^{a'}(k', i)$. Given $T(e^{j\omega})$ at $N_l + 1$ different frequencies $\omega_i, i = 0 \cdots N_l$, the low-delay gain shaping method calculates the $\mathbf{c_{eq}}$ values according to equation (5.3). Similarly, the spectral values $\mathbf{U}(k', i), i = 0 \cdots N_g - 1$ for the microphone signal $u(n)$ are used for energy monitoring to detect offending frequencies. The adaptive notch filters are used as described in Section 4.1.2.1 to monitor frequency range of the i^{th} band.

The reset algorithm works on the frequency domain adaptive filters coefficients $\mathbf{W}(k, j), j = 0 \cdots N_f - 1$. The reset algorithm monitors the j^{th} frequency bin of the adaptive filter coefficient $W(k, j)$ at time k to reset parametric EQ filters in the j^{th} frequency range - $[\frac{2\pi(j-1/2)}{N_f}, \frac{2\pi(j+1/2)}{N_f}]$. The reset algorithm also calculates a reinitialization indicator to start the howling suppression algorithm. The reinitialization indicator is set when at least N_f^r out of N_f bins deem the feedback path change. The feedback path change in the reset algorithm is described in Section 4.1.2.2.

Finally, the step size of the adaptive filter is modified based on the prescribed gain vector $\mathbf{g}$ and the modified prescribed gain vector $\mathbf{g}^a(k)$. The prescribed gain values in the vector $\mathbf{g}$ remains the same over time and can be calculated at the time of the hearing aid fitting from the audiogram of a patient. The N_f modified hearing aid gain values $g^a(k, j), j = 0 \cdots N_f - 1$ at time k are calculated from the N_g modified gain values at $g^{a'}(k', i), i = 0 \cdots N_g - 1$ by suitably interpolating N_f values from N_g values. With the above description, the complete perceptually motivated signal processing is listed in Table 7.1.

Table 7.1: Update equations for the perceptually motivated low-delay signal processing.

Initialization

$\mathbf{\Psi}(0)$	...	A diagonal matrix with large numbers
$\mathbf{S}(0)$	...	A vector with small positive constant
$\mathbf{W}(0)$	...	A vector with all zeros
$g_i^a(0) = g_i(0)$	...	for each band i
$\mathbf{L}_i(0)$	...	A column vector of length N_s with all zeros
$\mathbf{M}_i(0)$	...	A column vector of length N_s with all zeros
$\gamma_i^o(0)$	...	0

Sample Processing Iterations (for $n = 1, 2 \cdots$)

$$\mathbf{x}(n) = \left[\begin{array}{cccc} x(n) & x(n-1) & \cdots & x(n-N+1) \end{array} \right]^T$$

$$e(n) = u(n) - \mathbf{w}^T(n)\mathbf{x}(n)$$

$$e_w(n) = \mathbf{L_w}(n) \left[\begin{array}{cccc} e(n) & e(n-1) & \cdots & e(n-M_a) \end{array} \right]^T$$

$$x_w(n) = \mathbf{L_w}(n) \left[\begin{array}{cccc} x(n) & x(n-1) & \cdots & x(n-M_a) \end{array} \right]^T$$

Finding Linear Predictor Coefficients

$$\mathbf{z}(n) = \left[\begin{array}{cccc} e(n-1) & e(n-2) & \cdots & e(n-M_a) \end{array} \right]^T$$

$$e_w(n) = e(n) - \mathbf{z}^T(n)\mathbf{p}(n)$$

Calculate $D_s(n)$ according to (5.7)

$$\lambda(n) = \frac{\lambda_{max} - \lambda_{min}}{D_{max} - D_{min}}(D_s(n) - D_{min}) + \lambda_{min}$$

$$\mathbf{r}(n) = \frac{\mathbf{\Psi}(n)\mathbf{z}(n)}{\lambda(n) + \mathbf{z}^T(n)\mathbf{\Psi}(n)\mathbf{z}(n)}$$

$$\mathbf{p}(n+1) = \mathbf{p}(n) + \mathbf{r}(n)e_w(n)$$

$$\mathbf{\Psi}(n) = \frac{1}{\lambda(n)}(\mathbf{\Psi}(n) - \mathbf{r}(n)\mathbf{z}^T(n)\mathbf{\Psi}(n))$$

Adaptive notch filter update

$$s_i(n) = u(n) + \rho a_i(n-1)s_i(n-1) - \rho^2 s_i(n-2)$$

$$z_i(n) = s_i(n) - a_i(n-1)s_i(n-1) + s_i(n-2)$$

$$P_i(n) = \lambda_s P_i(n-1) + (1-\lambda_s)s_i^2(n-1)$$

$$a_i(n) = a_i(n-1) + \frac{\alpha_a}{P_i(n) + \epsilon_a} s_i(n-1)z_i(n)$$

$$a_i(n) = \begin{cases} 2\cos(2\pi f_i^l) & ; a_i(n) > 2\cos(2\pi f_i^l) \\ 2\cos(2\pi f_i^u) & ; a_i(n) < 2\cos(2\pi f_i^u) \\ a_i(n) & ;\text{otherwise} \end{cases}$$

ANF tracking monitor

$$a_i^m(n) = \lambda_m a_i^m(n-1) + (1-\lambda_m)a_i(n)$$

$$\gamma_i^a(n) = \begin{cases} \gamma_i^a(n-1) + 1 & ;|a_i(n) - a_i^m(n)| < \delta_q \\ 0 & ;\text{otherwise} \end{cases}$$

Spectral Gain Update (for $n = r, 2r \cdots$, $k' = n/r$, $i = 0 \cdots N_g - 1$)

$$p^r(k', i) = \begin{cases} 0 & \text{if } |Q(k', i)|^2 < T(k', i) \\ 1 & \text{else} \end{cases}$$

$$g^{a'}(k', i) = p^r(k', i)g'(k', i) + (1 - p^r(k', i))\eta g^{a'}(k', i)$$

$$g^{a'}(k', i) = \max[g^{a'}(k', i), G_m(k', i)]$$

Table 7.1 continued.

Energy growth monitor

$P^u(k',i) = |U(k',i)|^2$ and $\overline{P^u}(k',i) = \lambda_u \overline{P^u}(k'-1,i) + (1-\lambda_u)P^u(k',i)$

$P^b(k',i) = \min(\delta_b P^b(k'-1,i), \overline{P^u}(k',i))$

$$\gamma^r(k',i) = \begin{cases} \gamma^r(k'-1,i) + \Phi(P^\Delta(k',i)) & ;P^u(k',i) > T_b P^b(k',i) \\ 0 & ;\text{otherwise} \end{cases}$$

$\gamma^r(k',i) = \max(\gamma^r(k',i), \gamma^r_m)$

Offending frequency detection (when $n = rk'$)

if $\gamma^a_i(n) > T_a$ and $\gamma^r(k',i) > T_r$

$\Rightarrow$ Offending frequency detected, Add a parametric EQ at $\frac{1}{2\pi}\cos^{-1}(a(n)/2)$

$\Rightarrow \gamma^a_i(n) = 0, \gamma^r(k',i) = \gamma^r_m$

Frequency domain adaptive filtering (for $n = R, 2R\cdots$, $k = n/R$, $j = 0\cdots N_f - 1$)

$$\mathbf{e}_w(k) = \begin{bmatrix} e_w(kR) & e_w(kR+1) & \cdots & e_w((kR+R-1) \end{bmatrix}^T$$

$$\mathbf{E}_W(k) = \text{FFT}\left(\begin{bmatrix} \mathbf{0} \\ \mathbf{e}_w(k) \end{bmatrix}\right)$$

$$W(k+1,j) = W(k,j) + \frac{\mu_0}{S(k,j)}\left(\frac{g^a(k,i)}{g(k,i)}\right)^2 X_W(k,j)E^*_W(k,j) \text{ for } j = 0,\cdots,N_f-1$$

$$\mathbf{W}(k+1) = \text{FFT}\left(\begin{bmatrix} \text{the first N elements of IFFT}(\mathbf{W}(k+1)) \\ \mathbf{0} \end{bmatrix}\right)$$

$$\mathbf{S}(k+1) = \beta\mathbf{S}(k) + (1-\beta)\mathbf{X}_W(k+1) \bigodot \mathbf{X}^*_W(k+1)$$

Reset algorithm

$L(k,j) = \lambda_l L(k-1,j) + (1-\lambda_l)W(k,j)$

$M(k,j) = \lambda_h M(k-1,j) + (1-\lambda_h)W(k,j)$

$D(k,j) = L(k,j) - M(k,j)$ and $\kappa(k,j) = \dfrac{|D(k,j)|^2}{|L(k,j)|^2 + \epsilon_r}$

$$\gamma^o(k,j) = \begin{cases} \gamma^o(k-1,j) + 1 & ;\kappa(k,j) > \delta_o \\ 0 & ;\text{otherwise} \end{cases}$$

Detection

if $\gamma^o(k,j) > T_o$

$\Rightarrow$ Remove all parametric EQs in the frequency range $\left[\dfrac{2\pi(j-1/2)}{N_f}, \dfrac{2\pi(j+1/2)}{N_f}\right]$

Reinitialization indicator

$$B_r(k,j) = \begin{cases} 1 & ;\gamma^o(k,j) > T_o \\ 0 & ;\text{otherwise} \end{cases}$$

if $\mathbf{B}^T_r(k)\mathbf{B}(k) > N^r_f$

$\Rightarrow$ Recalculate adaptive filter coefficients using the howling suppression method in Section 6.2

- $\bigodot$ denotes element-by-element multiplication and $\mathbf{0}$ denotes column vector of length $N-1$.

7.2 Results and discussion

This section presents the results from MATLAB simulations of the hearing aid algorithms to demonstrate the performance of the perceptually motivated signal processing (PMSP) method and the classical scheme described in Section 2.2.2. The parameters for the classical subband method were $M = 128, L = 16, L_p = 128$. Both methods were evaluated in terms of the output sound quality and the hearing aid stability. The sampling frequency f_s used for all experiments was 16000 Hz. The true feedback path was simulated using a 192-tap FIR filter in parallel with a homogeneous quadratic nonlinearity, as described in Section 3.2. Coefficients for the linear component of the feedback paths were obtained from measurements of an inside-the-ear (ITE) hearing aid, as shown in Figure 4.2. The description of these feedback paths are provided in Section 4.2. Three feedback cases, as described in Section 4.2, were studied for both methods. Four hearing aid gain profiles shown in Figures 4.3a - 4.3d were used for evaluations of the both methods. Some of the parameters for the PMSP method were $T_r = 150$, $\delta_b = 1.0002$, $T_b = 6$, $\lambda_l = 0.99$, $\lambda_h = 0.7$, $\lambda_u = 0.9$ $\epsilon_r = 10^{-4}$, $\delta_o = 0.1$, $T_o = 10$, $r = 8$, $N_f^r = 32$, $g_c = 2$ and $N_g = 64$. Other parameters that were used in the experiment, but not mentioned here, were the same as given in Chapters 4, 5 and 6.

Six 80 seconds long input speech signals were used in this experiment. Additionally, car noise was added to the speech signals to create a signal-to-noise-ratio of 10 dB. The output sound quality in the steady state was subjectively evaluated for both methods. The perceived output sound quality of the hearing aid system for both structures was assessed with normal-hearing listeners. In order to work with normal-hearing listeners, the output of both methods was further processed with long linear-phase filters that equalized for the effects of the insertion gain of the hearing aid. To assess sound quality, six subjects participated in the listening test. The processed sounds were presented to them in both ears with a pair of headphones in a quiet place. Subjects rated each system under test on a scale from 1 to 5 as described in Section 5.2.4. The mean values with 95% confidence intervals of the user ratings, mTRI values and the processing delays for the PMSP method and the classical subband based method in the three feedback cases and four hearing aid gain profiles are listed in Table 7.2. In Table 7.2, "ST" indicates that the system was stable during the experiment and "US" indicates the system went into howling and did not became stable. When the system went into instability, user ratings were not obtained for that experiment. User ratings in Table 7.2 indicate that the classical method and the PMSP method yielded good output sound quality for profiles 1 to 3 in the steady state. In transient situations of the experiments, both methods were stable for the profiles 1 and 2 in all the feedback cases. The classical method went into instability for 0.6 second for the feedback case 3 when the hearing aid gain profile 3 was used. For the same situation (feedback case 3 and profile 3), the PMSP method kept the hearing aid system stable, as indicated by the mTRI

Table 7.2: Output sound quality for the perceptually motivated signal processing method and the classical method.

Profile	Measures	Feedback situation					
		1		2		3	
		PMSP	Classical	PMSP	Classical	PMSP	Classical
1	User ratings	4.1±0.3	4.0±0.4	4.0±0.4	4.1±0.3	4.0±0.3	4.1±0.3
	mTRI	ST	ST	ST	ST	ST	ST
	Max delay(ms)	2.1	8	2.3	8	2.0	8
2	User ratings	4.1±0.3	4.0±0.4	4.1±0.3	4.0±0.3	4.1±0.4	4.1±0.3
	mTRI	ST	ST	ST	ST	ST	ST
	Max delay(ms)	1.9	8	2.1	8	2.1	8
3	User ratings	4.0±0.3	4.1±0.4	4.0±0.3	4.1±0.4	4.0±0.4	4.1±0.3
	mTRI	ST	ST	ST	ST	ST	0.6
	Max delay(ms)	2.1	8	2.4	8	2.3	8
4	User ratings	4.0±0.3	US	4.1±0.4	US	4.1±0.4	US
	mTRI	0.1	US	0.1	US	0.3	US
	Max delay(ms)	4.2	8	3.9	8	4.1	8

values in Table 7.2. In each situation, the PMSP method required lower delay values compared to the classical subband design. The classical subband method was unstable for all the feedback cases when the hearing aid gain profile 4 was used. On the other hand, the PMSP system was stable and the output sound quality was good in the steady state as indicated by the user ratings in Table 7.2 for all the three feedback cases. The PMSP method was briefly unstable during transient periods for the feedback case 3 and the hearing aid gain profile 4. However, the instability was detected and suppressed in less that 0.3 second. Finally, it is clear from Table 7.2 that the overall hearing aid delay in the forward path for the PMSP method was smaller than the classical subband method in all the experiments.

CHAPTER 8

CONCLUSION AND FUTURE WORK

This dissertation presented methods for modifying the forward path gain in a hearing aid to improve adaptive feedback cancellation efficiency. The gain modification is based on perceptual redundancy in the input signal and gain reductions in narrowband frequency regions with parametric EQ filters. MATLAB simulations with speech and music signals indicate that the gain modifications presented in this dissertation provide $8-12$ dB of additional stable gain over traditional approaches. The reset algorithm successfully eliminated unnecessary filters placed in the signal path during the transient periods. Psychophysical experiments suggest that this dissertation's method also delivers perceptually better output sound quality without compromising loudness in the output sound. Consequently, the method of this dissertation may be a better alternative to currently used techniques for hearing aid signal processing.

A major advantage of the method of this dissertation is that it reduces broadband delays in the forward path for signal processing in hearing aids. The key element of the low-delay hearing aid structure presented in this dissertation is the spectral gain shaping method that utilizes parametric equalization filters. Results of extensive performance evaluation presented in the dissertation reveal that the low-delay signal processing used in this work requires much smaller forward path delays than a state-of-the-art subband-based method. A comparison of our implementations of this system has indicated that the low-delay structure has comparable or lower computational complexity than subband realizations evaluated in this dissertation. This work paves the way for an alternative solution to the widely used subband method for implementing hearing aid signal processing algorithms and reducing the unwanted effects of the long and broadband forward path delays.

Finally, a novel howling suppression scheme based on the least-squares method is presented in this dissertation. This scheme has faster convergence than conventional howling suppression methods. The least-squares estimate used in the howling suppression method is implemented with a linear complexity. The system also employs a perceptually motivated gain control algorithm that allows stable operation. The distortions occurring during the transition period are kept below the perceptual threshold of the listener because they are masked by the temporal masking phenomenon in the human auditory system.

8.1 Future work

In the adaptive gain processing, we only considered frequency-based masking models. Temporal masking can be included in the work to get more added stable gains. Several models on temporal masking are available in the literature [99, 136–138]. Many of these models were developed to achieve higher efficiency in audio coding by reducing redundant components. These models can be included to adaptively change gain of the hearing aid for the input signal if it is masked due to components that occurred earlier in time. Furthermore, the computational efficiency of the adaptive gain processing can be improved using low-complexity masking models [98, 139, 140].

In this research, we have used auditory models from the normal-hearing listeners. The normal-hearing auditory model was used because it is straight-forward to implement and provides us with the benefits of the methods presented in this dissertation. On the other hand, modeling hearing-impaired auditory systems is challenging because it depends on the degree and the type of hearing loss and is substantially different from normal-hearing listeners [141–145]. Specifically, auditory filters are wider for hearing-impaired listeners than normal-hearing listeners [146, 147], the additive masking effect is larger in hearing-impaired listeners than in normal-hearing listeners [148, 149] and the growth of masking is more gradual in hearing-impaired listeners [150–153]. We believe that the benefits will be even greater and more suitable for hearing-impaired listeners if the auditory models for hearing-impaired listeners are used. Researchers have developed mathematical models that can predict some of the parameters for the hearing-impaired auditory systems [154–157]. These models can be used for the processing developed in this dissertation to provide greater benefits to hearing-impaired listeners on an individual basis.

The computational load of the hearing aid structure in this dissertation can be further reduced by incorporating the parametric EQ bank into the low-delay spectral gain shaping. This can be achieved by incorporating the frequency response of a parametric EQ filter into the desired response at the time of optimization in the low-delay spectral gain shaping. Finally, the computational complexity of the howling suppressor presented in the dissertation can be further reduced using superfast Toeplitz solvers [158–162].

APPENDIX A

SOLVING LINEAR TOEPLITZ SYSTEMS

In this appendix, we present an algorithm to solve the N linear Toeplitz equations for $N = 2^k$ where k is a positive integer [45]. The algorithm requires $2N^2 + 8N\log_2 N - N$ operations to solve it. Consider the the set of linear equations given by equation (A.1)

$$\mathbf{X}^T(n)\hat{\mathbf{w}}(n) = \mathbf{d}(n) \tag{A.1}$$

where $\mathbf{X}^T(n)$ is a $N \times N$ Toeplitz matrix and its $(j,k)^{th}$ entry is $x(n-N+1+(j-k))$. $\mathbf{d}(n)$ (6.3) is a $N \times 1$ vector. Now, we define some notations that will be used in the algorithm presented here. "$\sim$" on a column vector represents reverse order of entries. $\mathbf{0}_{N\times 1}$ is a column vector with N zeros. The steps of the algorithm are given below.

Step 1. **Initialization:**

$$\lambda_0 = x(n-N+1)$$

$$a_0 = b_0 = r_0 = s_0 = \text{Null vector}$$

Step 2. **Recursions:** for $k = 0$ to $N-2$

$$\alpha_k = \frac{-1}{\lambda_k}(x(n-N+1+k+1) + \mathbf{a}_k^T\tilde{\mathbf{r}}_k) \tag{A.2}$$

$$\beta_k = \frac{-1}{\lambda_k}(x(n-N+1-k-1) + \mathbf{s}_k^T\tilde{\mathbf{b}}_k) \tag{A.3}$$

$$\mathbf{a}_{k+1} = \begin{bmatrix} \mathbf{a}_k + \alpha_k\tilde{\mathbf{b}}_k \\ \alpha_k \end{bmatrix} \quad \mathbf{b}_{k+1} = \begin{bmatrix} \beta_k \\ \tilde{\mathbf{b}}_k + \beta_k\mathbf{a}_k \end{bmatrix} \tag{A.4}$$

$$\lambda_{k+1} = \lambda_k(1-\alpha_k\beta_k) \tag{A.5}$$

$$\mathbf{r}_k = \begin{bmatrix} \mathbf{r}_k \\ x(n-N+2) \end{bmatrix} \quad \mathbf{s}_k = \begin{bmatrix} \mathbf{s}_k \\ x(n-N-k) \end{bmatrix} \tag{A.6}$$

Step 3. i) **Extend Vectors**

$$\mathbf{a_e} = \begin{bmatrix} 1 \\ \mathbf{a}_{N-1} \\ \mathbf{0}_{N\times 1} \end{bmatrix} \quad \mathbf{b_e} = \begin{bmatrix} 1 \\ \mathbf{0}_{N\times 1} \\ \tilde{\mathbf{b}}_{N-1} \end{bmatrix} \quad \mathbf{d_e} = \begin{bmatrix} \mathbf{d}(n) \\ \mathbf{0}_{N\times 1} \end{bmatrix} \tag{A.7}$$

ii) **Compute FFTs**

$$\mathbf{a_e^f} = \text{FFT}(\mathbf{a_e}), \mathbf{b_e^f} = \text{FFT}(\mathbf{b_e}), \mathbf{d_e^f} = \text{FFT}(\mathbf{d_e})$$
$$\mathbf{u^f} = \mathbf{a_e^f} \bigodot \mathbf{d_e^f}, \quad \mathbf{v^f} = \mathbf{b_e^f} \bigodot \mathbf{d_e^f}$$

Note: $\bigodot$ denotes element by element multiplication of vectors.

iii) **Compute IFFTs**

$$\mathbf{u} = \text{IFFT}(\mathbf{u^f}), \quad \mathbf{v} = \text{IFFT}(\mathbf{v^f})$$
$$\mathbf{p}(m) = \mathbf{v}(m), \mathbf{q}(m) = \mathbf{u}(m+N) \text{ for } 1 \le m \le N$$
$$\mathbf{p}(m) = \mathbf{q}(m) = 0 \text{ for } N+1 \le m \le 2N$$

iv) **Desired Output**

$$\mathbf{x^f} = \mathbf{a_e^f}(m)\mathbf{p}(m) + (-1)^m \mathbf{b_e^f}(m)\mathbf{q}(m) \text{ for } 1 \le m \le 2N \tag{A.8}$$

$$\text{Compute} \quad \mathbf{x} = \text{IFFT}(\mathbf{x^f})$$
$$\hat{\mathbf{w}}(n) = \frac{\mathbf{x}(1:N)}{\lambda_{N-1}} \tag{A.9}$$

APPENDIX B

NOISE SUPPRESSION FILTER

In this appendix, we briefly describe a method to determine the postfilter weights $W_n(k, \omega_l)$ [36] to reduce noise in a band of frequencies centered around ω_l at time k for audio signal $X(k, \omega_l)$. These weights are obtained from the instantaneous spectral power $P_x(k, \omega_l) = |X(k, \omega_l)|^2$. Sub-band components are used to obtain instantaneous spectral power in each band whereas off-the-forward-path discrete Fourier transform (DFT) is used to obtain spectral power to generate the postfilter weights for the low-delay method. Given the instantaneous spectral power in the l^{th} band, the postfilter weight that represents the amount of suppression for that band is calculated as

$$W_n(k, \omega_l) = \frac{\hat{\xi}(k, \omega_l)}{1 + \hat{\xi}(k, \omega_l)} \tag{B.1}$$

where $\hat{\xi}(k, \omega_l)$ denotes estimate of the *a priori* signal-to-noise ratio and is calculated using a decision-directed approach as

$$\hat{\xi}(k, \omega_l) = \alpha_p \frac{|\hat{P_x}^c(k-1, \omega_l)|^2}{E(|P_x^n(k-1, \omega_l)|^2)} + (1 - \alpha_p)\text{max}(\gamma(k, \omega_l) - 1, 0) \tag{B.2}$$

where $0 < \alpha_p < 1$, $\gamma(k, \omega_l)$ is the *a posteriori* estimate of the signal-to-noise ratio defined as

$$\gamma(k, \omega_l) = \frac{|P_x(k, \omega_l)|^2}{E(|P_x^n(k, \omega_l)|^2)} \tag{B.3}$$

$\hat{P_x}^c(k, \omega_l - 1)$ is an estimate of the power of the clean audio in the last time frame given by

$$\hat{P_x}^c(k-1, \omega_l) = W_n(k-1, \omega_l) P_x(k-1, \omega_l) \tag{B.4}$$

and $P_x^n(k-1, \omega_l)$ is an estimate of the background noise power estimated as

$$P_x^n(k, \omega_l) = \text{min}(\epsilon_n P_x^n(k-1, \omega_l), P_x(k, \omega_l)) \tag{B.5}$$

where ϵ_n is a constant such that $\epsilon_n > 1$.

REFERENCES

[1] Frost and Sullivan, *World Audiology Product Markets*. San Diego, CA: Frost and Sullivan, 1997.

[2] J. E. Greenberg, P. M. Zurek, and M. Brantley, "Evaluation of feedback-reduction algorithms for hearing aids," *Journal of the Acoustical Society of America*, vol. 108, no. 5, pp. 2366–2376, Nov. 2000.

[3] S. Wyrsch and A. Kaelin, "Subband signal processing for hearing aids," *Proc. IEEE Intl. Symposium on Circuits and Systems*, vol. 3, no. 3, pp. 29–32, Orlando, FL, Jul. 1999.

[4] J. M. Kates and K. H. Arehart, "Multichannel dynamic-range compression using digital frequency warping," *EURASIP Journal on Applied Signal Processing*, vol. 18, no. 1, pp. 3003–3014, Jan. 2005.

[5] J. E. Greenberg, "Modified LMS algorithms for speech processing with an adaptive noise canceller," *IEEE Trans. on Speech and Audio Processing*, vol. 6, no. 4, pp. 338–350, Jul. 1998.

[6] J. A. Maxwell and P. M. Zurek, "Reducing acoustic feedback in hearing aids," *IEEE Trans. on Speech and Audio Processing*, vol. 3, no. 4, pp. 304–313, Jul. 1995.

[7] M. G. Siqueira and A. Alwan, "Steady-state analysis of continuous adaptation in acoustic feedback reduction systems for hearing aids," *IEEE Trans. on Speech and Audio Processing*, vol. 8, no. 4, pp. 443–453, Jul. 2000.

[8] H.-F. Chi, S.-X. Gao, S.-D. Soli, and A. Alwan, "Band-limited feedback cancellation with a modified filtered-XLMS algorithm for hearing aids," *Speech Communication*, vol. 39, pp. 147–161, 2003.

[9] R. Brennan and T. Schneider, "A flexible filterbank structure for extensive signal manipulations in digital hearing aids," *Proc. IEEE Intl. Symposium on Circuits and Systems*, vol. 6, no. 31, pp. 569–572, Monterey, CA, Jun. 1998.

[10] H. A. L. Joson, F. Asano, and T. Sone, "Adaptive feedback cancellation with frequency compression for hearing aids," *Journal of the Acoustical Society of America*, vol. 94, no. 6, pp. 3248–3254, Dec. 1993.

[11] Y.-C. Park, I.-Y. Kim, and S.-M. Lee, "An efficient adaptive feedback cancellation for hearing aids," *Proc. 25th Annual Intl. Conf. of the IEEE on Engineering in Medicine and Biology Society*, vol. 2, pp. 1647–1650, Apr. 2004.

[12] B. Farhang-Boroujeny, *Adaptive Filter: Theory and Applications*, 1st ed. Chichester, UK: John Wiley and Sons, 1998.

[13] A. Kaelin, A. Lindgren, and S. Wyrsch, "A digital frequency domain implementation of a very high gain hearing aid with compensation for recruitment of loudness and acoustic echo cancellation," *Signal Processing*, vol. 64, pp. 71–85, 1998.

[14] J. Hellgren, “Analysis of feedback cancellation in hearing aids with filtered-XLMS and the direct method of closed loop identification,” *IEEE Trans. on Speech and Audio Processing*, vol. 10, no. 2, pp. 119–131, Feb. 2002.

[15] J. M. Kates, “Room reverberation effects in hearing aid feedback cancellation,” *Journal of the Acoustical Society of America*, vol. 109, no. 1, pp. 367–378, Jan. 2001.

[16] R. Wang and R. Harjani, “Suppression of acoustic oscillations in hearing aids using minimum phase techniques,” *Proc. IEEE Intl. Symposium on Systems and Circuits*, pp. 3–6, Minneapolis, US, May 1993.

[17] J. M. Harte and S. J. Elliott, “A comparison of various nonlinear models of cochlear compression,” *Journal of the Acoustical Society of America*, vol. 117, no. 6, pp. 3777–3786, Jun. 2005.

[18] T. Gansler and P. Eneroth, “Influence of audio coding on stereophonic acoustic echo cancellation,” *Proc. IEEE Intl. Conf. Acoustics Speech and Signal Processing*, vol. 6, pp. 3649 – 3652, May 1998.

[19] W. Jesteadt, S. P. Bacon, and J. R. Lehman, “Forward masking as a function of frequency, masker level, and signal delay,” *Journal of the Acoustical Society of America*, vol. 71, pp. 950–962, Apr. 1982.

[20] G. Kidd Jr. and L. L. Feth, “Effects of masker duration in pure-tone forward masking,” *Journal of the Acoustical Society of America*, vol. 72, pp. 1384–1386, Nov. 1982.

[21] B. C. J. Moore and B. R. Glasberg, “Growth of forward masking for sinusoidal and noise maskers as a function of signal delay; implications for suppression in noise,” *Journal of the Acoustical Society of America*, vol. 73, pp. 1249–1259, Apr. 1983.

[22] D. E. Tsoukalas, J. N. Mourjopoulos, and G. Kokkinakis, “Speech enhancement based on audible noise suppression,” *IEEE Trans. on Speech and Audio Processing*, vol. 5, no. 6, pp. 497–514, Nov. 1997.

[23] J. D. Johnston, “Transform coding of audio signals using perceptual noise criteria,” *IEEE Journal on Selected Areas in Communications*, vol. 6, no. 2, pp. 314–323, Feb. 1988.

[24] M. R. Schroeder, B. S. Atal, and J. L. Hall, “Optimizing digital speech coders by exploiting masking properties of the human ear,” *Journal of the Acoustical Society of America*, vol. 66, no. 6, pp. 1647–1651, Dec. 1979.

[25] S. M. Kuo and J. Chen, “New adaptive IIR notch filter and its application to howling control in speakerphone system,” *Electronics Letters*, vol. 28, no. 8, pp. 764–766, Apr. 1992.

[26] V. Hamacher, J. Chalupper, J. Eggers, E. Fischer, U. Kornagel, H. Puder, and U. Rass, “Signal processing in high-end hearing aids: State of the art, challenges, and future trends,” *EURASIP Journal on Applied Signal Processing*, vol. 18, pp. 2915–2929, 2005.

[27] D. Troxel, “Method and apparatus for identifying feedback in a circuit,” U.S. Patent 20 060 215 852A1, Sep., 2006.

[28] M. Harteneck, S. Weiss, and R. W. Stewart, “Design of near perfect reconstruction oversampled filter banks for subband adaptive filters,” *IEEE Trans. on Circuits and Systems*, vol. 46, no. 8, pp. 1081–1086, Aug. 1999.

[29] M. B. Sachs, I. C. Bruce, R. L. Miller, and E. D. Young, “Biological basis of hearing-aid design,” *Annals of Biomedical Engineering*, vol. 30, no. 2, pp. 157–168, Feb. 2002.

[30] J. Ryan and S. Tewari, "A digital signal processor for musicians and audiophiles," *Hearing Review*, vol. 16, no. 2, pp. 38–41, Feb. 2009.

[31] J. Agnew and J. M. Thornton, "Just noticeable and objectionable group delays in digital hearing aids," *Journal of the American Academy of Audiology*, vol. 11, no. 6, pp. 330–336, Jun. 2000.

[32] M. A. Stone and B. C. J. Moore, "Tolerable hearing aids delays. I: Estimation of limits imposed by the auditory path alone using simulated hearing losses," *Ear and Hearing*, vol. 20, no. 3, pp. 182–192, Jun. 1999.

[33] ——, "Tolerable hearing aids delays. II: Estimation of limits imposed during speech production," *Journal of the American Academy of Audiology*, vol. 11, no. 6, pp. 325–338, Aug. 2002.

[34] S. A. White, "Design of a digital biquadratic peaking or notch filter for digital audio equalization," *Journal of the Acoustical Society of America*, vol. 34, no. 6, pp. 479–483, Jun. 1986.

[35] S. J. Orfanidis, "High-order digital parametric equalizer design," *Journal of the Acoustical Society of America*, vol. 53, no. 11, pp. 1026–1046, Nov. 2005.

[36] E. Hansler and G. Schmidt, *Acoustic Echo and Noise Control: A Practical Approach*, 1st ed. NJ: John Wiley and Sons, 2004.

[37] G. Ramos, J. J. Lopez, and J. Lloret, "Direct method with random optimization for loudspeaker equalization using IIR parametric filters," *Proc. Intl. Conf. on Acoustics Signal and Systems Processing*, vol. 5, no. 10, pp. 97–100, Montreal, Quebec, Canada, May 2004.

[38] D. Wit, P. Robert, A. J. Kaizer, O. D. Beek, and J. Frans, "Numerical optimization of the crossover filters in a multiway loudspeaker system," *Journal of the Audio Engineering Society*, vol. 34, no. 3, pp. 115–123, Mar. 1986.

[39] W. A. Yost and N. D. W., *Fundamentals of Hearing: An Introduction*, 1st ed. San Diego, CA: Academic Press, 1985.

[40] D. R. Morgan and J. C. Thi, "A delayless subband adaptive filter structure," *IEEE Trans. on Signal Processing*, vol. 43, pp. 1819–1830, Aug. 1995.

[41] J. Hellgren, "Variations in the feedback of hearing aids," *Journal of the Acoustical Society of America*, vol. 106, no. 5, pp. 2821–2833, Nov. 1999.

[42] J. Cioffi and T. Kailath, "Fast recursive-least-squares transversal filters for adaptive filtering," *IEEE Trans. on Acoustics Speech and Signal Processing*, vol. 32, no. 1, pp. 304–337, Apr. 1984.

[43] J. M. Cioffi and T. Kailath, "An efficient RLS data-driven echo canceller for fast initialization of full-duplex data transmission," *IEEE Trans. on Communications*, vol. 33, no. 7, pp. 601–611, Jul. 1985.

[44] J. J. Shynk, "Adaptive IIR filtering," *IEEE ASSP Magazine*, vol. 6, no. 2, pp. 4–21, Apr. 1989.

[45] J. R. Jain, "An efficient algorithm for a large Toeplitz set of linear equations," *IEEE Trans. on Acoustics Speech and Signal Processing*, vol. 27, no. 6, pp. 612–615, Dec. 1979.

[46] R. Brent, F. Gustavson, and D. Yun, "Fast solution of Toeplitz systems of equations and computation of padé approximants," *Journal of Algorithms*, vol. 1, pp. 259 –295, 1980.

[47] F. D. Hoog, "A new algorithm for solving Toeplitz systems of equations," *Linear Algebra and its Applications*, vol. 88, pp. 123–138, 1987.

[48] T. Chan and J. Olkin, "Circulant preconditioners for Toeplitz-block matrices," *Numerical Algorithms*, vol. 6, pp. 1079–1090, 1992.

[49] R. Freund, "A transpose-free quasi-minimal residual algorithm for non-Hermitian linear systems," *SIAM Journal on Scientific Computing*, vol. 14, no. 2, pp. 470–482, Mar. 1993.

[50] R. Kumar, "A fast algorithm for solving a Toeplitz system of equations," *IEEE Trans. on Acoustics Speech Signal and Processing*, vol. 33, no. 1, pp. 254–267, Feb. 1985.

[51] G. Golub and C. V. Loan, *Matrix Computations*, 2nd ed. Baltimore, MD: The John Hopkins University Press, 1989.

[52] H. Dillon, *Hearing Aids*, 1st ed. New York, NY: Thieme Medical Publishers Inc., 2001.

[53] B. Rafaely and J. L. Hayes, "On the modeling of the vent path in hearing aid systems," *Journal of the Acoustical Society of America*, vol. 109, no. 4, pp. 1747–1749, Apr. 2001.

[54] H. Nyquist, "Regeneration theory," *Bell Systems Technology Journal*, vol. 11, pp. 126–147, 1932.

[55] B. Rafaely and M. Roccasalva-Firenze, "Control of feedback in hearing aids - a robust filter design approach," *IEEE Trans. on Speech and Audio Processing*, vol. 8, no. 6, pp. 531–534, Nov. 2000.

[56] D. K. Bustamante, T. L. Worral, and M. Williamson, "Measurement of adaptive suppression of acoustic feedback in hearing aids," *Proc. IEEE Intl. Conf. Acoustics Speech and Signal Processing*, vol. 3, pp. 2017–2020, Glasgow, UK, May 1989.

[57] J. Agnew, "Application of a notch filter to reduce acoustic feedback," *Hearing Journal*, vol. 46, no. 3, pp. 37–43, 1993.

[58] A. Beex, "Moving average notch filter," U.S. Patent 4 232 192, Nov., 1980.

[59] J. M. Kates, "Feedback cancellation in hearing aids: Results from a computer simulation," *IEEE Trans. on Signal Processing*, vol. 39, pp. 553–562, Mar. 1991.

[60] H. Levitt, R. S. Gugot, and K. W. Kopper, "Programmable digital hearing aid system," U.S. Patent 4 731 850, Mar., 1988.

[61] M. Bennett and L. Browne, "A controlled feedback hearing aid," *Hearing Aid Journal*, vol. 33, no. 5, pp. 42–43, Dec. 1980.

[62] M. R. Schroeder, "Improvement of acoustic feedback stability in public address systems," *Journal of the Acoustical Society of America*, vol. 31, no. 6, pp. 851–852, Jun. 1959.

[63] L. Ljung, *System Identification: Theory for the User*, 2nd ed. Upper Saddle River, NJ: Prentice Hall, 1999.

[64] B. Strope and A. Alwan, "A novel structure to compensate for frequency-dependent loudness recruitment of sensorineural hearing loss," *Proc. IEEE Intl. Conf. on Audio Speech and Signal Processing*, vol. 5, pp. 3539–3542, Detroit, MI, May 1995.

[65] J. P. Campbell and T. E. Tremain, "Voiced/unvoiced classification of speech with applications to the U.S. government LPC-10E algorithm," *Proc. IEEE Intl. Conf. Acoustics, Speech and Signal Processing*, vol. 1, pp. 473–476, Tokyo, Japan, Apr. 1986.

[66] V. Parsa and D. G. Jamieson, "Adaptive modelling of digital hearing aids using a subband affine projection algorithm," *Proc. IEEE Intl. Conf. on Acoustics Speech and Signal Processing*, vol. 2, pp. 1937–1940, May 2002.

[67] O. Dyrlund and N. Bisgaard, "Acoustic feedback margin improvements in hearing instruments using a prototype DFS (digital feedback suppression) system," *Scand Audiology*, vol. 20, pp. 49–53, 1991.

[68] O. Dyrlun, L. B. Henningsen, N. Bisgaard, and J. H. Jensen, "Digital feedback suppression (DFS): Characterization of feedback margin improvements in a DFS hearing instrument," *Scand Audiology*, vol. 23, pp. 135–138, 1994.

[69] A. M. Engebretson and M. French-St. George, "Properties of an adaptive feedback equalization algorithm," *Journal of Rehabilitation Research and Development*, vol. 30, no. 1, pp. 8–16, 1993.

[70] A. M. Engebretson, M. P. O'Connell, and F. Gong, "An adaptive feedback equalization algorithm for the CID digital hearing aid," *Proc. 12th Annual Intl. Conf. of the IEEE on Engineering in Medicine, Part 5*, vol. 12, no. 5, pp. 2286–2287, Philadelphia, PA, Nov. 1990.

[71] M. Ali, "Stereophonic acoustic echo cancellation system using time-varying all-pass filtering for signal decorrelation," *Proc. IEEE Intl. Conf. Acoustics Speech and Signal Processing*, pp. 3689–3692, Apr. 1998.

[72] Y.-C. Park, D.-W. Kim, and I.-Y. Kim, "An efficient feedback cancellation for multiband compression hearing aids," *Proc. 20th Annual Intl. Conf. of the IEEE on Engineering in Medicine and Biology Society*, vol. 5, pp. 2706–2709, Hong Kong, Oct. 1998.

[73] J. M. Kates, "Constrained adaptation for feedback cancellation in hearing aids," *Journal of the Acoustical society of America*, vol. 106, pp. 1010–1019, Aug. 1998.

[74] D. Graupe, J. Grosspietsch, and S. P. Basseas, "Method of and means for adaptively filtering screeching noise caused by acoustic feedback," U.S. Patent 4 783 818, Nov., 1988.

[75] M. French-St. George, D. J. Wood, and A. M. Engebretson, "Behavioral assessment of adaptive feedback cancellation in a digital hearing aid," *Journal of Rehabilitation Research and Development*, vol. 30, pp. 17–25, Jan. 1993.

[76] H. F. Chi, "Adaptive feedback cancellation for hearing aids: Theories, algorithms, computations, and systems," Ph.D. dissertation, Department of Electrical Engineering, UCLA, CA, 1999.

[77] J. Hellgren and U. Forssell, "Bias of feedback cancellation algorithms in hearing aids based on direct closed loop identification," *IEEE Trans. on Speech and Audio Processing*, vol. 9, no. 7, pp. 906–913, Nov. 2001.

[78] B. Farhang-Boroujeny, "Fast LMS/Newton algorithms based on autoregressive modeling and their application to acoustic echo cancellation," *IEEE Trans. on Signal Processing*, vol. 45, pp. 1987–2000, Aug. 1997.

[79] A. Spriet, M. Moonen, and I. Proudler, "Feedback cancellation in hearing aids: An unbiased modelling approach," *Proc. European Signal Processing Conf. EUSIPCO*, vol. 1, pp. 531–534, Sep. 2002.

[80] S. Haykin, *Adaptive Filter Theory*, 2nd ed. Upper Saddle River, NJ: Prentice Hall, 1991.

[81] P. Estermann and A. Kaelin, "Feedback cancellation in hearing aids: Results from using frequency-domain adaptive filters," *Proc. IEEE Intl. Symposium on Circuits and Systems*, vol. 2, pp. 257–260, London, UK, Jun. 1994.

[82] F. Thomas and P. Jacques, "Acoustic feedback cancellation for hearing-aids using multi-delay filter," *Proc. NORSIG Signal Processing Symposium*, Trondheim, Norway, Oct. 2002.

[83] R. E. Crochiere and L. R. Rabiner, *Multirate Digital Signal Processing*, 1st ed. Upper Saddle River, NJ: Prentice Hall, 1996.

[84] T. Glzow, A. Engelsberg, and U. Heute, "Comparison of a discrete wavelet transformation and a nonuniform polyphase filterbank applied to spectral-subtraction speech enhancement," *Signal Processing*, vol. 64, no. 1, pp. 5–19, Jan. 1998.

[85] I. Cohen, "Enhancement of speech using Bark-scaled wavelet packet decomposition," *Proc. 7th European Conference on Speech Communication and Technology*, pp. 1933–1936, Sep. 2001.

[86] T. Fillon and J. Prado, "Evaluation of an ERB frequency scale noise reduction for hearing aids: A comparative study," *Speech Communication*, vol. 39, no. 1-2, pp. 23–32, 2003.

[87] I. Cohen and B. Berdugo, "Speech enhancement for non-stationary noise environments," *Signal Processing*, vol. 81, pp. 2403–2418, Aug. 2001.

[88] Y. Deng, V. Mathews, and B. Farhang-Boroujeny, "Low-delay nonuniform pseudo-QMF banks with application to speech enhancement," *IEEE Trans. on Signal Processing*, vol. 55, no. 5, pp. 2110–2121, May 2007.

[89] S. Weiss, A. Stenger, R. W. Stewart, and R. Rabenstein, "Steady-state performance limitations of subband adaptive filters," *IEEE Trans. on Signal Processing*, vol. 49, no. 9, pp. 1982–1991, Sep. 2001.

[90] R. Dong, D. Hermann, R. Brennan, and E. Chau, "Joint filterbank structures for integrating audio coding into hearing aid applications," *Proc. IEEE Intl. Conf. Acoustic Speech and Signal Processing*, vol. 5, pp. 1533–1536, Las Vegas, NV, Apr. 2007.

[91] B. Widrow and S. D. Stearns, *Adaptive Signal Processing*, 1st ed. Upper Saddle River, NJ: Prentice Hall, 1999.

[92] S. C. Douglas and T.-Y. Meng, "Normalized data non-linearities for LMS adaptation," *IEEE Trans. on Signal Processing*, vol. 42, no. 6, pp. 1352–1356, Jun. 1994.

[93] J. M. D. Haan, N. Grbic, I. Claesson, and S. Nordholm, "Design of oversampled uniform DFT filter banks with delay specification using quadratic optimization," *Proc. IEEE Intl. Conf. Acoustics Speech and Signal Processing*, vol. 6, pp. 3633–3636, Salt Lake City, UT, May 2001.

[94] R. W. Buml and W. Srgel, "Uniform polyphase filter banks for use in hearing aids: design and constraints," *Proc. 16th European Signal Processing Conference*, pp. 3615–3622, Lausanne, Switzerland, Aug. 2008.

[95] P. Vary, “An adaptive filter-bank equalizer for speech enhancement,” *Signal Processing*, vol. 86, no. 6, pp. 1206–1214, 2006.

[96] H. W. Lollmann and P. Vary, “Uniform and warped low delay filter-banks for speech enhancement,” *Speech Communication*, vol. 49, no. 7, pp. 574–587, 2007.

[97] N. Virag, “Single channel speech enhancement based on masking properties of the human auditory system,” *IEEE Trans. on Speech and Audio Processing*, vol. 7, no. 2, pp. 126–137, Mar. 1999.

[98] C. Taal and R. Heusdens, “A low-complexity spectro-temporal based perceptual model,” *Proc. IEEE Intl. Conf. Acoustics Speech and Signal Processing*, vol. 5, pp. 153 – 156, Taipei, Taiwan, Apr. 2009.

[99] S. Ganapathy, P. Motlicek, H. Hermansky, and H. Garudadri, “Temporal masking for bit-rate reduction in audio codec based on frequency domain linear prediction,” *Proc. Intl. Conf. Acoustics Speech and Signal Processing*, vol. 5, pp. 4781 – 4784, Las Vegas, NV, Apr. 2008.

[100] S. A. Gelfand, *Essentials of Audiology*, 3rd ed. New York, NY: Thieme Medical Publishers, 2009.

[101] E. Terhart, “Calculating virtual pitch,” *Hearing Research*, vol. 1, pp. 155–182, 1979.

[102] E. Zwicker and H. Fastl, *Psychoacoustics: Facts and Models*, 2nd ed. Berlin, Germany: Springer Verlag, 1999.

[103] S. A. Gelfand, *Hearing: An Introduction to Psychological and Physiological Acoustics*, 4th ed. New York, NY: Informa Healthcare, 2004.

[104] B. Scharf, “Critical Bands, in foundations of modern auditory theory,” *New York: Academic Press*, 1970.

[105] R. Hellman, “Asymmetry of masking between noise and tone,” *Perception and Psychophysics*, vol. 11, no. 3, pp. 241–246, Mar. 1972.

[106] N. Jayant, “Signal compression based on models of human perception,” *Proc. IEEE*, vol. 81, no. 10, pp. 1385–1422, Murray Hill, NJ, Oct. 1993.

[107] B. S. Atal and L. R. Rabiner, “A pattern recognition approach to voiced-unvoiced-silence classification with applications to speech recognition,” *IEEE Trans. on Acoustics Speech and Signal Processing*, vol. 24, no. 3, pp. 201–212, Jun. 1976.

[108] T. Painter and A. Spanias, “A review of algorithms for perceptual coding of digital audio signals,” *Proc. IEEE Intl. Conf. on Digital Signal Processing*, vol. 1, pp. 179–208, Santorini, Greece, Jul. 1997.

[109] J. M. Kates, “Feedback cancellation apparatus and methods,” U.S. Patent 6 072 884, Jun., 2000.

[110] B. D. V. Rao and S.-Y. Kung, “Adaptive notch filtering for the retrieval of sinusoids in noise,” *IEEE Trans. on Acoustics Speech and Signal Processing*, vol. ASSP-33, no. 4, pp. 791–802, 1984.

[111] A. Nehorai, “A minimal parameter adaptive notch filter with constrained poles and zeros,” *IEEE Trans. on Acoustics Speech and Signal Processing*, vol. ASSP-33, no. 4, pp. 983–996, 1985.

[112] T. S. Ng, “Some aspects of an adaptive digital notch filter with constrained poles and zeros,” *IEEE Trans. on Acoustics Speech and Signal Processing*, vol. ASSP-35, no. 2, pp. 158–161, 1987.

[113] J. M. Travassos-Ramano and M. Bellanger, “Fast least-squares adaptive notch filtering,” *IEEE Trans. on Acoustic Speech and Signal Processing*, vol. ASSP-36, no. 9, pp. 1536–1540, 1988.

[114] P. A. Regalia and S. K. Mitra, “Tunable digital frequency response equalization filters,” *IEEE Trans. on Acoustics Speech and Signal Processing*, vol. 35, no. 1, pp. 118–120, Jan. 1987.

[115] Y. Matsuda, N. Nagasawa, and Y. Nomura, “Development of parametric equalizer LSI,” *IEEE Trans. on Consumer Electronics*, vol. 36, no. 3, pp. 354–359, Aug. 1990.

[116] R. Martin, “Noise power spectral density estimation based on optimal smoothing and minimum statistics,” *IEEE Trans. on Speech and Audio Processing*, vol. 9, no. 5, pp. 504–512, Jul. 2001.

[117] A. Pandey and V. J. Mathews, “Improving adaptive feedback cancellation in digital hearing aids through offending frequency suppression,” *Proc. IEEE Intl. Conf. Acoustics Speech and Signal Processing*, pp. 173–176, Dallas, TX, Mar. 2010.

[118] D. Bryce and W. Tonisson, “Selecting the gain of hearing aids for persons with sensori-neural hearing impairments,” *Scand Audiology*, vol. 5, no. 1, pp. 51–59, 1976.

[119] I.-T. R. P.862, “Perceptual evaluation of speech quality (PESQ): An objective method for end-to-end speech quality assessment of narrow band telephone networks and speech coders,” Feb. 2001.

[120] T. V. Waterschoot and M. Moonen, “Adaptive feedback cancellation for audio applications,” *Signal Processing*, vol. 89, no. 11, pp. 2185–2201, Nov. 2009.

[121] A. V. Oppenheim, R. W. Schafer, and J. R. Buck, *Discrete-time Signal Processing*, 2nd ed. Upper Saddle River, NJ: Prentice Hall, 1999.

[122] J. G. Proakis and D. K. Manolakis, *Digital Signal Processing*, 4th ed. Upper Saddle River, NJ: Prentice Hall, 2006.

[123] N. Karaboga and B. Cetinkaya, “Design of minimum phase digital IIR filters by using genetic algorithm,” *Proc. 6th Nordic Signal Processing Symposium*, pp. 29 – 32, Espoo, Finland, Jun. 2004.

[124] A. Marques and D. Freitas, “Infinite impulse response (IIR) inverse filter design for the equalization of non-minimum phase loudspeaker systems,” *IEEE Workshop on Applications of Signal Processing to Audio and Acoustics*, pp. 170–173, Mohonk Mountain House, New Paltz, New York, 16-19 Oct. 2005.

[125] A. Spriet, I. Proudler, M. Moonen, and J. Wouters, “Adaptive feedback cancellation in hearing aids with linear prediction of the desired signal,” *IEEE Trans. on Signal Processing*, vol. 53, no. 10, pp. 3749–3763, Oct. 2005.

[126] M. Veinovic, B. D. Kovacevic, and M. M. Milosavljevic, “Time-varying AR speech analysis using robust RLS algorithm with variable forgetting factor,” *Proc. 12th Intl. Conf. on Pattern Recognition*, vol. 3, pp. 211–213, Oct. 1994.

[127] C. H. Lee, “On robust linear prediction of speech,” *IEEE Trans. on Acoustics Speech and Signal Processing*, vol. 36, no. 5, pp. 642–650, May 1988.

[128] M. Bodson, "An adaptive algorithm with information-dependent data forgetting," *Proc. American Control Conf.*, vol. 5, pp. 3485–3489, Seattle, WA, Jun. 1995.

[129] T. F. Quatieri, *Discrete-time Speech Signal Processing: Principles and Practice*, 1st ed. Upper Saddle River, NJ: Prentice Hall, 2001.

[130] M. A. Stone and B. C. J. Moore, "Tolerable hearing aids delays. III: Effects on speech production and perception of across frequency variation in delay," *Ear and Hearing*, vol. 24, no. 2, pp. 175–183, Apr. 2003.

[131] ——, "Tolerable hearing aids delays. IV: Estimation of limits imposed by the auditory path alone using simulated hearing losses," *Ear and Hearing*, vol. 26, no. 2, pp. 225–235, Apr. 2005.

[132] D. Byrne and W. Noble, "Optimizing sound localization with hearing aids," *Trends in Amplification*, vol. 3, no. 2, pp. 49–73, 1998.

[133] B. Gardner and K. Martin. (1994, May) HRTF measurements of a KEMAR dummy-head microphone. [Online]. Available: http://sound.media.mit.edu/KEMAR.html [Accessed: May 12, 2010].

[134] Y. Hu and P. Loizou, "Subjective evaluation and comparison of speech enhancement algorithms," *Speech Communication*, vol. 49, pp. 588–601, 2007.

[135] K. Steinert, M. Schonle, C. Beaugeant, and T. Fingscheidt, "Hands-free system with low-delay subband acoustic echo control and noise reduction," *Proc. Intl. Conf. Acoustics Speech and Signal Processing*, vol. 5, pp. 1521 – 1524, Las Vegas, NV, Apr. 2008.

[136] F. Sinaga, T. Gunawan, and E. Ambikairajah, "Wavelet packet based audio coding using temporal masking," *Proc. 4th Intl. Conf. Information, Communications and Signal Processing and Pacific-Rim Conference On Multimedia*, vol. 3, pp. 4781 – 4784, Singapore, Dec. 2003.

[137] J. Wen, "Fourier domain speech enhancement by constrained optimization and temporal masking," *Proc. 12th Digital Signal Processing Workshop and 4th Signal Processing Education Workshop*, pp. 585 – 589, Teton National Park, Wyoming, Sep. 2006.

[138] N. Cvejic, A. Keskinarkaus, and T. Seppanen, "Audio watermarking using m-sequences and temporal masking," *IEEE Workshop on the Applications of Signal Processing to Audio and Acoustics*, pp. 227–230, New Platz, NY, Aug. 2001.

[139] H. Krishnamoorthi, V. Berisha, A. Spanias, and H. Kwon, "Low-complexity sinusoidal component selection using loudness patterns," *Proc. IEEE Intl. Conf. Acoustics Speech and Signal Processing*, vol. 5, pp. 301 – 304, Taipei, Taiwan, Apr. 2009.

[140] X. Hu, G. He, and X. Zhou, "An efficient low complexity encoder for MPEG advanced audio coding," *Proc. 8th Intl. Conf. Advanced Communication Technology*, vol. 3, pp. 1501–1505, Phoenix Park, Korea, Feb. 2006.

[141] W. Jesteadt, P. G. Stelmachowicz, and B. P. Callaghan, "Predicting masked thresholds in impaired listeners from combinations of normal masked thresholds and hearing loss (a)," *Journal of the Acoustical Society of America*, vol. 81, no. S1, pp. S77–S77, May 1987.

[142] R. P. Derleth, T. Dau, and B. Kollmeier, "Modeling temporal and compressive properties of the normal and impaired auditory system," *Hearing Research*, vol. 159, no. S1, pp. 132–149, Aug. 2001.

[143] A. C. Schroeder, N. F. Viemeister, and D. A. Nelson, "Pure-tone intensity discrimination in normal-hearing and hearing-impaired listeners," *Journal of the Acoustical Society of America*, vol. 96, pp. 2683–2693, 1994.

[144] B. C. J. Moore, *An Introduction to the Psychology of Hearing*, 1st ed. San Diego, CA: Academic Press, 1997.

[145] M. Florentine, S. Buus, B. Scharf, and E. Zwicker, "Frequency selectivity in normally-hearing and hearing-impaired observers," *Journal of Speech and Hearing Research*, vol. 23, pp. 646–669, Sep. 1980.

[146] M. S. Zilany and I. C. Bruce, "Modeling auditory-nerve responses for high sound pressure levels in the normal and impaired auditory periphery," *Journal of the Acoustical Society of America*, vol. 120, no. 3, pp. 1446–1466, Sep. 2006.

[147] D. A. Nelson and T. W. Fortune, "High-level psychophysical tuning curves: simultaneous masking with different noise bandwidths," *Journal of Speech and Hearing Research*, vol. 34, no. 2, pp. 374–378, Apr. 1991.

[148] R. A. Lutfi, "Masking additivity in the hearing-impaired," *Hearing Research*, vol. 25, no. 1, pp. 3–10, 1987.

[149] A. J. Oxenham and B. C. J. Moore, "Additivity of masking in normally hearing and hearing-impaired subjects," *Journal of the Acoustical Society of America*, vol. 98, pp. 1921–1934, 1995.

[150] D. A. Nelson and A. C. Schroeder, "Release from upward spread of masking in regions of high-frequency hearing loss," *Journal of the Acoustical Society of America*, vol. 100, no. 4, pp. 2266–2277, Oct. 1996.

[151] J. T. S. Smith and H. Duifhuis, "Masking and partial masking in listeners with a high frequency hearing loss," *Audiology*, vol. 21, pp. 310–324, 1982.

[152] D. E. Trees and C. W. Turner, "Spread of masking in normal subjects and in subjects with high frequency hearing loss," *Audiology*, vol. 24, pp. 678–693, 1991.

[153] P. Stelmachowicz, D. E. Lewis, L. Larson, and W. Jesteadt, "Growth of masking as a measure of response growth in hearing-impaired listeners," *Journal of the Acoustical Society of America*, vol. 81, pp. 1881–1887, 1987.

[154] B. C. J. Moore and B. R. Glasberg, "A revised model of loudness perception applied to cochlear hearing loss," *Hearing Research*, vol. 188, no. 1-2, pp. 70–88, Feb. 2004.

[155] L. E. Humes, B. Espinoza-Varaasn, and C. S. Watson, "Modeling sensorineural hearing loss. i. model and retrospective evaluation," *Journal of the Acoustical Society of America*, vol. 83, no. 1, pp. 188–202, Jan. 1988.

[156] B. Edwards, C. Struck, P. Dharan, and Z. Hou, "New digital processor for hearing loss compensation based on the auditory system," *Hearing Journal*, vol. 51, no. 8, pp. 38–49, Jan. 1998.

[157] T. Dau, D. Puschel, and A. Kohlrausch, "A quantitative model of the "effective" signal processing in the auditory system. I. model structure," *Journal of the Acoustical Society of America*, vol. 99, no. 6, pp. 3615–3622, Jun. 1996.

[158] G. Strang, "A proposal for Toeplitz matrix calculations," *Studies in Applied Mathematics*, vol. 74, pp. 171–176, 1986.

[159] M. Gutknecht, "Stable row recurrences for the padé table and generically superfast lookahead solvers for non-Hermitian Toeplitz systems," *Linear Algebra and its Applications*, vol. 188, pp. 351–421, 1993.

[160] J. Olkin, "Linear and nonlinear deconvolution problems," Ph.D. dissertation, Rice University, Houston, TX, 1986.

[161] B. Friedlander, M. Morf, T. Kailath, and L. Ljung, "New inversion formulas for matrices classified in terms of their distance from Toeplitz matrices," *Linear Algebra and its Applications*, vol. 27, pp. 31–60, Oct. 1979.

[162] R. Chan and M. Ng, "Toeplitz preconditioners for Hermitian Toeplitz systems," *Linear Algebra and its Applications*, vol. 190, pp. 181–208, 1993.